2007

A Search for the Counter-Immune Mechanisms of Mycobacterium Tuberculosis

Meghan Alida Kirksey

A SEARCH FOR THE COUNTER-IMMUNE MECHANISMS OF *MYCOBACTERIUM TUBERCULOSIS*

A Thesis Presented to the Faculty of

The Rockefeller University

in Partial Fulfillment of the Requirements for

the degree of Doctor of Philosophy

by

Meghan Alida Kirksey

June 2007

A SEARCH FOR THE COUNTER-IMMUNE MECHANISMS OF *MYCOBACTERIUM TUBERCULOSIS*

Meghan Alida Kirksey, Ph.D.

The Rockefeller University 2007

Tuberculosis is characterized by dynamic interactions between *M. tuberculosis* (Mtb) and the human immune response. The cytokine IFN-γ triggers macrophage production of bactericidal nitric oxide by inducible nitric oxide synthase (NOS2) and is essential for mammalian control of Mtb infection. Mice lacking NOS2 are unable to control replication of Mtb and rapidly succumb to infection. The persistent nature of TB infection suggests that Mtb has evolved counter-immune mechanisms to survive in the face of NOS2 and other pathways downstream of IFN-γ.

A differential signature-tagged transposon mutagenesis screen was conducted to identify mutants attenuated in $NOS2^{-/-}$ mice, but retaining virulence in IFN-$\gamma^{-/-}$ mice. Such mutants may be deficient in counter-immune responses to IFN-γ -dependent, NOS2-independent immune pathways.

Four mutants with the phenotype of interest were pulled from a screen of 96: *pks6*/Rv0405 - a polyketide synthase, Rv0072 - a membrane spanning domain of a putative glutamine transporter, Rv2958c - a glycosyl-transferase, and *pstA1*/Rv0930 - a membrane spanning domain of an inorganic phosphate transporter.

Monotypic IV infections confirmed that these mutants replicate freely in the tissues of IFN-$\gamma^{-/-}$ mice and kill these mice with similar kinetics to wild-type Mtb. In contrast, the mutants have little or no growth advantage in NOS2$^{-/-}$ mice and are highly attenuated in these mice.

It was discovered that none of the four mutants were producing a key mycobacterial surface lipid: phthiocerol dimycocerate (PDIM). *In vivo* phenotypes of the mutants were reproduced in a PDIM deficient strain cloned from a subpopulation pre-existing in the parent stock. Hence it was discovered that PDIM deficiency causes IFN-γ dependent, NOS2 independent attenuation of H37Rv. Moreover, the PDIM deficient strains demonstrated NOS2 dependent attenuation as well as early IFN-γ independent attenuation.

Autonomously from PDIM, the *pstA1* mutant is impaired for survival during WT and NOS2$^{-/-}$ macrophage infection and during *in vitro* P_i starvation. It is also deficient for uptake of orthophosphate and is hyper-sensitive to H_20_2, SDS, and acidified nitrite exposure. Phosphate starvation of H37Rv induces hypersensitivity to H_20_2 and SDS suggesting that disruption of *pstA1* may disrupt metabolism and/or gene regulation in a manner consistent with the effects of phosphate starvation.

I would like to thank everyone who has stood by me in support of this work and my sanity. My heart goes to my family, my friends, and my Love.

Acknowledgements-

I would like to acknowledge the following people for their invaluable contributions to this project:

John McKinney for inspiring me to pursue science for the benefit of humanity and for providing the scientific insight and support to see this project through.

My committee members: Michael Glickman, George Cross, Charles Rice, Sabine Ehrt, and Gilla Kaplan for your guidance, insight, and enthusiasm.

The members of the McKinney lab, current and past, for all of their teaching, assistance, patience, and humor.

My collaborators for sharing their thoughts, reagents, and data: Christophe Guilhot, Gilla Kaplan, Cheryl Vos, Keno Onwueme, Eric Rubin, and Jyothi Rengarajan.

Table of Contents:

List of Figures:

Chapter 1:

Chapter 3:

List of Tables:

Chapter 2:

Appendix:

List of Abbreviations:

ABC – ATP binding cassette

BMMO – bone marrow-derived macrophages

Cfu – colony forming units

Cim – counter immune mutants

dSTM – differential signature tagged mutagenesis

IFN-γ - interferon-γ

MDDC- monocyte derived dendritic cell

MDM – monocyte derived macrophage

MSD – membrane spanning domain

Mtb – *Mycobacterium tuberculosis*

NBD – nucleotide binding domain

NOS2 – inducible nitric oxide synthase/nitric oxide synthase 2

PDIM – phthiocerol dimycoserosate

PGL – phenolic glycolipid

phox – phagocyte oxidase

*p*HBA – *p*-hydroxy benzoic acid

*p*HBAD – *p*-hydroxy benzoic acid derivative

pks – polyketide synthase

ROS –reactive oxygen species

ROI – reactive oxygen intermediates

RNI – reactive nitrogen intermediates

SBD – substrate binding domain

TB – tuberculosis

Chapter 1:

Introduction to *Mycobacterium tuberculosis* Virulence and Immunity

History of Tuberculosis

Evidence from ancient Egyptian mummified remains demonstrates that humans have been afflicted with tuberculosis (TB) for at least 5,400 years [1]. However, it wasn't until 1882 that Robert Koch established that TB was a communicable disease caused by infection with the tubercle bacillus (*Mycobacterium tuberculosis*). Genetic analysis of *M. tuberculosis* (Mtb) and its close relatives suggests that the common progenitor of these pathogens may have infected our early hominid ancestors as long as 3 million years ago [2].

A complex and dynamic series of interactions between Mtb and the human immune response have allowed this pathogen to successfully parasitize the human host over the millennia with no sign of abatement. Today, in spite of widespread vaccination and use of chemotherapeutic agents, nearly 2 billion individuals worldwide are thought to be infected with Mtb, and each year 2-3 million deaths are attributed to TB [3].

Approximately 6.5 million of the world's 8 million annual new cases of TB occur in Southeast Asia, the Western Pacific, and Africa [3]. 95 % of all cases are in the developing world; however, poverty is a strong correlate of TB even in Western Europe and North America where the overall incidence is low [4]. Globally, TB is rivaled only by HIV-AIDS as an infectious killer, and TB is the leading cause of death among those infected with HIV. In addition, HIV is the most important risk factor for progression from Mtb infection to active clinical disease. This synergy is in large part responsible for the recent global resurgence of TB [5, 6]. In the United States, data suggests that HIV co-infection is present in more than 20 % of TB cases in patients age 25-44 [7]. Other immuno-compromised states that impact on the severity of mycobacterial infections

include anti-tumor necrosis factor-α (anti TNF-α) treatment and generation of interferon-γ (IFN-γ) autoantibodies [8-10].

Vaccines

The only vaccine that is currently used to prevent TB, the live-attenuated bacille Calmette Guérin (BCG) vaccine, is problematic. In large-scale, placebo-controlled, double-blinded clinical trials, the apparent protective efficacy of BCG against TB ranged from 80 % to nil [11]. The design, development, and evaluation of new vaccine candidates to replace BCG will require a more thorough understanding of the interaction of Mtb and the human immune system.

Evidence for the existence of protective immunity is indicated by the fact that 90 % of individuals who are infected by Mtb never develop active TB, despite the lifelong persistence of viable tubercle bacilli in their tissues [12-15]. The risk of disease progression rises precipitously in individuals who are immuno-compromised (e.g., due to HIV-AIDS), underscoring the critical role of the immune response in determining the outcome of infection. Novel vaccines cannot just imitate natural infection with Mtb; they must generate more substantial and enduring immune responses than are seen in the course of natural infection in order to be truly protective.

Chemotherapy

Between 1941 and 1952, in one of the most remarkable medical advances in history, the work of three independent groups led to the development of a trio

of drugs that could cure TB. Then, as now, TB had the dubious distinction of being one of the most devastating of human diseases. Approximately one billion people had died from tuberculosis in the two hundred years preceding these first chemotherapeutic discoveries. Without antibiotic treatment, the 5 year mortality rate of uncomplicated pulmonary TB was more than 50% [16]. In contrast, the combination of para-aminosalicylate (PAS), streptomycin, and isoniazid could, if administered properly, cure TB completely and nearly universally. In the decade following the discovery of these three drugs, several other effective drugs were identified and treatment times were shortened. While these drugs represent a critical advance in our ability to treat TB, inadequate healthcare infrastructure, financial limitations, individual patient non-compliance, the spread of HIV, and the surge in circulation of multi-drug resistant strains of Mtb have prevented universal control of the disease [17].

The current standard of care for treatment of TB in developed countries is 6-9 month "short-course" therapy using a combination of four of the first-line medications: isoniazid (INH), rifampin (RIF), pyrazinamide (PZA), and either ethambutol (EMB) or streptomycin (SM) [18]. With such a long treatment period, problems with patient compliance are inevitable and this has resulted in the emergence and spread of a significant number of drug-resistant strains of Mtb. Directly Observed Therapy (DOT) regimens, where administration of each dose is supervised by a health care or social worker, have been efficacious where implemented. However, only one fifth of patients worldwide are treated under DOT programs and some consider these programs to be ethically questionable [19]. Meanwhile, according to various studies, rates of multidrug resistant (MDR) TB reach percentiles in the teens in many countries and as high as 34 % in

Gujarat, India and 48 % in Nepal [20, 21]. The newest of our first-line anti-TB drugs, rifampicin, is over 40 years old and the emergence and spread of MDR-TB reminds us of the risks of relying on these old-line drugs for future control of this ancient disease.

Further complicating treatment options are issues of toxicity. Among the most common severe side-effect of TB treatment is isoniazid hepatotoxicity which occurs in approximately 1-5 % of patients and has a case-fatality rate approaching 5 % [22]. This and other adverse effects, including neurological and gastrointestinal effects, lead to drug discontinuation in nearly 10 % of patients [22]. It is essential for the global health community to discover and develop novel high-potency, low-toxicity drugs to treat TB, including MDR strains. Furthermore, the course of TB therapy must be shortened to help improve patient adherence to therapy, and thereby prevent emergence of further drug resistance.

The not-for-profit consortium, the Global Alliance for TB Drug Development (http://www.tballiance.org/), is working with government, industry and academia to pursue the essential if potentially "unprofitable" goal of anti-Mtb drug discovery, development, distribution, and equitable access. The recent publication of the genome of Mtb and modern developments in microbiological methodology afford us unique opportunities for identification of novel bacterial drug targets and rational drug design. A better understanding of the interactions between Mtb and the mammalian host will allow us to identify targets in the bacterial repertoire that are essential for *in vivo* survival and virulence.

The Tubercle Bacillus

Mycobacteria are rod shaped bacteria composing a genus of fast growing soil microbes and slow growing pathogens including Mtb, *Mycobacterium leprae*, *Mycobacterium bovis*, and *Mycobacterium marinum*. The Mtb complex consists of several closely related species with minimal genetic variation and includes *Mycobacterium tuberculosis* (Mtb), *Mycobacterium canettii*, *Mycobacterium africanum*, *Mycobacterium microti*, *Mycobacterium bovis*, and the live-attenuated vaccine strain *M. bovis* bacille Calmette-Guerin (BCG) [23]. While Mtb is overwhelmingly the most important mycobacterial pathogen of *Homo sapiens*, all of these strains can cause disease in immuno-competent humans, with the exceptions of *M. microti* and BCG.

In the pre-genomic era, much research was conducted in an effort to characterize the *Mycobacterium tuberculosis* cell envelope. The complex Mtb cell envelope consists of a plasma membrane, a cell wall, and a capsule-like outer layer (Figure 1.1). The cell wall consists of, from innermost to outermost, peptidoglycan (PG), arabinogalactan (AG), mycolic acids (MA), and peripheral lipids. Lipoarabinomannan (LAM) is thought to be anchored in the plasma membrane and is also found in the capsule-like layer anchored in the MAs [24].

The distinctive thickness and complexity of the Mtb cell wall is likely to impact on the host's ability to mount an effective anti-bacterial attack on the intra-phagosomal bacteria. Consistent with this hypothesis, the cell envelope components phthiocerol dimycocerate (PDIM), phenolic glycolipid (PGL), and LAM have been implicated in virulence and/or immunomodulatory effects of Mtb [25-27]. PDIM deficient mutants are attenuated in the mouse model of infection [26]. LAM has been shown to directly scavenge reactive oxygen species

(ROS), inhibit protein kinase C activity, and block transcription of IFN-γ dependent genes in macrophages [25]. Macrophages infected with Mtb lacking PGL secrete increased levels of tumor necrosis factor-α (TNF-α), interleukin-6 (IL-6), and IL-12; purified PGL suppresses these pro-inflammatory cytokines [27].

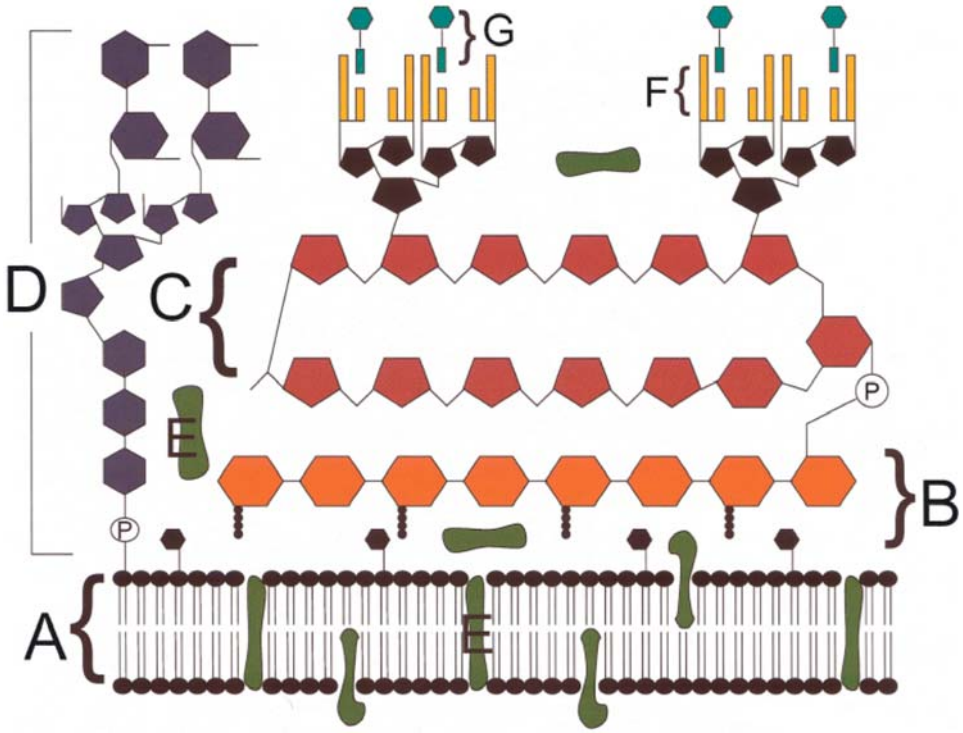

Figure 1.1: Schematic of Mycobacterial Cell Envelope [28]. (A) plasma membrane, (B) peptidoglycan, (C) arabinogalactan, (D) mannose-capped lipoarabinomannan, (E) plasma membrane- and cell envelope-associated proteins, (F) mycolic acids and (G) glycolipid surface molecules associated with the mycolic acids.

The thick Mtb cell wall has low permeability that may contribute to the organism's relative insensitivity to β-lactams and resistance to many other antibiotics that have low minimal inhibitory concentrations (MICs) for other bacteria. The unique cell wall characteristics of Mtb also allow it to retain the carbol fuchsin stain even after an acid alcohol wash, thus enabling identification

of mycobacteria based upon their unusual "acid fast" staining.

In addition to structural, biochemical, and genetic analysis of the cell wall, much research has been done to characterize clinically relevant secreted and immunodominant antigens of Mtb. Such antigens have potential as elements of improved vaccines and as novel diagnostic markers of infection and disease. Among the best characterized antigens are Esat-6, MPT-64, the 19 kDa antigen, the 38 kDa antigen, and the Antigen 85 (Ag85) complex [29, 30]. In one recent vaccine study, a subunit vaccine containing Ag85B and Esat-6 in combination was shown to have substantial protective efficacy in macaques [31].

In the quest for new diagnostics, a study of 196 culture positive TB patients found that approximately 77% produced antibodies to the 38kDa antigen and confirmed that the antigen successfully induced skin reactions in Mtb sensitized outbred guinea pigs [32]. However, BCG sensitized animals also responded to the 38kDa antigen, recapitulating the false-negative potential of the PPD skin test (see pp.14-15). In contrast, Esat-6 is a protein that is encoded in a region of the Mtb chromosome that is deleted in the BCG vaccine (region RD1); hence, Esat-6 and other proteins encoded by RD1 are being developed as potential diagnostic reagents that can be used in previously vaccinated individuals [33, 34].

The genome of the commonly utilized laboratory strain of Mtb, H37Rv, was sequenced and published in 1998 [35]. The sequence revealed, among other things, that the bacteria dedicate 8 % of their genome to lipid metabolism alone. The genes encompassed by this grouping include an extensive collection of genes for lipid catabolism as well as many used for synthesis of the complex mycobacterial cell wall. The genome sequence also described 167 PE and PPE

genes that encoded products of unknown function grouped based on N-terminal ProGlu or ProProGlu motifs and repetitive C-terminal extensions [35, 36]. Subsequent sequence analysis of the highly transmissible clinical strain CDC1551 revealed that it was nearly identical to H37Rv, confirming the utility of H37Rv as a model of clinically relevant strains of Mtb [37]. Moreover, despite over 10,000 years of evolution, when 16 genetically diverse clinical strains were examined for conservation of 24 genes known to encode antigenic proteins, minimal variation was observed [38]. In fact, 19 genes were identical across all strains examined, suggesting a recent common ancestor of the majority of modern clinical strains as well as the laboratory strain H37Rv.

Since the publication of the Mtb genome and the development of molecular biology techniques for use in Mtb research, the focus of much research has shifted to the genetics of Mtb virulence and pathogenesis. While development of diagnostics and vaccines remains a challenge, renewed emphasis has been placed on the identification of putative targets for novel drug design. Genetics promises to be a key for unlocking pathways essential to Mtb survival and replication and identification of those gene products that can be targeted by chemotherapeutics. Impressively, an exhaustive mutagenesis was conducted to identify a potential list of essential Mtb genes for which no mutants could be isolated [39]. While it should be noted that several of these putatively essential genes have since been successfully deleted, this study remains a useful broad screen for genes likely to be important for bacterial survival.

It should be noted that in recent years the only new anti-TB drugs to enter clinical trials have been identified by industry through non-specific high-throughput screening of chemicals for bacteriostatic or bactericidal activity.

There exists immense practical potential for brute force pharmaco-chemical screening in combination with rational target identification. Much promise lies in public-private partnerships enabling such collaboration.

Pathogenesis of Disease

Infection by Mtb occurs via inhalation of 1-5 μm droplets containing one or several bacteria. These small droplets deposit into alveolar airspace, while larger particles are efficiently cleared by the pulmonary mucociliary system [40]. Infecting bacteria are phagocytosed by resident alveolar macrophages and can begin to replicate within the membrane-bound phagocytic vesicles. Eventually the bacterial burden overwhelms the macrophages leading to the rupture of the cells and the release of numerous bacilli. These bacteria are then taken up by other alveolar macrophages and by monocyte-derived macrophages (MDMs) emigrating from the bloodstream [40]. After approximately 2 weeks bacteria begin to spill over from the primary lesion into surrounding tissue and are carried to regional lymph nodes from which they spread to other organs. By three weeks post-infection, a specific T-cell response emerges. Release of the lymphokines interferon-γ (IFN-γ) and tumor necrosis factor-α (TNF-α) activates macrophages and thereby checks bacterial replication. A mature granuloma forms consisting of a ring of CD4+ and CD8+ T cells surrounding a ring of macrophages containing intracellular bacteria. A caseating granuloma may develop with a central core of necrotic tissue and extracellular bacteria (Figure 1.2) [40].

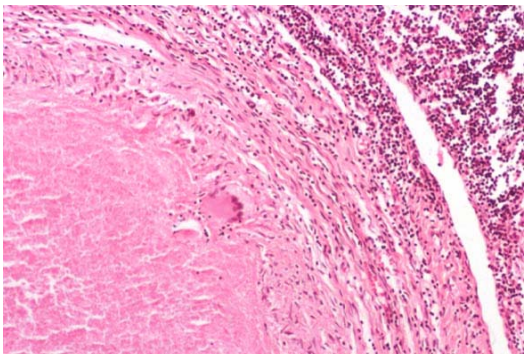

Figure 1.2: **Histology of a Caseating Granuloma.** [41]

In a healthy individual, tuberculous granulomas can be contained indefinitely and may even be completely sterilized over time. However, in approximately 5 % of cases, primary progressive TB develops within several years of infection. Moreover, in another 5 % of cases, reactivation of latent infection occurs years or decades after primary exposure [40]. Progression to a disease state is most often seen in infants, the elderly, the malnourished, or those who are immuno-compromised by steroids, genetic predisposition, or HIV. In severe post-primary disease, gross cavitation can occur in the lung and necrotic tissue can spill over into airways. The associated cough provides the perfect vehicle for spread of bacteria within the lung of an individual and between an individual and his or her contacts.

Active TB disease can be diagnosed based on symptomology, microscopic analysis of sputum stained to reveal acid-fast bacilli, sputum culture, DNA or RNA amplification assays, and/or chest radiograph. Signs and symptoms of TB include: night sweats, productive cough, bloody sputum, weight loss, and consolidated opacities (esp. apical) and/or upper lobe cavitation on lung X-ray. However, it should be noted that with severe immunodeficiencies such as HIV,

patients with disseminated Mtb lung infection can display non-typical signs and symptoms mimicking other lung pathologies.

Model Systems

Our understanding of Mtb pathogenesis and the mammalian immune response to Mtb infection has been enhanced by the use of several key model systems. Tissue culture models utilizing murine bone marrow derived macrophages (BMMOs) or human peripheral blood monocytes (PBMCs) have provided insights into the interactions between Mtb and the phagocytic host cell. However, the macrophage cannot reproduce the complexity of the immune response in an intact animal. Therefore, several small animal models have been commonly employed in the study of Mtb virulence and host immunity, especially mice, guinea pigs, and rabbits.

Mice are often the model of choice for Mtb infection because of the widespread availability of species-specific reagents, inbred strains, and transgenic and gene knockout technology, as well as their small size and relatively low cost. Mice also demonstrate reduced susceptibility to Mtb infection compared to other models, allowing for study of a persistent phase of infection that models latency in humans [42]. Mice do not, however, demonstrate the stages of well organized granuloma development seen in advanced human disease.

For the study of granuloma formation and development, guinea pigs and rabbits provide valuable models. Guinea pigs are highly susceptible to Mtb infection and form early stage granulomas before succumbing to disease [43]. Rabbits progress through all of the stages of granuloma formation seen in

humans including caseation, liquefaction, and cavitation [44]. However, maintenance costs and the lack of inbred strains and biological reagents prohibit the use of rabbits and guinea pigs for the majority of Mtb studies.

A few groups have recently pursued studies of Mtb infection using non-human primate models [45] . These models are valuable in that they demonstrate the broad spectrum of progression seen in humans, from true latency to fulminant disease. Moreover, an array of immunologic reagents are available for non-human primates. Unfortunately, primates are contagious to both humans and other animals and biocontainment following Mtb infection is a major challenge. In addition, the cost of acquisition and maintenance of primates is exorbitant. These challenges limit the utility of non-human primate models.

Immune Response

Infection with Mtb elicits primarily a cell-mediated immune (CMI) response dominated by macrophages and T lymphocytes (Figure 1.3). Early recognition of Mtb is mediated by the macrophage mannose receptor, CD14, and Toll-like receptors (TLR2, 4, and 9) [46-48]. Surfactant receptors, complement receptors, and Fc receptors recognize host molecules bound to Mtb [49]. The receptor mediating bacterial entry can affect the subsequent host response; IgG opsonized Mtb entering via the Fc receptor trigger antibacterial macrophage activation, however, complement opsonized Mtb entering via complement receptors fail to trigger macrophage effector mechanisms [50, 51]. Triggering of the appropriate activating receptors by Mtb can result in early production of pro-inflammatory cytokines such as interleukin-12 (IL-12) and TNF-α [52].

The development of an acquired immune response to Mtb, and

subsequent control of infection, is dependent on both $CD4^+$ and $CD8^+$ T cells; neither cell type can fully compensate for lack of the other [53], [54]. $CD4^+$ depletion causes reactivation of previously stable persistent Mtb infection in the mouse model and MHC class II deficient mice are highly susceptible to Mtb infection [53],[55]. Mice deficient in MHC class Ia, CD1, and TAP1 are also more susceptible to Mtb, implicating $CD8^+$ T cells in resistance [56]-[57]. Moreover, CD8 deficient mice demonstrate enhanced susceptibility to infection by Mtb [58].

CD1 proteins are similar in structure to MHC molecules, but present lipid antigens instead of peptide antigens. $CD4^+$ and $CD8^+$ T cells as well as $CD4^-$ $CD8^-$ T cells have been shown to respond to mycobacterial lipid antigen presentation via CD1 [59-61]. $CD4^+$ and $CD8^+$ CD1 restricted T cells are capable of Th1 cytokine production, lysis of infected cells, and reduction of bacterial loads [61-63]. There are five isoforms of CD1 in humans: CD1A-E. However, it is worth noting that the group 1 molecules (A-C) are not present in rodents and CD1D deficient mice are no more susceptible to Mtb infection than wildtype mice [57].

Dendritic cells (DCs) are specialized antigen presenting cells that serve in the innate immune response as sentinals of infections and as adjuvants in stimulating the adaptive immune response. DCs carry antigens to the lymphoid organs and present them to T cells via MHC and CD1 molecules. Dendritic cells are also involved in directing differentiation of T cells via either the T helper 1 (Th1) or Th2 pathway. Upon interaction with Mtb, DCs upregulate antigen presenting and T cell co-stimulatory molecules [64]. DCs are capable of presenting Mtb antigens via CD1 as well as cross-presenting antigens from apoptotic Mtb infected cells and presenting antigens via MHC class I [56, 65]. Thus, DCs might play a key role in mediating CD8+ T cell response to Mtb. DCs

also increase expression of IL-12, IL-1, and TNF-α when exposed to Mtb and likely stimulate $CD4^+$ responses as well.

When an Mtb infected person is injected subcutaneously with a preparation of partially purified protein derivative (PPD) from Mtb, antigen presenting cells display the antigens to T cells. Antigen specific T cells then recruit macrophages to the area and activate them, generating a local delayed type hypersensitivity (DTH) reaction. It was recognized early in the study of TB that this DTH would be a valuable tool for detecting Mtb infection, even in those people who were sputum negative for bacteria. Today, the tuberculin skin test for DTH remains the gold standard for detection of Mtb infection. It should be noted, however, that a false negative rate as high as 20 % has been reported for patients with HIV and other forms of immunosuppression [4]. Moreover, false positive results can be elicited in patients with a history of exposure to environmental mycobacteria and/or the BCG vaccine. In the USA, where there is little endemic tuberculosis and limited exposure to confounding environmental mycobacteria, vaccination has been avoided in favor of enhanced detection of infection by skin test.

It is clear that there are elements of the innate and the adaptive immune response that are essential for control of TB, and attempts have been made to dissect the elements of this response during the course of human infection. Many important experiments have been conducted with macrophage-like cell lines and *ex vivo* human PBMCs. In addition, studies have been performed using cells and fluid obtained by bronchoalveolar lavage. In cell culture experiments, infection of human monocyte-derived macrophages (MDMs) with Mtb has been shown to stimulate secretion of the pro-inflammatory cytokines TNF-α, IL-1, IL-

6, and IL-18 [66]. However, infected MDMs were also shown to secrete the immuno-suppressive cytokine IL-10, which is a potent inhibitor of IL-12 synthesis. Conversely, IL-10 was not produced by infected human monocyte-derived dendritic cells (MDDCs) and these MDDCs released copious amounts of IL-12. Using a combined transcriptomic and proteomic approach, it has been demonstrated that there is induction of osteopontin, IL-8, MCP-1, and RANTES, as well as the proinflammatory cytokines IL-1, IL-2, and TNF-α in the human THP1 macrophage-like cell line after infection with *M. tuberculosis* [67].

IFN-γ and TNF-α are crucial for macrophage activation and are thought to be key elements of the mammalian immune response that controls Mtb infection. In the late 1980s, it was demonstrated that application of exogenous IFN-γ was able to activate murine bone-marrow derived macrophages and cause inhibition of mycobacterial growth [68]. When IFN-γ knockout mice became available, it was shown that this cytokine is essential for control of Mtb infection [69, 70]. Similarly, it was shown that both TNF-α 55 kDa receptor knockout mice and TNF-α depleted mice quickly succumb to Mtb infection [71]. It is noteworthy that humans with naturally occurring IFN-γ receptor mutations are more susceptible to mycobacterial infections and rheumatoid arthritis patients treated with anti- TNF-α antibody are at high risk of Mtb reactivation [72, 73].

One of the primary roles of IFN-γ is to trigger macrophage production of inducible nitric oxide synthase (NOS2), thereby providing bactericidal nitric oxide and other reactive nitrogen intermediates (Figure 1.3). Microarray analysis of murine bone marrow-derived macrophages (BMMΦs) revealed strong induction of NOS2 and various chemokines, including MIG and RANTES, in

response to IFN-γ, Mtb, or IFN-γ plus Mtb [74]. In 1999, it was demonstrated that NOS2 knockout mice are highly susceptible to infection with Mtb [75]. However, the phenotype of NOS2 knockout mice is not as severe as that of IFN-γ deficient mice, indicating that NOS2 independent, IFN-γ dependent pathways play a role in control of Mtb infection [76, 77]. Recently it was shown that LRG-47, an IFN-γ inducible GTPase, accounts for a significant part, but not all, of the NOS2 independent control of Mtb infection [78].

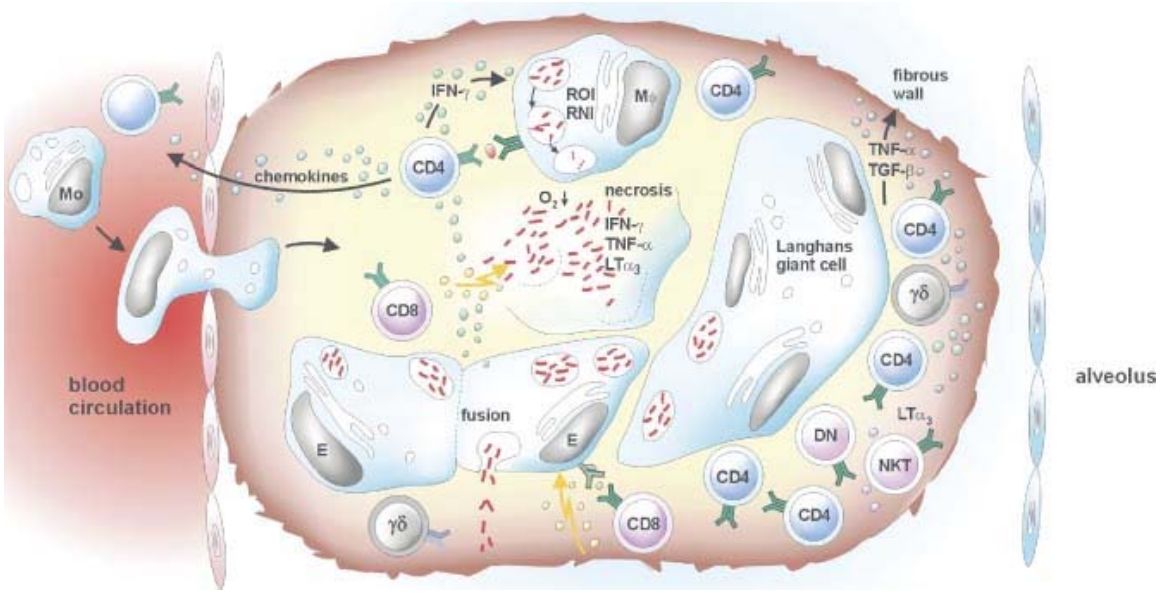

Figure 1.3: Schematic of Immune Mechanisms Involved in Defense Against Mtb [79]. Cells: MΦ, macrophage; CD4, CD4+ T cell; CD8, CD8+ T cell; NKT, natural killer T cell; E, epithelial cell; γδ, γδ T cell. Cytokines: TNF-α, tumor necrosis factor-α; IFN-γ, interferon-γ; TGF-β, transforming growth factor-β; $LT\alpha_3$, leukotriene α_3. Reactive species: ROI, reactive oxygen intermediates; RNI, reactive nitrogen intermediates.

Bacterial Survival

A complex set of requirements must be met in order for bacteria to ensure their survival and replication, even in the most hospitable of environments. Rationally based targeted gene disruption of Mtb followed by animal or macrophage infection with mutant bacteria has been a valuable tool for testing the importance of many genes suspected to be involved in *in vivo* pathogenesis. For example, in the 1950's, Segal observed that Mtb grown *in vitro* culture preferred carbohydrate nutritional substrates, while those grown *in vivo* seemed to prefer fatty acids, suggesting that there is a difference between the *in vivo* and *in vitro* metabolic requirements of Mtb [80]. These observations suggested that enzymes necessary for metabolism of non-carbohydrate substrates, such as those involved in the glyoxylate shunt of the Krebs cycle, might be required for virulence. Using targeted gene disruption, it has been demonstrated that isocitrate lyase (ICL), a key enzyme involved in metabolism of fatty acids via the glyoxylate shunt, is required for replication and persistence of *M tuberculosis* in mice [81, 82]. ICL, which is not required for growth *in vitro* in carbohydrate-rich media, was thus identified as an enzyme essential for *in vivo* survival and as a potential drug target.

In another example of successful rational identification of a virulence gene, the extracellular repeat protein (Erp) of Mtb was known to be a secreted protein produced only by pathogenic mycobacteria. A suspected virulence factor, it was targeted for gene disruption and was thus identified to be required for growth during the acute phase of mouse infection, though not essential *in vitro* [83]. Other examples include: a Mg^{++} transporter, a heat-shock protein transcription factor, and a mycolic acid cyclopropanase (encoded by *mgtC, hspR,*

and *pcaA* respectively) which were shown to be required for growth of Mtb in mice, but not in nutrient rich media *in vitro* [84-86].

It is important to note that extensive time and resources have been invested in rational targeted disruption and characterization of genes that were subsequently found to be dispensable for virulence. Hence, a number of screening approaches have been employed to directly identify genes important for virulence of Mtb. In one study, McAdam generated a transposon library of over 10,000 H37Rv mutants representing disruptions in 351 genes [87]. Severe combined immunodeficient (SCID) mice, which are unable to control Mtb replication, were used to facilitate screening of these mutants for virulence defects. While several slightly attenuated and several mildly hypervirulent mutants were identified, the use of severely immunocompromised mice in these experiments limited their utility as a screening tool for genes involved in growth and survival in an immunocompetent host.

Mtb faces substantial challenges as it colonizes a mammalian host and must survive the onslaught of both innate and adaptive immune responses. The complexities of the dynamic host-pathogen interaction require a unique set of genes, proteins, and pathways for the *in vivo* survival and virulence of Mtb. A better understanding of the essential pathways required for bacterial growth and survival *in vivo* may allow us to identify drug targets that would facilitate shortening of disease therapy and prophylaxis against reactivation of latent infections.

Several approaches have been used to identify genes required for survival in an immunocompetent host. Gene expression studies have been conducted in an attempt to identify genes that are specifically upregulated *in vivo* and

potentially essential for virulence of mycobacteria. Tools employed for such expression studies include: subtractive hybridization [88], selective capture of transcribed sequences (SCOTS) [89], promoter-fusion libraries [90, 91], and most recently DNA microarrays [92, 93]. Using a fluorescence-activated cell sorter (FACS) based screen for differential fluorescence induction, one group demonstrated that two genes encoding PE/PE-PGRS family proteins were highly expressed by *M. marinum* in frog granulomas, but not *in vitro* or in cultured macrophages. These proteins were then shown to be essential for virulence of the bacteria in frogs, but not for their survival *in vitro* [94]. While expression based screens for virulence factors have potential, activity of specific promoters *in vitro* depends on the specific *in vitro* culture conditions used. For a professional pathogen like Mtb, *in vitro* growth conditions are highly artificial. It is difficult, therefore, to distinguish between genes artifactually downregulated *in vitro* from those of significance to virulence that are upregulated *in vivo*. Genes that are less active *in vitro* are not necessarily required for virulence *in vivo* and vice versa.

To avoid investing resources into studying pathways that are not essential for pathogenesis, it can be useful to screen directly for genes of interest based on their *in vivo* virulence profiles. Signature-tagged transposon mutagenesis (STM) was developed as a tool for directly screening large numbers of transposon mutants for attenuation *in vivo* by negative selection (Figure 1.4) [95]. In STM, a library of transposons is constructed so that each transposon carries a unique, short variable DNA region that acts like a barcode, allowing for PCR based detection of individual transposons within a pool of many. Bacteria are mutagenized using the tagged transposons and pools of uniquely tagged mutants are injected into animals. At predetermined timepoints, surviving

bacteria are collected from the animals and genomic DNA is prepared from the recovered bacteria. The DNA tags are PCR amplified from the genomic DNA and the PCR products are hybridized to a membrane array of the individual tags (Figure 1.4). The membrane is compared to one that has been probed with PCR products amplified from the inoculum, revealing tags that are absent or under-represented in the pools after infection. Mutants that were present in the inoculum but were selected against during passage through the mouse are potentially attenuated. The insertion point of the transposon can be sequenced and the disrupted virulence gene or operon identified.

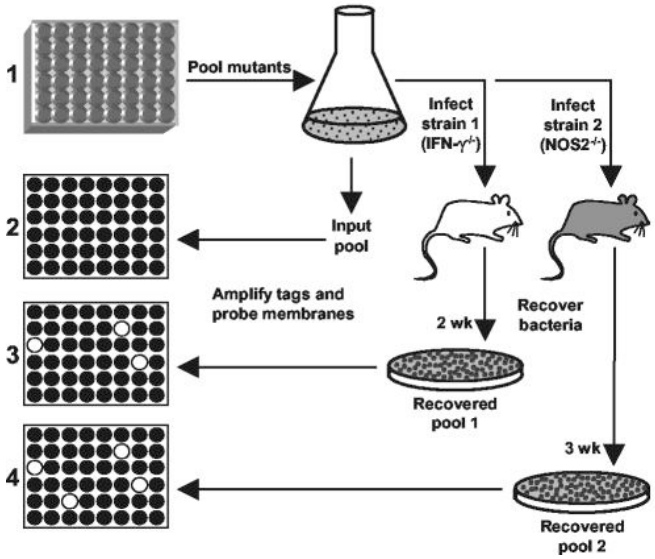

Figure 1.4: Schematic of STM Screen [76].

STM was first described in *Salmonella typhimurium* in 1995 and has since proven to be an invaluable tool in the study of other pathogens, including Mtb [95]. Using STM, Camacho et al. (1999) identified 16 Mtb mutants that were attenuated in Balb/c mice and Cox et al. (1999) identified 14 in C57BL/6 mice

[26, 96]. Both of these groups examined bacteria from lungs of mice infected by tail-vein and harvested three weeks post infection. The potential uses of STM to identify virulence genes in different mouse backgrounds, by different routes of infection, at different times post-infection, in different organs, and under different stress conditions are numerous.

Differential Signature Tagged Mutagenesis (dSTM) Screen

Three genes are known to potentially be involved in IFN-γ dependent control of bacterial infections in mice: phagocyte oxidase (phox), NOS2, and LRG-47 [75, 78]. Phox knockout mice are not more susceptible to Mtb than wildtype mice and phox$^{-/-}$ NOS2$^{-/-}$ double knockout mice phenocopy NOS2$^{-/-}$ mice when infected with wildtype Mtb [76, 97]. Thus, it appears that phox plays a minimal role in control of Mtb in the mouse model of infection. NOS2$^{-/-}$ mice and LRG-47$^{-/-}$ mice are highly susceptible to Mtb infection, permitting rapid bacterial expansion and exhibiting accelerated mortality [75, 78]. However, neither of these knockout strains is as susceptible as IFN-γ$^{-/-}$ mice. Moreover, LRG-47$^{-/-}$ mice treated with aminoguanidine, an inhibitor of NOS2 function, are not as susceptible to infection as IFN-γ$^{-/-}$ mice [78]. These observations indicate the existence of at least one as yet unknown effector pathway of IFN-γ that contributes to host defense against Mtb.

Mtb has evolved mechanisms to counter the immune pressures it faces *in vivo*. It may do this by interfering directly with IFN-γ signaling and/or by blocking its downstream effectors (Figure 1.5). For example, the mycobacterial catalase (KatG) plays a role in detoxification of reactive oxygen species (ROS).

katG deficient bacteria are attenuated in WT mice, but fully virulent in phox$^{-/-}$ mice, thus demonstrating that catalase is able to effectively neutralize the impact of phox on bacterial control; *katG* mutants exhibit phox dependent attenuation [97]. Similarly, the Mtb proteasome has been shown to play a role in countering the toxic effects of reactive nitrogen species (RNS) produced by NOS2 and proteasome mutants exhibit NOS2 dependent attenuation [98].

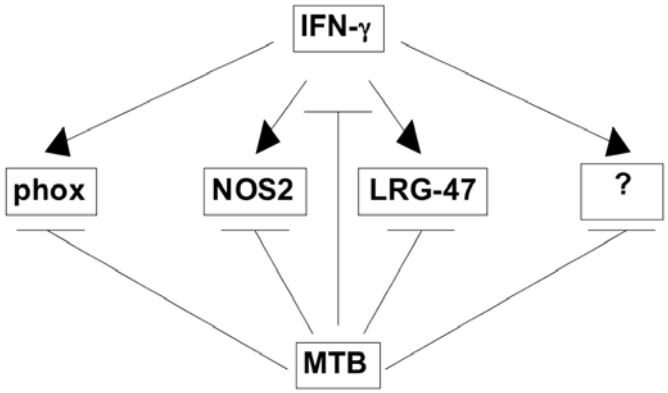

Figure 1.5: Schematic of Immune and Counter-immune Pathways.

In an effort to identify other Mtb genes involved in counter-immune (*cim*) defense, our lab conducted a differential STM (dSTM) screen to identify mutants that are attenuated in NOS2 knockout mice, but remain highly virulent in IFN-γ knockout mice. The *cim* genes identified in this screen are candidates for bacterial defense mechanisms that provide specific protection against IFN-γ-dependent, NOS2-independent host immune pressures.

Results of dSTM Screen

Four mutants of interest were isolated from a screen of 96 transposon mutants: (1) ***pks6*/Rv0405**, encoding a polyketide synthase; (2) **Rv0072**, encoding a membrane spanning domain (MSD) protein of a putative glutamine ATP

Binding Cassette (ABC) transporter; (3) **Rv2958c**, encoding a glycosyltransferase; (4) ***pstA1*/Rv0930**, encoding an MSD protein of an inorganic phosphate ABC transporter. The phenotypes of all four mutants were confirmed by monotypic intravenous (IV) infection (Figure 1.6). As expected, the mutants were more severely attenuated in NOS2$^{-/-}$ mice than in IFN-γ$^{-/-}$ mice as evidenced by both colony forming units (cfu)/lung and mouse survival.

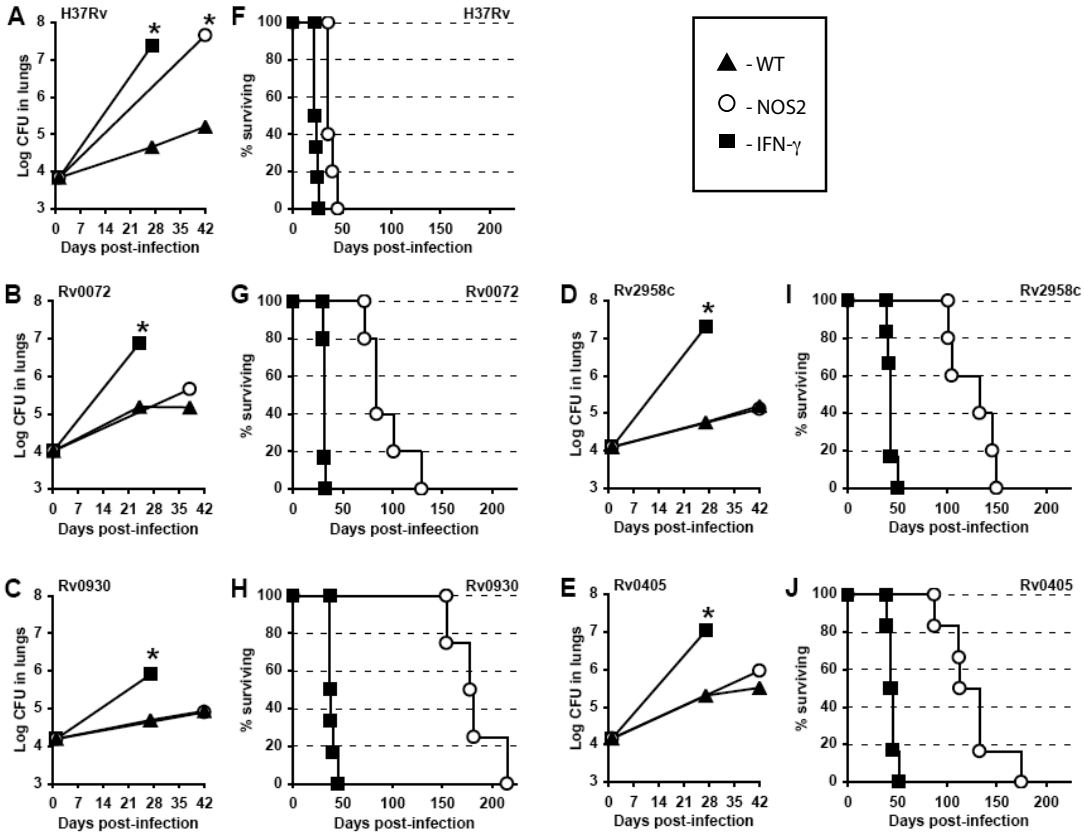

Figure 1.6: IV Retest of Virulence Phenotype of *cim* Mutants. Mice were infected by tail vein injection of H37Rv (A, F), Rv0072 (B, G), Rv0930/*pstA1* (C, H), Rv2958c (D, I), and Rv0405/*pks6* (E, J) strains of *M. tuberculosis*. Lung cfu from WT (black triangles), NOS2$^{-/-}$ (white circles), and IFN-γ$^{-/-}$ (black squares) mice were quantified at 28 and 42 days post infection (A-E). Mouse survival curves were generated (F-J) for NOS2$^{-/-}$ (white circles), and IFN-γ$^{-/-}$ (black squares) mice.

Unexpectedly, the phenotypes of our mutants were found to be due predominantly to spontaneously arising pthiocerol dimycocerosate (PDIM) deficiency. However, the most well characterized mutant, *pstA1*, also displays significant PDIM-independent phenotypes.

Chapter 2:

Introduction to Pst Systems and the Pho Regulon

Introduction to the Pst System

The bacterial high affinity inorganic phosphate transport (Pst) system has been explored in numerous species and is best characterized in *E. coli*. In spite of the confounding effects of PDIM deficiency, a *pstA1* mutant isolated from the Mtb dSTM screen was found to have significant PDIM independent phenotypes of interest. This mutant was therefore studied in further detail.

***E. coli* Pst and the Pho Regulon**

E. coli has two inorganic phosphate transport systems: Pst, a derepressible high affinity ATP binding cassette (ABC) importer, and Pit, a constitutive low affinity importer. Pst has a K_t of approximately 0.2 μM, while Pit has a K_t of about 25 μM [99]. The Pit system consists of two independent single-protein transporters, PitA and PitB. The Pst system is encoded in an operon encompassing four genes in the following order: *pstS*, *pstC*, *pstA*, and *pstB*. *pstS* encodes the substrate binding domain (SBD) subunit, *pstB* encodes the nucleotide binding domain (NBD) subunit, and the membrane spanning domain (MSD) subunits are encoded by *pstC* and *pstA* [100]. It is hypothesized that inorganic phosphate dianions are imported across a discontinuous charged amino acid relay system via the PstA and PstC MSD subunits [101]. The *E. coli pst* operon also encodes a gene that is not involved in phosphate uptake but is postulated to be involved in regulation: *phoU* [100, 102, 103]. Transcriptional analysis reveals that the operon is transcribed in its entirety and cleaved into distinct mRNAs post-transcriptionally. The dominant transcript is that of the first gene, *pstS*, encoding the SBD protein [104]. This is consistent with previous

reports that the SBD subunit genes of ABC transporters are often expressed at higher levels than downstream genes in the operon [104].

The Pho regulon, which is normally repressed in high phosphate environments, is composed of phosphate scavenging genes including the *pst* genes and the gene for alkaline phosphatase. Alkaline phosphatase activity is a commonly utilized indicator of Pho regulon activity. In addition to its role in inorganic phosphate uptake, the *E. coli* Pst system has been shown to be required for repression of the Pho regulon. Most *E. coli pst* mutants exhibit derepression of the Pho regulon and constitutive alkaline phosphatase activity even under high phosphate conditions [105]. Two amino acid residues of the NBD, PstB, have been shown to be required for both phosphate uptake and Pho regulon repression [106]. However, although Arg-237 and Glu-241 of PstC and Arg-220 of PstA are required for phosphate transport, they are not required for repression of alkaline phosphatase [106, 107]. This observation suggests that the regulatory function of the Pst system may be independent of its role in Pi transport.

It is worth noting that overexpression of *pitA* or *pitB* can restore phosphate responsiveness of the Pho regulon to a *pstS* mutant in the presence of *pstCAB* and the putative regulator *phoU* [108]. Taken together, these results demonstrate that active transport through the Pst system is not required for Pst dependent Pho regulon repression and phosphate mediated repression can be partially mediated by Pit transporters. However, regulation of the Pho regulon is not restored by Pit in the complete absence of *pstSCAB* and *phoU*.

In *Bacillus subtilis*, *pst* has been shown to be specifically upregulated by alkali stress even in the presence of normal phosphate concentrations [109]. The Pit system does not function under alkaline conditions; however, increased levels

of extracellular phosphate were able to overcome the alkali induced *pst* expression. It has been postulated that a third phosphate transporter is functioning under these conditions, enabling repression of the Pst system [109]. However, the dysfunction of the Pit system might cause functional P_i limitation and might therefore induce *pst* gene upregulation. Thus, residual phosphate uptake under alkaline conditions could be mediated by the Pst system itself.

The *E. coli* Pho regulon is controlled via the PhoB/PhoR two-component signal transduction system. PhoR is a histidine kinase that phosphorylates the response regulator PhoB, which in turn stimulates transcription of downstream genes when phosphate concentrations drop below 4 μM [103, 110]. PhoR is also capable of dephosphorylating PhoB in order to repress the genes of the Pho regulon. It has been suggested that PhoU plays a role in mediating signaling between the Pst transporter and the PhoB/PhoR signal transduction system. Hoffer and Tommassen (2001) postulated that by interacting directly with the Pst transporter, PhoU immediately detects local changes in intracellular phosphate and signals downstream to PhoB/PhoR. In the absence of PstS, they suggested that high intracellular phosphate concentrations accumulated by overexpression of Pit may allow for signaling via PhoU [108]. This interpretation is consistent with the observation that some Pst mutants that do not transport phosphate are still able to mediate repression of the Pho regulon under high extracellular phosphate concentrations. However, this interpretation does not explain why most *pst* mutants are unable to repress the Pho regulon under high phosphate concentrations when even normal levels of Pit allow for accumulation of high intracellular phosphate concentrations (30 mM) [111]. The molecular details of the putative Pst/PhoU/PhoR interactions remain unclear, as does the direct link

between phosphate transport and the Pho regulon.

While Muda et al. (1992) reported that *phoU* mutants were deficient in phosphate uptake [101], it was later reported by Steed et al. (1993) that *phoU* mutants have no inherent defect in phosphate acquisition [102, 112]. Instead, *phoU* mutants have a severe growth defect in rich medium that is largely eliminated by compensatory mutations in the PstSCAB transporter or the PhoB/PhoR two-component system [102]. In another study, an *E. coli phoU* mutant was identified that accumulated excess inorganic phosphate in both high and low phosphate environments [113]. This mutant demonstrated a slow growth phenotype consistent with the observations of Steed et al. (1993) [102, 113]. This *phoU* mutant also accumulated high levels of intracellular polyphosphate (polyP) in a Pst dependent manner. PolyP is a long chain polymer of inorganic phosphate that is produced from ATP by polyphosphate kinase as a response to stress. Inorganic phosphate (P_i) can be liberated from polyP via hydrolysis by exopolyphosphatases or endopolyphosphatases. Excess accumulation of polyP in the *phoU* mutant was enhanced more than two-fold by overexpression of polyphosphate kinase (*ppk*) [113]. The aforementioned evidence suggests that PhoU plays an important role in preventing growth restriction caused by Pst mediated P_i and/or polyP hyper-accumulation. Furthermore, a *Streptomyces lividans ppk* mutant overexpresses the PstS protein, indicating another link between the Pst and polyP systems [114].

Defects in polyP production have been linked to decreased stationary phase survival, morphological variation, and sensitivity to oxidative, osmotic, and heat stress [115]. PolyP has also been shown to directly bind the Lon protease of *E. coli* and participate in ribosomal protein degradation, indicating a

role for polyP in amino acid scavenging during nutrient restriction [116].

In yet another link between the Pst/Pho system and polyP accumulation, Ault-riche et al. (1998) have shown that *phoB* mutants and *rpoS* mutants fail to demonstrate nitrogen limitation dependent and osmotic stress dependent polyP accumulation [117]. SigmaS, an alternative sigma factor encoded by *rpoS*, regulates the stationary phase response of *E. coli*. When *pst* genes are mutated leading to constitutive activity of the Pho regulon, Hfq dependent upregulation of *rpoS* translation occurs even during exponential growth [118]. Hfq is an RNA binding protein that is required for the activity of a number of small RNAs (sRNAs). Several sRNAs have been shown to affect *rpoS* expression in an Hfq dependent manner, suggesting a role for sRNAs in *pst* mediated regulation of *rpoS* [119, 120]. Interestingly, sigmaS negatively regulates expression of several members of the Pho regulon including *phoB*, but positively regulates the *pst* operon [121]. These studies suggest a feedback between the Pst/PhoU/PhoB/PhoR system and sigmaS dependent gene regulation.

SigmaS accumulates as cells enter stationary phase and stimulates transcription of a number of genes involved in stationary phase survival and stress responses. Among the more than 70 sigmaS dependent genes identified in *E. coli* are several which are involved in resistance to oxidative stress including genes encoding catalases (*katE* and *katG*), xanthine oxidase (*xthA*), and the ferritin-like DNA binding protein Dps (*dps*) [122, 123]. Consistent with this observation, cells in stationary phase are more resistant to hydrogen peroxide (H_2O_2) than cells in exponential phase [122]. Cells undergoing continuous aerobic respiration during stationary phase produce endogenous reactive oxygen species (ROS) via leakage of electrons from the respiratory chain [124].

Endogenously generated ROS may account for the stationary phase stress necessitating sigmaS mediated antioxidant gene expression.

Moreau et al. (2001) hypothesized that if endogenous production of ROS is a source of stationary phase stress, bacteria enduring P_i limited growth yet maintaining glycolysis would be subject to a significant oxidative stress challenge [125]. In order to test this hypothesis, the group examined the survival of catalase (*katG*) and alkylhydroperoxide reductase (*ahpCF*) mutants under phosphate starvation versus glucose starvation conditions. It was found that *ahpCF* was specifically necessary for protection of aerobic phosphate starved cultures in a manner that was enhanced by the presence of *katG*. *oxyR* and *rpoS* are known to increase antioxidant gene expression in response to glucose starvation [126]. However, while *oxyR* and *rpoS* mutations are severely detrimental to glucose starved cultures, they have little effect on survival of cultures starved for phosphate [125]. Moreau et al. (2001) suggested that basal levels of AhpCF production may be sufficient to mediate defense against oxidative stress during phosphate starvation [125]. However, their results leave open the possibility that there could be another mediator of a phosphate dependent *ahpCF* response in addition to OxyR and sigmaS. The Pst/PhoU-regulated PhoB/PhoR system is an obvious candidate.

Pst gene expression changes have been detected in response to phosphate levels and are potentially linked to oxidative and stationary phase stress response pathways in *E. coli*. While *E. coli* does not upregulate its catalase genes in response to phosphate starvation, Yuan et al. (2005) recently demonstrated that *Sinorhizobium meliloti*, *Pseudomonas aeroginosa*, and *Agrobacterium tumefaciens* all do [127, 128]. *S. meliloti*, which was examined in detail, exhibited PhoB

dependent *katA* regulation that was distinct from the OxyR dependent response to H_2O_2 and was mediated via binding to a distinct promoter. Moreover, the group found that acclimation of wildtype *S. meliloti* to P_i limitation conferred significant protection against subsequent H_2O_2 challenge. In contrast, a phosphate starved *phoB* mutant was hypersensitive to H_2O_2. In fact, *phoB* mutants were even more sensitive to H_2O_2 than *katA* mutants, implying a role for other mediators of ROI defense downstream of *phoB* [128].

The Pst system clearly plays a central role in response to a number of *in vitro* stresses. The Pst system is also upregulated by several pathogens *in vivo*. *pstS* was induced nearly two-fold in a screen for *Streptococcus pneumoniae* genes upregulated during growth in the murine peritoneal cavity [129]. In addition, *pstS* and *phoA* (the gene encoding alkaline phosphatase) were upregulated in *Shigella flexneri* growing intracellularly in a Henle cell monolayer [130]. *In vivo* and *in vitro* regulatory changes reveal a potential role for the Pst system and phosphate responsive two-component systems in complex environmental stress responses and virulence pathways.

Downstream Effects of *pst* Gene Disruption

The effects of *pst* gene disruption in different bacterial species are multitudinous. The pleiotropic phenotypes of *pst* mutants have implicated the Pst system in a number of pathways that are not directly related to phosphate acquisition. The Pst system, like several other nutrient scavenging systems, seems to play a role in environmental sensing; it provides a hub capable of linking environmental phosphate changes to diverse downstream pathways including production of secondary metabolites, biofilm formation, and

expression of stress response factors and virulence factors.

Secondary Metabolites and Morphogenesis

It has long been known that inorganic phosphate is a repressor of secondary metabolite production in various bacteria. It has been suggested that the environmental stress of phosphate limitation has come to serve a signal for the production of secondary metabolites useful under stressful conditions. This phosphate dependent regulation is not metabolite specific and is not limited by biosynthetic group. Among the regulated secondary metabolites are macrolides, tetracyclines, anthracyclines, polyether compounds, aminoglycosides, and amino acid derived metabolites [131]. These molecules can aid in bacterial crosstalk, antagonize competing bacteria, and aid in stress survival. It has been demonstrated that much of the phosphate dependent control of this wide range of secondary metabolites is exerted at the transcriptional level. However, until recently, little was understood about the genetic mediators of this regulation.

Pseudomonas aureofaciens normally forms a zone of fungal inhibition mediated by antibiotic production. However, *P. aureofaciens pst* mutants fail to inhibit fungal growth [132]. In contrast, Slater et al. (2003) described *pstS* and *pstA* mutations in *Serratia* that led to hyperproduction of the antibiotics prodogiosin and carbapenem. These mutations mimicked the effects of phosphate starvation and exerted their effect in part through an overlap with the quorum sensing SmaI pathway [133]. As described previously, *pst* mutations often lead to constitutive activation of genes normally repressed under high phosphate conditions. The observation that *pst* mutations in *Serratia* lead to constitutive production of antibiotics normally only produced during phosphate

limitation is consistent with this pattern. Similarly, mutants in the *Streptomyces lividans* phosphate responsive two-component system, PhoP/PhoR, overexpressed the antibiotics actinorhodin and undecylprodigiosin [134]. Suprisingly, however, these mutants failed to express *phoA* demonstrating that in *S. lividans*, PhoP exerts positive regulation of *phoA* and negative regulation of secondary metabolites.

In addition to their role in antibiotic production, *pst* genes can affect morphogenesis. *Streptomyces coelicolor* and *S. lividans pstS* mutants demonstrate accelerated differentiation and sporulation on solid media [114]. They also ultimately produce more spores than wildtype bacteria. *P. aureofaciens* normally forms biofilms under phosphate replete conditions, but not in phosphate limited environments. *P. aureofaciens pstA* and *pstC* mutants fail to repress the Pho regulon and fail to form biofilms under high phosphate conditions. In contrast, the *phoR* mutants form biofilms even during phosphate starvation [132]. *Caulobacter crescentus* normally undergoes stalk elongation under low phosphate conditions. *C. crescentus pstB* mutants undergo stalk elongation regardless of phosphate concentration, whereas *phoB* mutants fail to elongate even during phosphate starvation [135].

Secondary metabolite production, sporulation, biofilm formation, and other morphogenic changes are tightly regulated by environmental bacteria. This regulation is necessary to reduce waste during growth under benign conditions and to cope efficiently in stressful environments. It seems that many bacteria have come to utilize the phosphate responsive Pst and Pho systems as environmental sensors that can turn on or turn off such systems as needed. Thus, disruption of *pst* and *pho* genes can lead to a range of pronounced

secondary phenotypes unrelated to phosphate acquisition *per se*. The central role of the phosphate sensing system seems to be shared by numerous bacteria, yet one must take care in extrapolating specific downstream pathways as they seem to have diverged in accordance with species-specific needs.

Stress Responses

The bacterium *Lactococcus lactis* is commonly utilized in the dairy industry. *L. lactis recA* mutants are hypersensitive to DNA damage, thermal stress, and H_2O_2, indicating that this gene mediates multiple stress responses [136]. In an effort to characterize interrelated genes, Duwat et al. (1999) positively selected from a pool of approximately 10 million insertion mutants for those that acquired thermal resistance in a *recA* mutant background [137]. Among the 18 insertions examined, seven different genes were disrupted; one was *pstS* and another was *pstB*. The primary source of phosphate in the M17 medium used in these experiments was sodium glycerophosphate; it is unclear how much free inorganic phosphate was available in the medium. However, it is worth noting that the thermoresistant phenotype of the *pstS* mutant was shown to be overcome by addition of 100 mM inorganic phosphate to the medium [137]. This observation indicates that the phenotype may have been reversed by phosphate acquisition through the Pit transporter, but does not rule out a Pst/Pho mediated regulatory defect. Emphasizing a role in multi-stress sensitivity, the *L. lactis recA*/*pstS* mutant was also shown to be resistant to carbon starvation and H_2O_2 [137].

A separate screen for acid resistant insertional mutants of wildtype *L. lactis* also recovered *pstS* and *pstB* mutants [138]. In this study, a modified M17

medium was used that lacked sodium glycerophosphate and was most likely phosphate limiting. Consistent with the previous study, the acid resistance could be overcome by administration of high levels of inorganic phosphate. Interestingly, in the wildtype background the *pstS* and *pstB* mutants were also resistant to oxidative stress, but not to heat [138]. The reason for this discrepancy between the two strain backgrounds is currently unclear. In contrast to the *L. lactis* mutants described above, an *E. coli* 078 *pst* mutant was shown to be hypersensitive to acid stress [139]. Despite these strain- and species-specific differences, it is notable that all of the aforementioned *pst* and *pho* mutants have pronounced, if disparate, stress response dysregulation.

Virulence

Lamarche et al. (2005) constructed a deletion mutant of the avian pathogen *E. coli O78:K80* (APEC) lacking the *pstCAB* segment of the *pst* operon [139]. In addition to its sensitivity to acid, this mutant was sensitive to killing by rabbit serum. Although it was not killed by chicken serum, the *pstCAB* mutant formed fewer extraintestinal lesions and achieved lower bacterial loads during chicken infection [139]. This virulence defect is similar to the attenuation observed in the pig septicemia model after infection with a *pstC* mutant of *E. coli* O115:K"V165":F165 [140]. Furthermore, *pstC* and *pstS* transposon mutants of the urinary tract pathogen *Proteus mirabilis* were attenuated in the murine model of ascending urinary tract infection (Jacobson 2004 ASM abstract).

Edwarsiella tarda is a freshwater and marine fish pathogen that is killed by fish serum and phagocytes. Srinivasa Rao et al. (2001) have demonstrated that cultured fish phagocytes achieve reduced superoxide levels when infected by

virulent *E. tarda* strains as compared to avirulent strains [141]. As reactive oxygen species (ROS) are known to be key phagocytic killing mechanisms, the group conducted a screen of 200 transposon mutants to identify genes in virulent *E. tarda* that might be involved in countering ROS production by fish phagocytes. Five of the mutants were permissive for ROS production as compared to WT and one of these mutants had a transposon insertion in the *E. tarda pstS* gene. This *pstS* mutant was also attenuated for growth within phagocytes and was hypersensitive to low pH [141]. In a subsequent screen of 490 *E. tarda* transposon mutants for genes required for disseminated infection in fish, 15 attenuated mutants were identified [142]. Three of these mutants were highly attenuated with a 50 % lethal dose (LD_{50}) over 3 logs higher than the parent strain: *pstC*, *pstB*, and *pstS*. These mutants grew normally in phosphate replete medium (tryptic soy broth), but grew poorly compared to wildtype in phosphate limited medium. It is interesting to note that unlike the previous paper, these *pst* mutants were described as low pH resistant [141, 142].

Srinivasa Rao et al. (2003) claimed that phosphate levels are reduced intracellularly in phagocytes and epithelial cells and postulated that the *pst* genes are required for environmental sensing and regulation of virulence genes [142]. However, it is unclear upon what data the group based its assertion of low intracellular phosphate. To our knowledge, a comparison of intracellular and intraphagosomal phosphate concentrations to concentrations required for *pst* gene regulation (as established *in vitro*) has yet to be published. It has been shown, however, that 24 hours post uptake, intraphagosomal Mtb has similar phosphate levels to extracellular bacteria (the absolute concentrations were not measured) [143]. Moreover, Mtb does not upregulate *pst* genes during

macrophage infection, suggesting that the low affinity Pit system is sufficient to achieve these normal intraphagosomal phosphate levels [144]. This would be unlikely to be the case under conditions of phosphate starvation. Furthermore, the lack of Mtb *pst* gene upregulation in the phagosome supports the hypothesis that phosphate is not limiting.

Corynebacterium glutamicum encodes a two-component system that shares 59% similarity (42% identity) with PhoR (Rv0758) and 81% similarity (66% identity) with PhoP (Rv0757) of Mtb. *Rhodococcus equi*, an equine pathogen, encodes a two component system, PhoPR, that is highly homologous to those encoded by Mtb and *C. glutamicum*. These *phoPR* genes have been named based on homology to the *Bacillus subtilis* phosphate responsive two-component system PhoPR and should not be confused with the Salmonella Mg^{++} responsive system PhoPQ. The actual functions of PhoP and PhoR in *R. equi* and Mtb have yet to be determined. However, Kocan et al. (2006) recently demonstrated that the *C. glutamicum phoPR* homologues control the phosphate starvation response, suggesting that the *R. equi* and Mtb PhoPR proteins may play a similar role [145]. It is therefore worth noting that an *R. equi phoPR* mutant overexpresses the genes of its virulence plasmid and is hypervirulent [146]. In contrast, an Mtb *phoP* mutant produces an altered manLAM profile and fails to replicate in the mouse model of infection [146, 147]. However, it should again be emphasized that even in closely related organisms, downstream pathways of homologous proteins can differ greatly. A recent paper describing transcriptional regulation in an Mtb *phoP* mutant revealed no obvious link between *phoP* and phosphate transport or regulation [148].

Chapter 3:

Pthiocerol Dimycocerosates (PDIMs)

Introduction to Phthiocerol Dimycocerosates (PDIMs)

Pathogenic mycobacteria are unique in their array of outer wall free lipids. The most abundant of these lipids, the phthiocerol dimycocerosates (PDIMs), are also among the best characterized. PDIMs contain long chain diols esterified by methyl-branched fatty acid chains [149]. The closely related phenolic glycolipids (PGLs) consist of a similar lipid core that is terminated by a glycosylated aromatic nucleus [150].

M. gastri and the pathogenic mycobacteria (*M. bovis, M. haemophilum, M. kansasii, M. leprae, M. marinum, M. tuberculosis, M. ulcerans*) all produce pthiocerols and PDIMs. Recent work has elucidated most of the genetic and biochemical steps involved in PDIM synthesis as summarized in Figure 3.1. Briefly, *pks15-1*, a fusion of two of 24 annotated *pks* genes in Mtb, is responsible for synthesis of a *p*-hydroxy-phenyl alkanoic acid phenolpthioceol precursor from *p*-hydroxy benzoic acid (*p*HBA). PpsA-E, members of a type 1 polyketide synthase (*pks*) system, are responsible for synthesis of a pthiocerol or phenolphthiocerol core from C22-C24 fatty acyl (phthiocerols) or 17-(*p*-hydroxy-phenyl)-heptadecanoyl derivative (phenolphthiocerols). The enzyme-bound phthiocerol and phenopthiocerol precursors are decarboxylatively released, reduced by the product of Rv1951c, methylated by the Rv2952 gene product, and acylated by PapA5 [151].

As early as 1974 it was known that a PDIM-free strain of H37Rv was attenuated in the guinea pig model of infection [152]. Shortly thereafter it was shown that *in vivo* survival of an avirulent Mtb strain was enhanced by coating the bacteria with cholesterol oleate and purified PDIM [153]. However, it wasn't until the first use of STM in Mtb, a quarter century later, that the genetics of

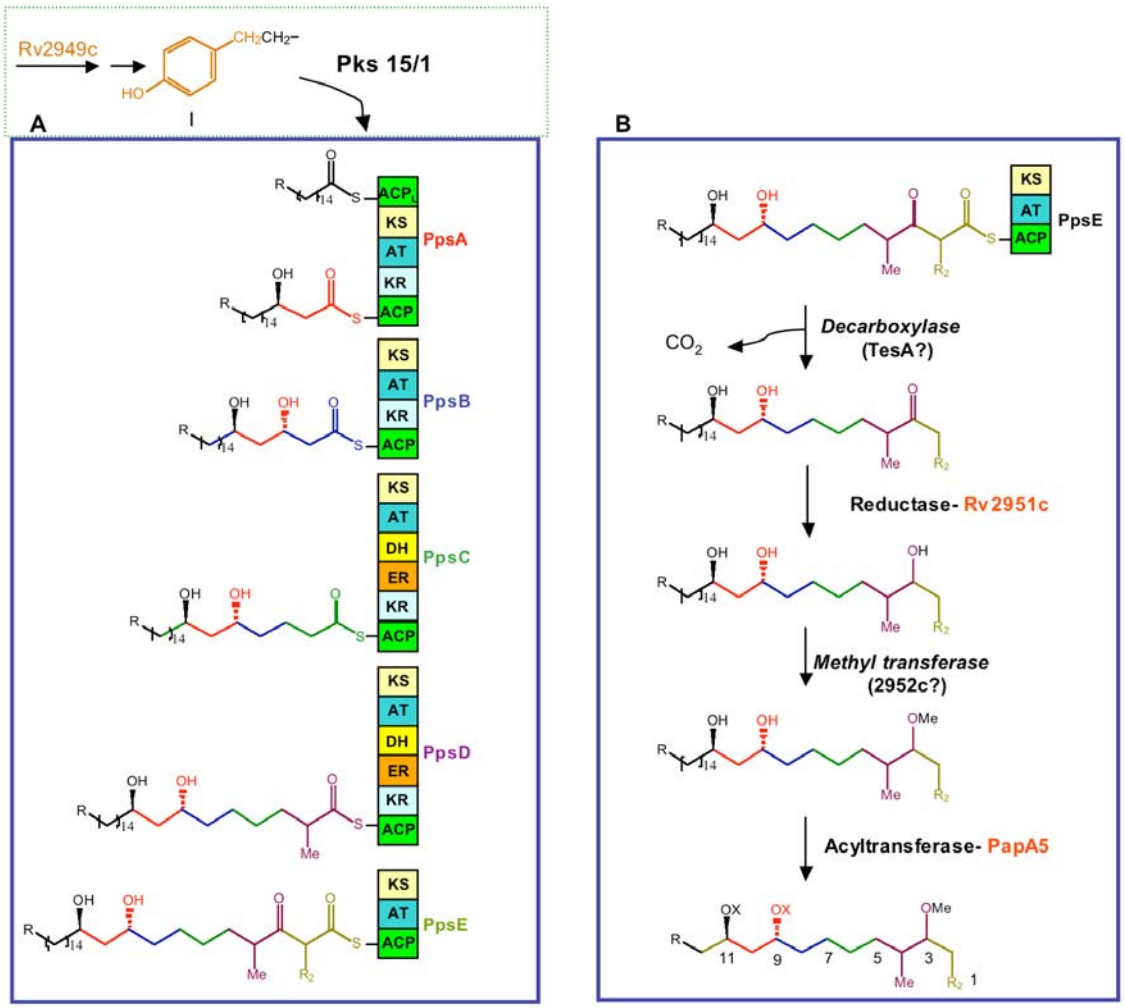

Figure 3.1: Biochemical and Genetic Schematic of the PDIM Biosynthetic Pathway. [151] (A) Addition of phenol and transformations by the polyketide synthase Pps family. (B) Post-Pps modifications generating PDIM.

PDIM synthesis were linked directly to virulence (Figure 3.2). In an STM screen of 1,927 H37Rv mutants, Camacho et al (1999) identified attenuated strains with insertions within *mmpL7*, *drrC*, and within and upstream of *fadD26* [96]. *fadD26*, encoding an acyl-CoA synthase, is upstream of and shares an operon with the PDIM *pps* biosynthesis gene cluster and Camacho et al. (2001) later demonstrated that *fadD26* mutants fail to synthesize PDIM [154]. They were also able to show that while the *mmpL7* and *drrC* mutants produce large amounts of PDIM, they accumulate it intracellularly, implicating these genes in transmembrane PDIM transport. Similarly, Cox et al. (1999) identified transposon insertion mutants in *mmpL7* and in the promoter region of *fadD26* in an STM screen of 576 mutants in the Erdman laboratory strain [26]. In addition, their screen identified an attenuated mutant with a transposon insertion in *fadD28*, encoding acyl-CoA synthase, which is also found in the PDIM synthesis locus [26]. Neither the promoter mutant nor the *fadD28* mutant strain synthesized PDIM, while the *mmpL7* mutant accumulated it due to a transport defect [26]. Interestingly, in the first report of a direct interaction between a synthase and the transporter of its product, PpsE has been shown to interact biochemically with MmpL7; these observations suggest that synthesis and transport of PDIM are coupled [155]. Recently the lipoprotein LppX, also encoded in the PDIM synthesis locus, was shown to be required for transport of PDIM [156].

Mutants lacking exported PDIM have altered colony morphology [26], and have enhanced membrane permeability as demonstrated by enhanced sodium dodecyl sulfate (SDS) sensitivity and chenodeoxycholate uptake [154]. In contrast, sensitivity to reactive nitrogen species (RNS) and drug minimal inhibitory concentrations (MICs) were unaffected in these mutants, suggesting

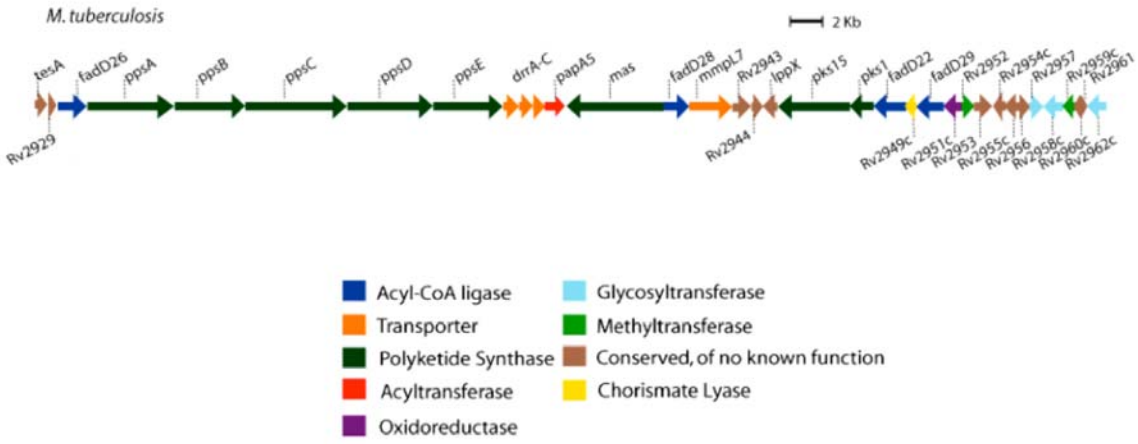

Figure 3.2: PDIM Synthesis Genetic Locus. [151]

that these stresses are relatively independent of PDIM mediated cell wall permeability. This interpretation is consistent with the observation that Mtb Ag85 mutants, which have increased cell wall permeability due to mycolic acid changes, maintain wildtype MIC levels [157]. It should be noted, however, that attenuation of a PDIM mutant in murine bone-marrow-derived macrophages was abolished by treatment with the NOS2 inhibitor L-NAME. This observation suggests that PDIM deficient strains might be hypersensitive to RNIs generated *in vivo* [158].

Mycobacterium leprae produces a phenolic glycolipid (PGL-1) that mediates bacterial binding to Schwann cells and macrophages [159]. Phagocytosis of *M. leprae* is promoted by binding of PGL-1 to laminin-2 of Schwann cells [159] and complement component 3 of macrophages [160]. Moreover, PGL-1 is associated with enhanced survival of *M. leprae* within macrophages [160]. However, while all Mtb strains produce PDIM and *p*HBA derivatives (*p*HBADs), very few produce PGL-tb [27, 161]. It has recently been demonstrated that a 7 bp deletion in *pks15-1*, resulting in a frameshift, is responsible for the lack of PGL-tb

production by H37Rv and most clinical strains of Mtb [162]. Nonetheless, Reed et al. (2004) recently demonstrated that the hyperlethality of clinical strain HN878 was attributable to its expression of an intact *pks15-1* and production of PGL-tb [27]. Furthermore, the virulence of H37Rv was enhanced by complemention with a plasmid encoding the intact *pks15-1* gene. Most intriguingly, the PGL producing strains repressed macrophage pro-inflammatory cytokine production in a way that was mimicked in a dose dependent manner by administration of purified PGL-tb. Notably, however, PDIM had no effect on cytokine production [27].

The potential importance of glycosylation to the bioactivities of PGLs was revealed by the discovery that the binding of *M. leprae* to Schwann cells is mediated by the saccharidyl moiety of PGL-1 [159]. It is also noteworthy that the PGL of BCG contains two fewer sugars than H37Rv and has differential effects on macrophage TNF-α and IL-6 production [27]. Based on bioinformatic analysis of genes in the Mtb complex, Onwueme et al. (2005) hypothesized that the glycosyltransferases encoded in the PDIM/PGL locus were involved in glycosylation of *p*HBADs and PGL-tb as depicted in Figure 3.3, suggesting that our Rv2958c mutant might be defective in the second glycosylation step [151].

In a paper published concurrently with our dSTM screen, Perez et al. (2004) demonstrated by analysis of targeted gene disruptions that the aforementioned hypothesis was essentially correct [161]. Wildtype H37Rv accumulates the tri-glycosylated *p*HBAD (*p*HBAD II) depicted in Figure 3.4. As expected the Rv2958c mutant accumulated a singly glycosylated *p*HBAD (*p*HBAD I), and the Rv2962c mutant failed to produce *p*HBAD entirely. Surprisingly, however, the Rv2957 mutant accumulated *p*HBAD I, but did not

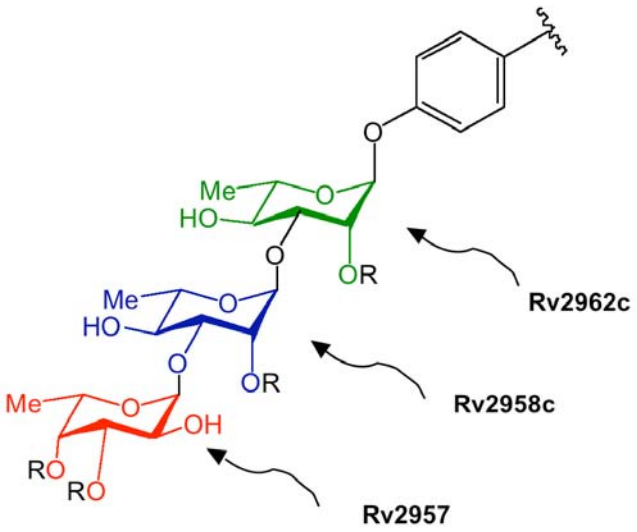

Figure 3.3: Biochemistry and Genetics of *p*HBAD and PGL_{tb} Glycosylation. [163]

produce a diglycosylated product (Figure 3.4). Rv2957 and Rv2958c may therefore function co-dependently in Mtb to add the final two sugars [161]. However, when BCG, which lacks a functional Rv2958c, was complemented with Rv2958c under the constitutively expressed *hsp60* promoter, a diglycosylated product (product E) was detected even in the absence of Rv2957 (Figure 3.4). This result demonstrates that Rv2958c is capable of independently adding the second sugar, suggesting that this intermediate is eliminated from H37Rv Rv2957 mutants, perhaps due to toxicity. As expected, when the H37Rv mutants were complemented with *pks15-1*, the bacteria accumulated PGL-tb with the same glycosylation patterns as the *p*HBAD molecules found in the strains lacking PGL [161].

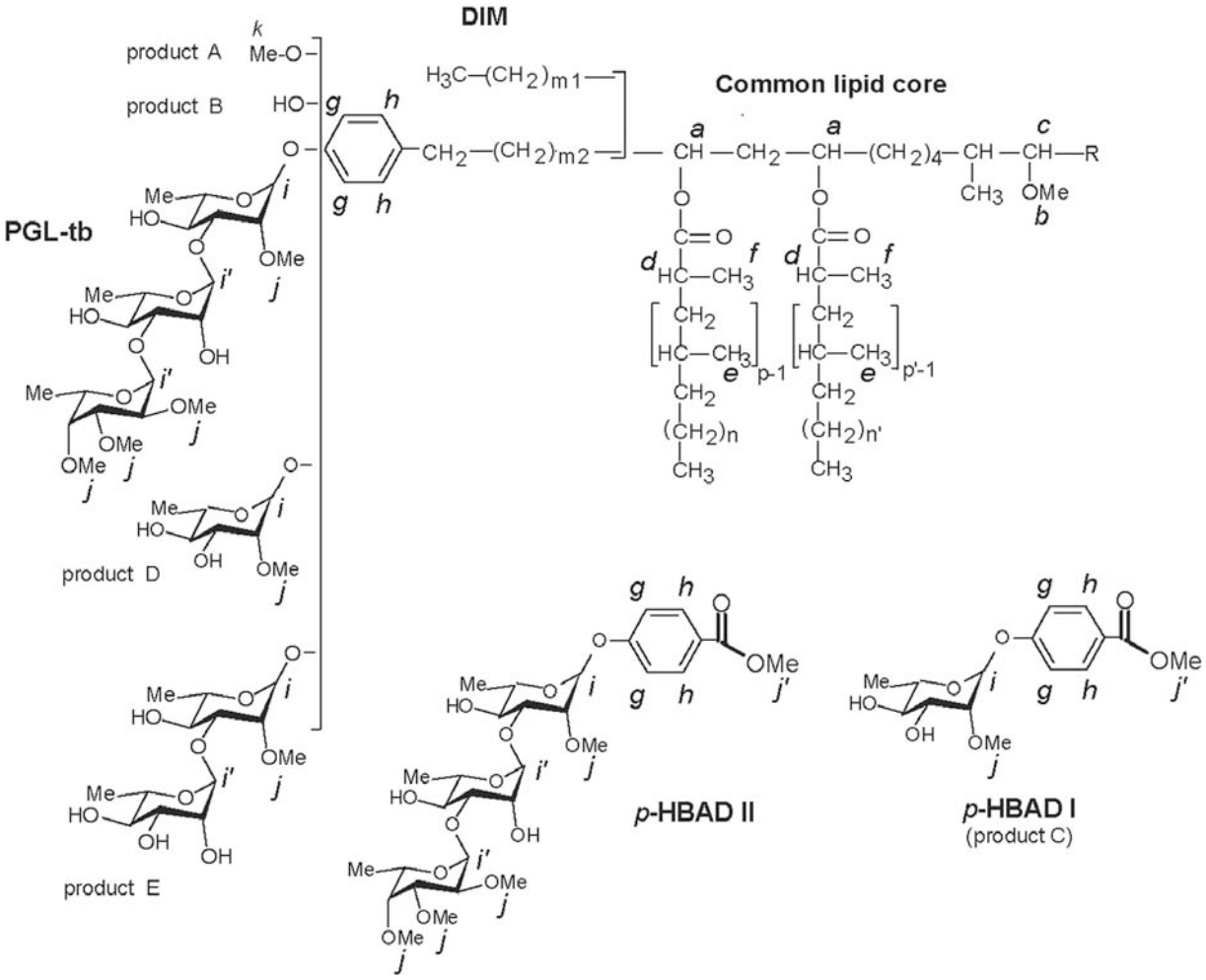

Figure 3.4: Biochemistry of *p*HBAD I, *p*HBAD II, and PGL$_{tb}$ [161]

PDIM Results and Discussion

A role for PGL-tb in virulence has been well established. However, it was thought that the *p*HBAD molecules were physiologically unimportant precursors, present in all strains of Mtb, that hyperaccumulated in the absence of *pks15-1*. It was surprising, therefore, that we found an Rv2958c mutant to be significantly attenuated in our dSTM screen and by intravenous monotypic retest (Figure 1.6) [76].

We proceeded to examine the detailed replication kinetics of the Rv2958c

mutant in wildtype and immunodeficient mice by monotypic aerosol infection. Consistent with the relative NOS2 independence of the attenuation that we sought in the dSTM screen, the Rv2958c mutant was profoundly attenuated in $NOS2^{-/-}$ mice, but replicated fairly well in IFN-$\gamma^{-/-}$ mice (Figure 3.5). The growth kinetics of the bacteria were reflected in the divergent survival curves of the two immunodeficient strains of mice (Figure 3.6). Consistent with our findings during IV versus aerosol monotypic infections with Rv2958c, an Erd2958c mutant was identified in our lab during an STM screen for Erdman mutants that were attenuated in wildtype mice by aerosol infection but not by IV infection. However, the phenotype of this Erdman mutant could not be reproduced in a monotypic infection experiment (N. Dhar, personal communication).

We sought to elucidate the role of glycosylation and methylation of the *p*HBADs in virulence of H37Rv by examining the knockout strains Guilhot and colleagues had used to characterize the biochemical role of the *p*HBAD glycosyltransferase and methyltransferase genes [161]. To our surprise, we found that none of the *p*HBAD mutants described in their paper demonstrated a significant virulence phenotype, including their Rv2958c mutant (Figure 3.7).

There has been some speculation in the scientific literature that a number of Mtb transposon mutants have secondary PDIM mutations that could be responsible for cryptic virulence phenotypes that are not due to the transposon insertions *per se*. Therefore, we had our Rv2958c and Erd2958c mutant strains examined for PDIM and *p*HBAD production. Consistent with the phenotype reported by Perez et al. (2004), our Rv2958c mutant failed to produce *p*HBAD II [161] (C. Guilhot, personal communication). Surprisingly, however, our mutant also failed to produce PDIM.

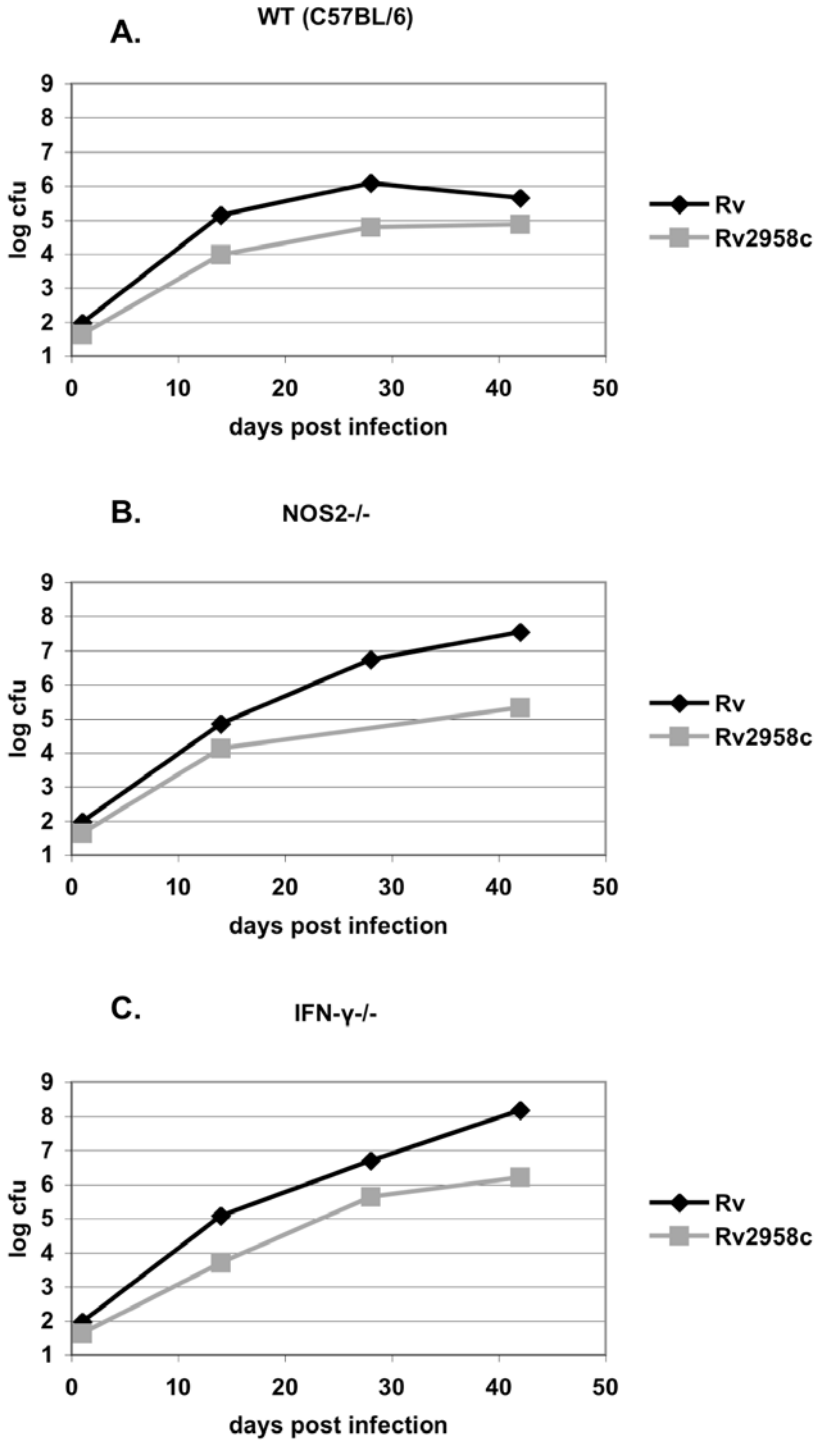

Figure 3.5: Aerosol Infection of Mice with McKinney Lab H37Rv and Rv2958c mutant. (A) WT (C57BL/6), (B) NOS2$^{-/-}$, and (C) IFN-γ$^{-/-}$ mice were aerosol-infected with H37Rv (black squares) or the Rv2958c mutant (grey squares).

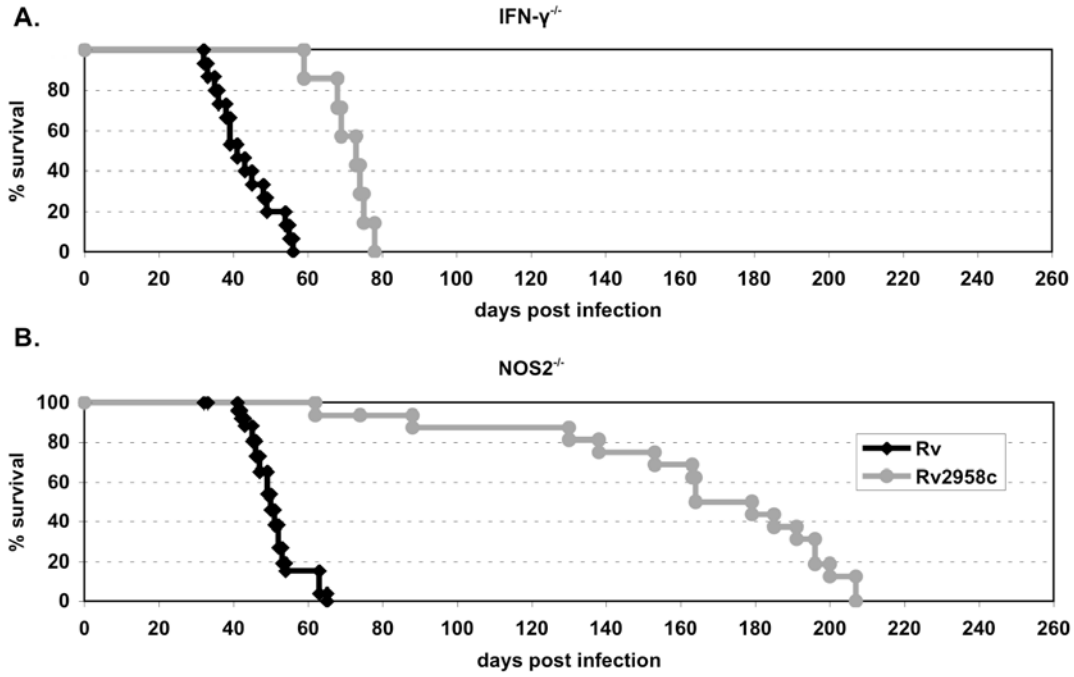

Figure 3.6: Survival of Mice after Aerosol Infection with McKinney Lab H37Rv and Rv2958c mutant. (A) IFN-$\gamma^{-/-}$ and (B) NOS2$^{-/-}$ mice infected with H37Rv (black diamonds) and the Rv2958c mutant (grey circles).

We are uncertain about the etiology of the loss of PDIM synthesis in our Rv2958c mutant. However, we observed that Guilhot's H37Rv strain (CGRv) was slightly more virulent in NOS2$^{-/-}$ mice than our H37Rv strain, suggesting possible PDIM deficiency in our parent strain (Figure 3.9). TLCs conducted on lipid extracts of our bacterial strains revealed that while our parent strain produced PDIM, all four of the mutants recovered from our dSTM screen were PDIM deficient. Moreover, a stock of H37Rv that had become attenuated after being subcultured from the parent stock no longer produced PDIM (Figure 3.8).

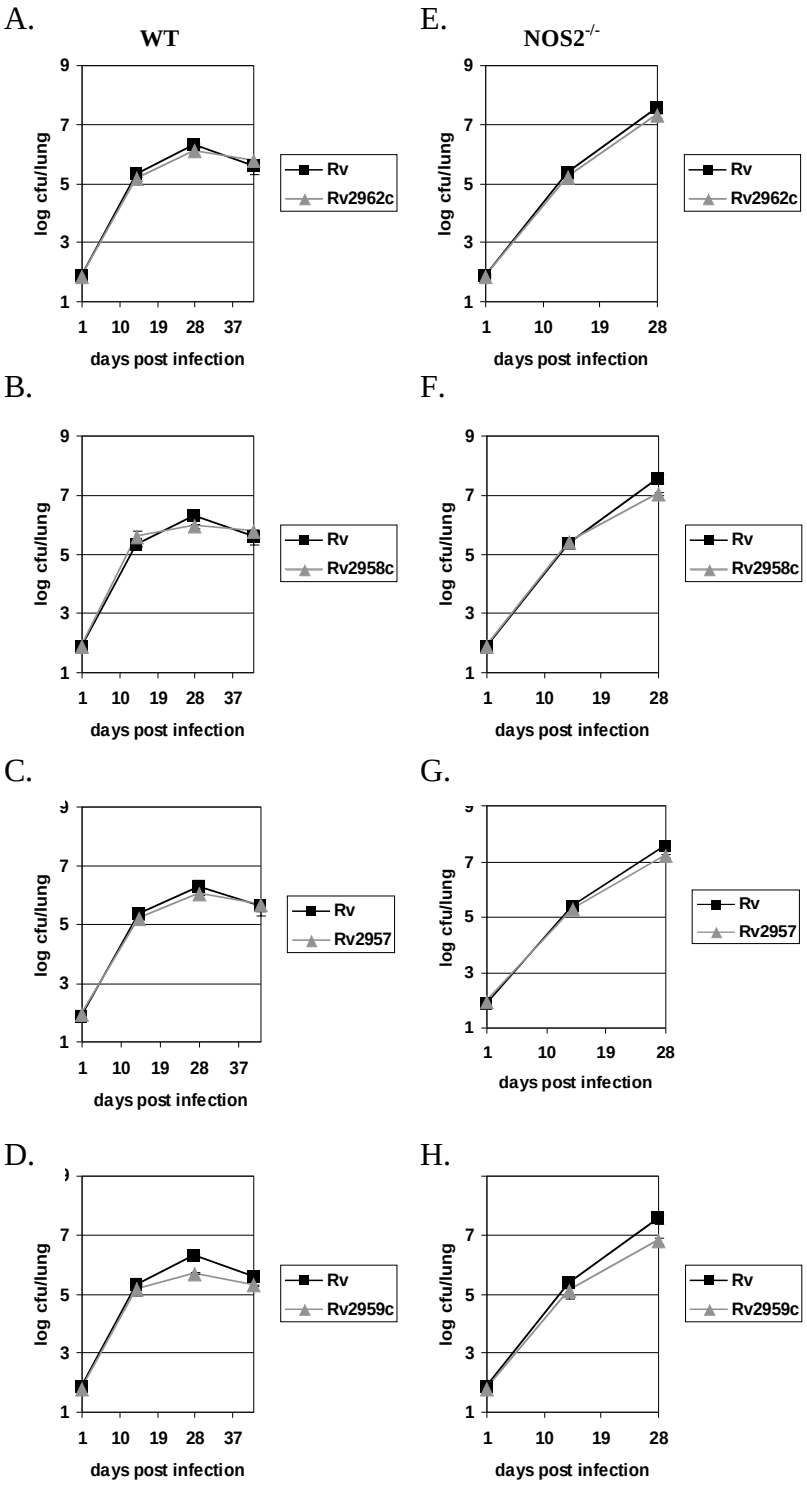

Figure 3.7: Aerosol Infection of Mice with Guilhot Lab H37Rv and Rv2957, Rv2958c, Rv2959c, and Rv2962 Mutants. (A-D) WT (C57BL/6) and (E-H) NOS2$^{-/-}$ mice were aerosol-infected with H37Rv (black squares) or the Rv2957, Rv2958c, Rv2959c, and Rv2962 mutants (grey triangles), as indicated.

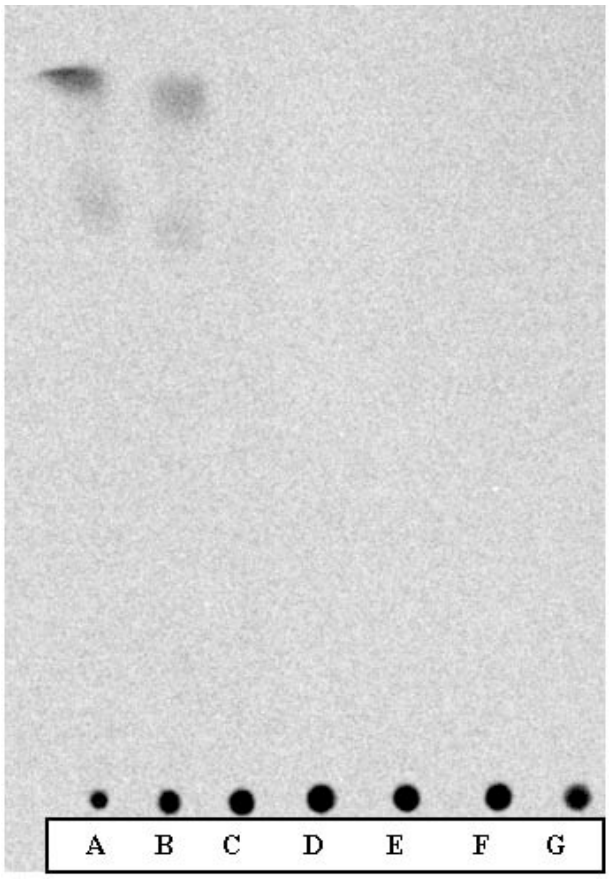

Figure 3.8: PDIM Synthesis in Mutant Strains Derived from H37Rv. Thin-layer chromatogram (TLC) of ^{14}C-propionate labeled lipids extracted from (A) Guilhot lab H37Rv, (B) McKinney lab H37Rv parent stock, (C) subcultured McKinney lab H37Rv, (D) Rv2958c mutant, (E) Rv0072 mutant, (F) Rv0405 (*pks6*) mutant, and (G) Rv0930 (*pstA1*) mutant.

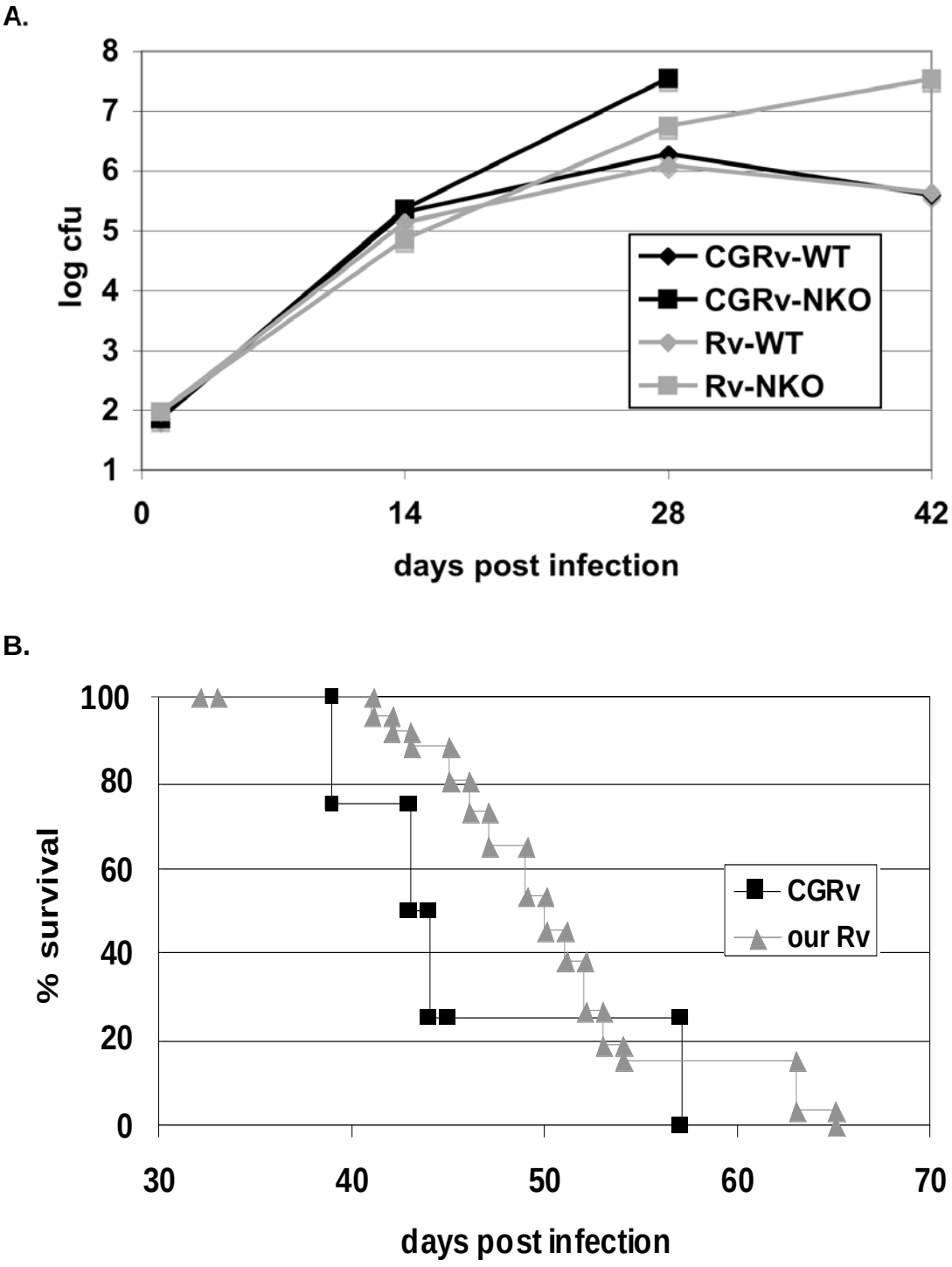

Figure 3.9: Aerosol Infection of Mice with Guilhot Lab H37Rv versus McKinney Lab H37Rv. (A) Bacterial cfu in the lungs and (B) mouse survival after aerosol infection of WT (C57BL/6) mice (diamonds) and NOS2$^{-/-}$ mice (squares) with Guilhot lab H37Rv (black) and McKinney lab H37Rv (grey).

Upon examination of subcultures cloned from the parent strain, it was found that approximately 50% of the bacteria in the original parent stock were PDIM deficient (PDIM-). This heterogeneity could explain the virulence difference observed between our H37Rv stock and the PDIM proficient (PDIM+) H37Rv of Guilhot and colleagues (Figure 3.9).

Direct comparisons of PDIM+ and PDIM- H37Rv replication and survival kinetics were conducted in mice. The PDIM deficient strain exhibited substantial early attenuation consistent with published work on PDIM mutants in wildtype mice [26, 158]. Consistent with the phenotype for which we had screened, PDIM- bacteria are well controlled by $NOS2^{-/-}$ mice, but are able to replicate rapidly in and kill IFN-$\gamma^{-/-}$ mice. Notably, PDIM deficiency also accounts for the unexpected IFN-γ independent early attenuation of the mutants (Figure 3.10).

Consistent with the results from the Guilhot lab's Rv2958c mutant, comparison of our Rv2958c mutant with its PDIM deficient parent strain revealed no significant attenuation of the mutant (Figure 3.11). Strikingly, none of the other mutants isolated from the dSTM screen appear to be significantly attenuated compared to the PDIM- parent (Figure 3.12).

Comparison of PDIM+ and PDIM- H37Rv *in vitro* revealed that PDIM- bacteria have a substantial *in vitro* growth advantage (Figure 3.13). This growth advantage is most distinct when cultures are started from a frozen stock and may reflect differential recovery from freezing. This *in vitro* advantage is sufficient to explain how a serially passaged culture can be overtaken by spontaneously arising mutants with defects in the 50kb genomic region required for PDIM synthesis.

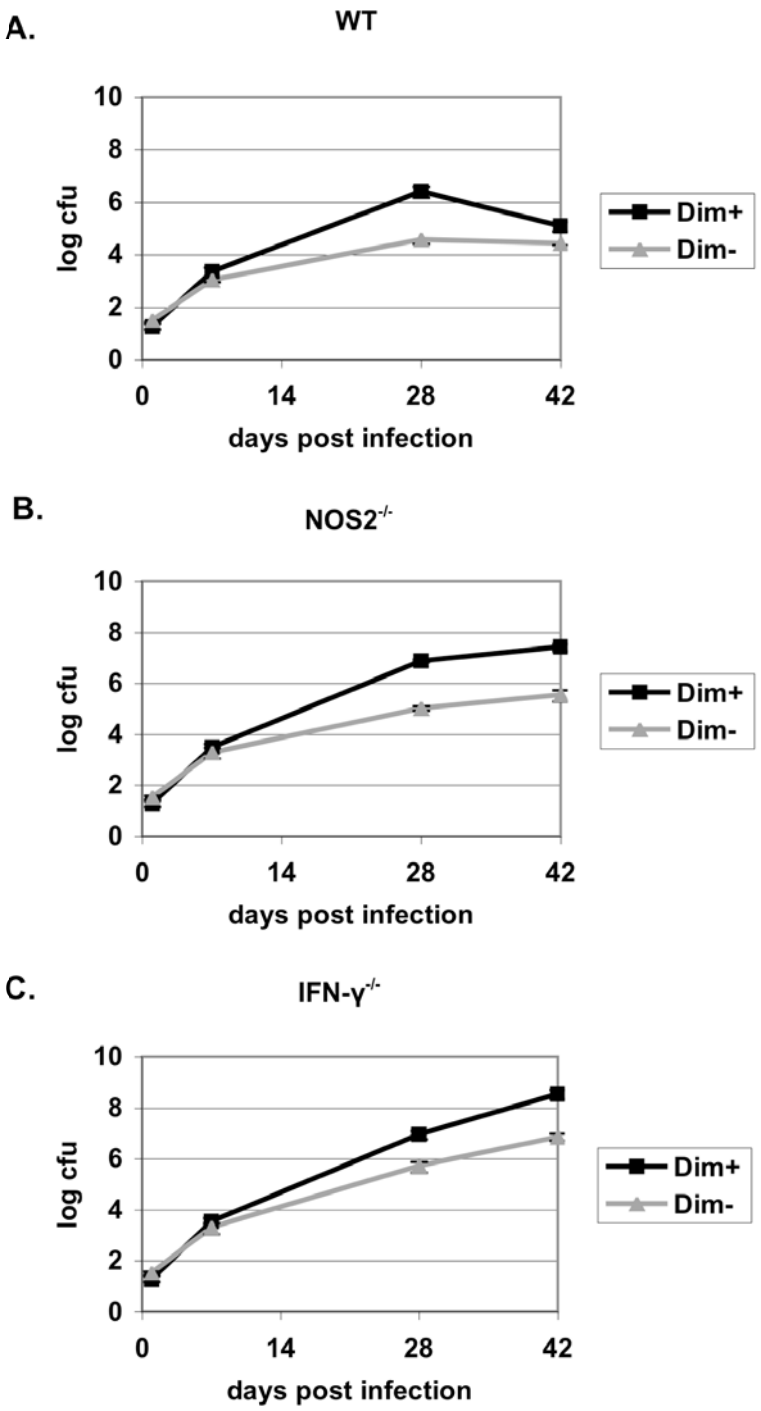

Figure 3.10: Aerosol Infection of Mice with McKinney Lab PDIM+ versus PDIM- H37Rv. (A) WT (C57BL/6), (B) NOS2$^{-/-}$, and (C) IFN-γ$^{-/-}$ mice were aerosol-infected with PDIM+ (black squares) and PDIM- (grey triangles) H37Rv.

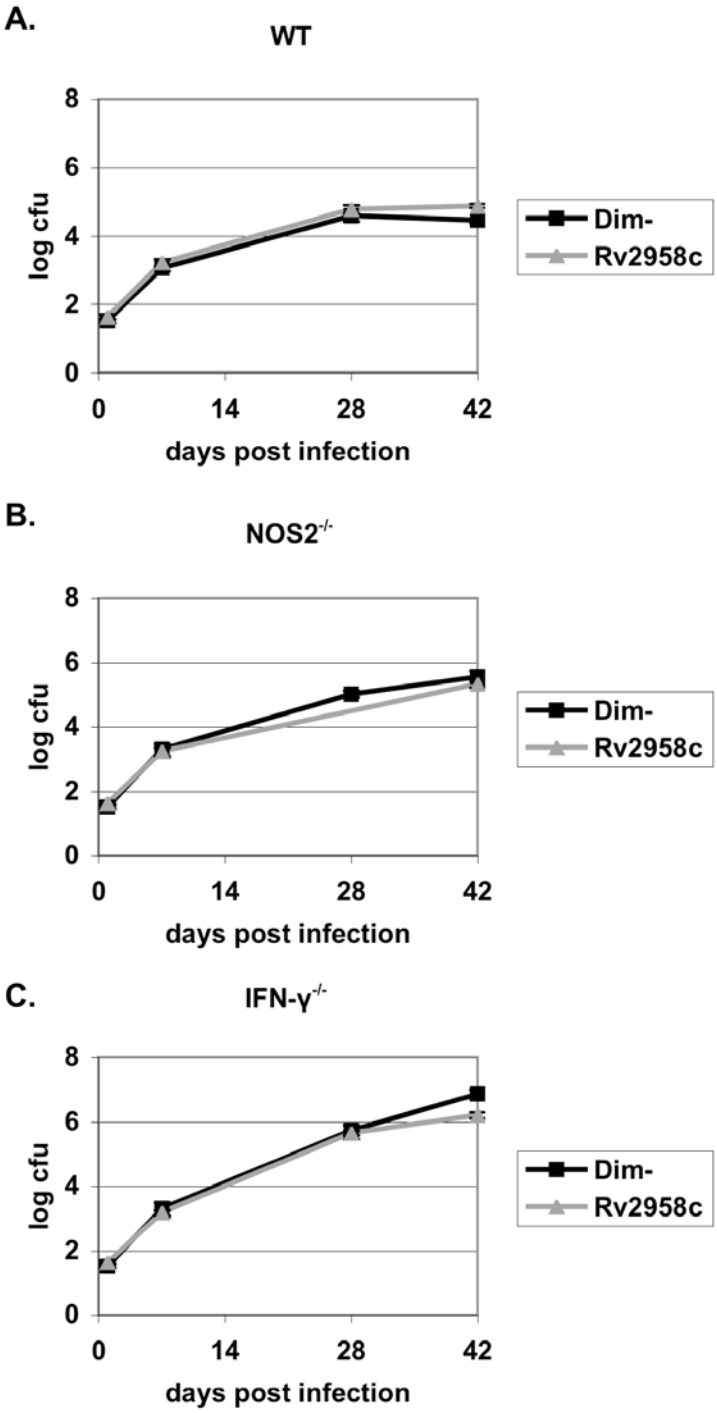

Figure 3.11: Aerosol Infection of Mice with McKinney Lab PDIM- H37Rv versus Rv2958c Mutant. (A) WT (C57BL/6), (B) NOS2$^{-/-}$, and (C) IFN-γ$^{-/-}$ mice were aerosol-infected with PDIM- H37Rv (black squares) and Rv2958c mutant (grey triangles).

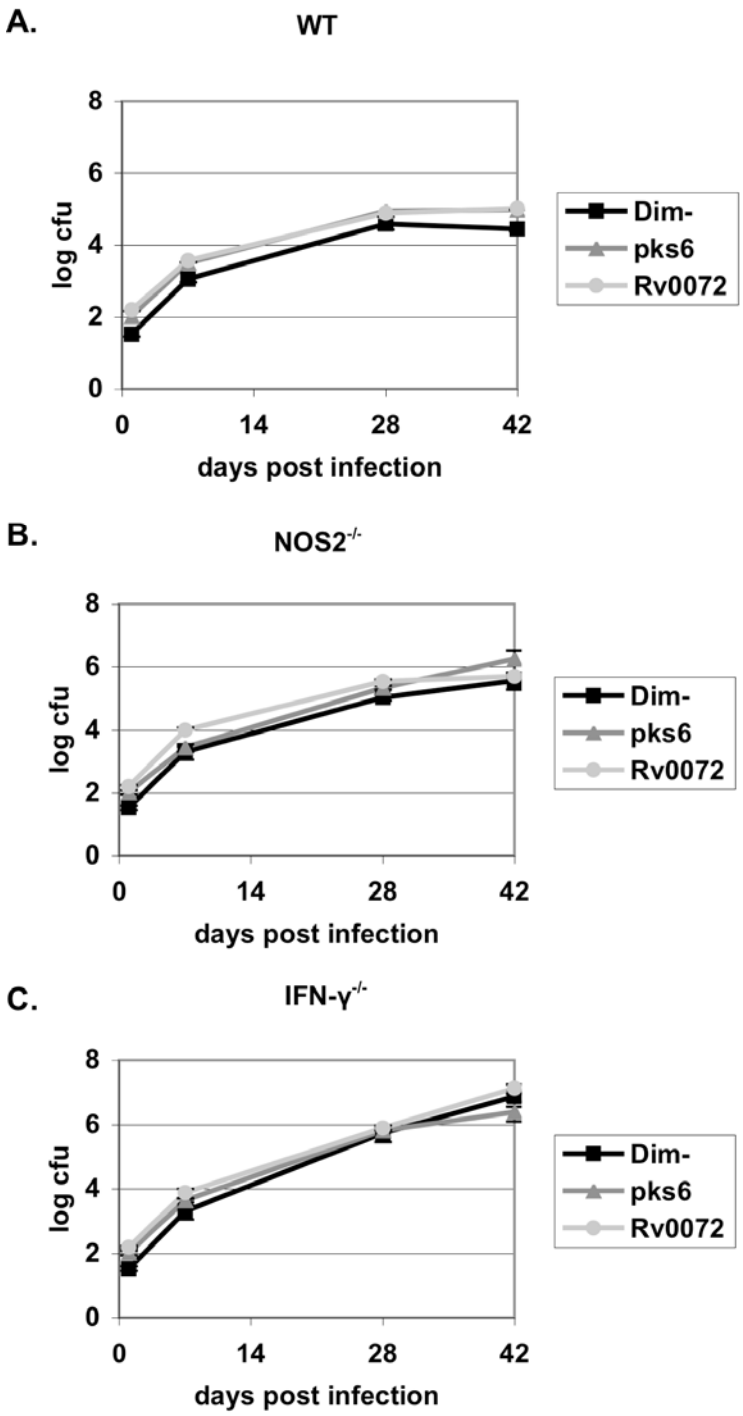

Figure 3.12: Aerosol Infection of Mice with McKinney Lab PDIM- H37Rv, Rv0405/*pks6* Mutant, and Rv0072 Mutant. (A) WT (C57BL/6), (B) NOS2$^{-/-}$, and (C) IFN-γ$^{-/-}$ mice were aerosol-infected with PDIM- H37Rv (black squares), Rv0405/*pks6* mutant (dark grey triangles), and Rv0072 mutant (light grey circles).

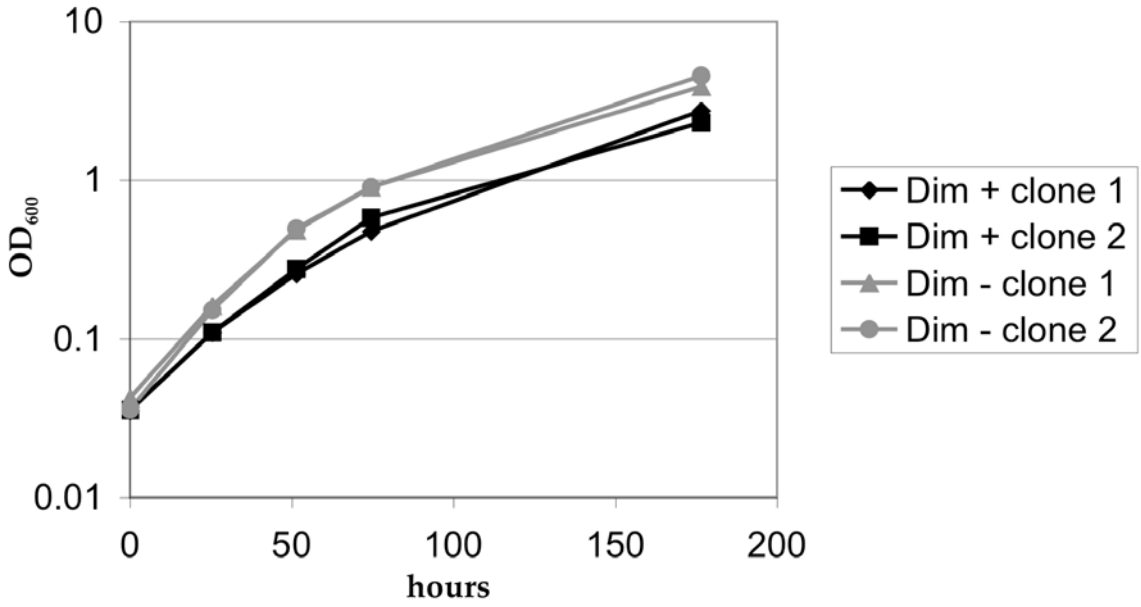

Figure 3.13: Differential *in vitro* Growth of McKinney Lab PDIM+ and PDIM- H37Rv. PDIM+ (black lines) and PDIM- (grey lines) H37Rv subclones were cultured in 7H9 broth and growth was monitored by measuring OD_{600} of the cultures.

Spontaneously arising PDIM deficient strains have been previously described in the literature and are probably far more common than reported or realized [27, 152]. It is likely that many uncomplemented attenuated mutants described in the scientific literature are defective due to cryptic spontaneous loss of PDIM production. Similarly, a number of mutants known to have lost PDIM production have had this loss attributed to loci with no confirmed role in PDIM synthesis; many of these mutants have not been complemented and may have lost PDIM due to occult spontaneous mutations (Table 1).

It has been suggested that loss of PDIM may result from locus instability during genetic manipulation [27]. However, the substantial presence of PDIM deficient bacteria in our otherwise PDIM+ parent strain suggests that we are

selecting for PDIM deficiency in our mutant screens (and during passaging) as opposed to generating PDIM deficiency when creating mutants.

Table 1: Genes with Unproven Roles in PDIM Synthesis.
Adapted from [151]

Gene	Parent Strain	Complementation
pks7	H37Rv	No
pks12	H37Rv	No
pks10	H37Rv	No
pks11	H37Rv	No
fadD28	M. bovis BCG	No
	Mtb103	Partial (15%)
	Erdman	No
fadD26	Mtb203	Partial (5%)
*Mb0100/Rv0097**	M. bovis	No

Chapter 4:

The Pst Inorganic Phosphate Transport Systems

The Mycobacterial Pst Systems

BCG vaccinated C57BL/6 mice have long been known to react strongly to a protein known as 38-kDa protein, Ag78, Ag5, and pAb. This protein, identified as a homologue of the *E. coli pstS* gene product, was later shown to be encoded by one of three *pstS* genes in the Mtb genome; this gene was called *pstS1* [164]. PstS1 was shown to be produced at a higher level in Mtb following phosphate starvation [165]. Lefevre et al. (1997) demonstrated that all three PstS proteins (PstS1-3) were present on the cell surface and in the culture filtrate of BCG and the proteins were upregulated in BCG after phosphate starvation [164]. It has also been shown by operon-*lacZ* fusion that *M. smegmatis* is capable of regulating Mtb *pst* operon expression in a phosphate dependent manner [166]. It is noteworthy that Lefevre et al. (1997) predict by molecular modeling that the 3 PstS proteins differ in their isoelectric points and in their electrostatic potential at the PstA/PstC (MSD) binding interface [164]. This prediction supports the hypothesis that the subunits may interact differentially in order to function optimally under various environmental conditions.

The *pst* gene cluster described by Lefevre et al. (1997) and later confirmed in the publication of the Mtb genome is as depicted in Figure 4.1 [164, 167, 168]. The three operons in the locus each encode an SBD protein (PstS), the first and last each encode a pair of MSD proteins (PstA and PstC), and the last operon is the only one to encode an NBD protein (PstB). Elsewhere in the genome is a second gene encoding an NBD protein (PhoT). Interestingly, PhoT is more closely related to the Pst NBD proteins of other bacteria than to PstB of Mtb. The multi-copy *pst* genes suggest redundancy or complexity of function.

The *M. bovis* genome encodes homologues of all of the *pst* genes present in

H37Rv with 100% amino acid similarity and 99% amino acid identity. *M. leprae* has one intact *pst* locus with a *pstS* gene 86% similar to H37Rv *pstS3*. The two loci with genes homologous to *pstS2* and *pstS1* consist only of psuedogenes. *M. avium* and *M. smegmatis* each encode one *pst* locus. *M. avium pstS* has 88% similarity to H37Rv *pstS3*, and *M. smegmatis pstS* is 61% similar to *pstS3*. Thus it seems that the first Mtb pst operon, encoding *pstS3*, is common to the mycobacteria.

There has been little analysis of regulation of the Pst system and phosphate dependent gene regulation in mycobacteria compared to the extensive work that has been published on *E. coli* and *Bacillus subtilis*. As described above, Mtb PstS proteins seem to be upregulated under phosphate starvation conditions. Phosphate dependent alkaline phosphatase activity has been demonstrated in *Mycobacterium smegmatis*, but not in other mycobacterial species. The *M. smegmatis* alkaline phosphatase has no genetic homologues in Mtb, *M. avium*, *M. bovis*, or *M. leprae* [169]. It remains to be determined what phosphate responsive and/or Pst regulated genes exists in the slow growing mycobacteria.

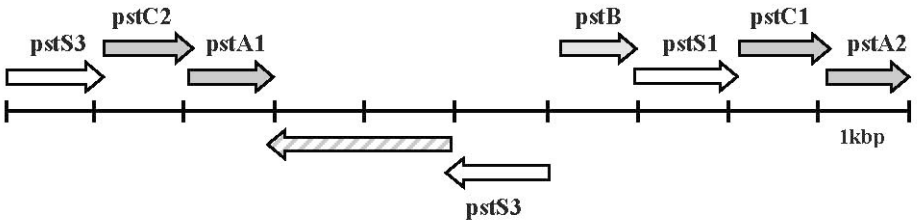

Figure 4.1: Mtb *pst* Locus. Substrate Binding Domain (SBD) genes (white arrows); Membrane Spanning Domain (MSD) genes (black arrows); Nucleotide Binding Domain (NBD) genes (grey arrows) A second NBD gene (*phoT*) is located elsewhere in the genome.

It should be noted that Mtb *pst* gene regulation has been detected in several microarray experiments that are not directly related to phosphate. *pstB* and *pstS1* were found to be downregulated after *in vitro* exposure to H_2O_2 [92]. In an *in vitro* nutrient starvation model where bacteria were cultured in phosphate buffered saline (PBS), *pstA1*, *pstB*, and *pstS1* were downregulated 5.32, 2.15, and 3.21 fold respectively. It is likely that this gene repression was due to the high phosphate concentrations in PBS relative to 7H9 medium; however, it is possible that nutrient starvation also contributed to the *pst* gene repression [170].

In *E. coli*, under nutrient starvation conditions, hyperphosphorylated guanine nucleotides, (p)ppGpps, accumulate and bind to RNA polymerase and alter expression of over 80 genes mediating what is called the stringent response. Mtb encodes a protein called Rel_{Mtb}, which is responsible for synthesis and hydrolysis of (p)ppGpp. Rel_{Mtb} mutants express lower levels of *pstS1* than wildtype bacteria in a 6 hr Tris-buffered saline (TBS) nutrient starvation model [171]. An interesting possibility is that Rel_{Mtb} plays a role in maintaining *pst* gene expression under nutrient starvation conditions, but that this role is overcome under conditions of high phosphate as seen in the PBS model discussed above.

Gene-specific gene expression assays are required to elucidate the response of *pst* genes to various *in vitro* stress conditions and *in vivo* environments. One such experiment found that *pstS1* is upregulated during growth in macrophages [172]. However, it is unclear what intraphagosomal environmental condition is responsible for inducing expression of this gene. It should also be noted that in our experiments, we did not observe any *pst* gene upregulation during macrophage infection. Consistent with our observations, microarray studies have not detected *pst* gene upregulation during Mtb

macrophage infection [92]. It is noteworthy that 1 hour and 24 hours after macrophage infection phagosomes containing Mtb *Mramp* mutant bacteria actually hyperaccumulate P_i and several divalent cations [173]. These observations suggest that Mtb is not phosphate starved *ex vivo*, but actively reduces intraphagosomal P_i concentrations via the Mramp transporter.

The aforementioned *in vitro* experiments remind us that it should not be assumed that regulation of *pst* genes is mediated solely by phosphate concentrations. Similarly, it cannot be assumed that the only role of the Pst system is in phosphate acquisition. In an interesting example of an unexpected role for the Pst system, Banerjee et al. (1998) found that a ciprofloxacin resistant (CIP^r) *M. smegmatis* mutant had a *pstB* gene duplication, overexpressed the gene, and exhibited an increased rate of phosphate uptake [174, 175]. A CIP^r mutant with the original copy of the *pstB* gene disrupted by insertion of a Kn cassette (CIP^{rd}) had a ciprofloxacin sensitivity and efflux profile intermediate between WT and CIP^r bacteria [176]. However, a *pstB* knockout created in the wildtype background (WT^d) was more sensitive to killing by ciprofloxacin, ofloxacin, and sparfloxacin than wildtype [175]. Both the WT^d and the CIP^{rd} mutants have reduced phosphate uptake capacity compared to wildtype even though the CIP^{rd} strain has a second functional *pstB* [176].

Banerjee et al. (1998) interpreted the aforementioned results to mean that the Pst transporter is involved in efflux mediated resistance to fluoroquinolones [176]. The WT^d mutant has no intact *pstB* gene, explaining its severe drug sensitivity and efflux deficiency phenotypes. However, insertion of a Kn cassette into the original *pstB* gene was likely polar on the downstream genes in the Pst transporter locus, explaining the severe disruption of phosphate uptake in both

the WT^{d} and CIP^{rd} mutants. Yet the CIP^{rd} mutant was able to maintain considerable ciprofloxacin efflux, suggesting that the remaining PstB nucleotide binding domain might mediate drug efflux via a different ABC transporter. While there is no direct evidence of drug efflux through a Pst transporter, it is noteworthy that at least one subunit of the transporter seems to contribute to drug efflux capacity of *M. smegmatis*.

Consistent with the aforementioned hypothesis, Collins et al. (2003) observed a two-fold increased sensitivity of a *Mycobacterium bovis phoT* mutant to ciprofloxacin. This mutant also had a defect in growth on limiting phosphate compared to its parent strain. This evidence suggests that *phoT* does encode a functional Pst related nucleotide binding domain protein and that, similar to *pstB* in *M. smegmatis*, it plays a role in ciprofloxacin resistance. The *M. bovis phoT* mutant is attenuated in the guinea pig and possum models of *M. bovis* infection, but not in the mouse model [177].

Several other recent papers have also examined the role of the Mtb Pst system in bacterial virulence. A *pstA1* mutant was one of 13 H37Rv transposon mutants to be tested for attenuation in the severe combined immune deficiency (SCID) mouse model and was found to be fully virulent in this mouse background [87]. In contrast, a TraSH (transposon site hybridization) screen for H37Rv mutants that were attenuated in wildtype macrophages uncovered a *phoT* mutant and a *pstA1* mutant [178]. More recently, insertion mutants were generated in *pstS1* and *pstS2* and each of these mutants was found to be attenuated in mouse lungs [179]. The insertion mutants in *pstS1* and *pstS2* were likely polar on the downstream genes in their respective operons.

These recent experiments suggest that *pstA1*, *phoT*, and each of the second

two *pstS* operons, are important for virulence of Mtb in immunocompetent mice and/or macrophages. It should be noted, however, that none of the Mtb *pst* mutants has been complemented and the *in vivo* phenotypes of the *pstS1* and *pstS2* mutants are consistent with those seen with spontaneous loss or deliberate elimination of PDIM production [178, 179].

pstA1 Results and Discussion

Recently we described a differential STM (dSTM) screen through which we identified three mutants that were deficient in counter-immune defense against an IFN-γ dependent pathway other than NOS2 [76]. This screen revealed a fourth mutant that was well controlled by a NOS2-independent, IFN-γ dependent response, but was also attenuated in IFN-$\gamma^{-/-}$ mice. This mutant had a transposon insertion approximately one third of the way into the gene encoding *pstA1* (Rv0930), membrane spanning domain protein of a putative inorganic phosphate ABC transporter (Figure 4.2B).

ABC transporters are large multi-subunit permeases that function in eukaryotic cells as exporters and in prokaryotes as both importers and exporters [180]. ABC transporters consist of two membrane spanning domain (MSD) proteins and two nucleotide binding domain (NBD) proteins. Prokaryotic ABC importers often include an additional high affinity substrate binding domain (SBD) subunit that specifies the cargo of the ABC transporter (Figure 4.2B).

pstA1/Rv0930 is highly homologous to an *E. coli* gene, *pstA*, encoding a high-affinity inorganic phosphate ABC transporter MSD protein. *pstA1* is the

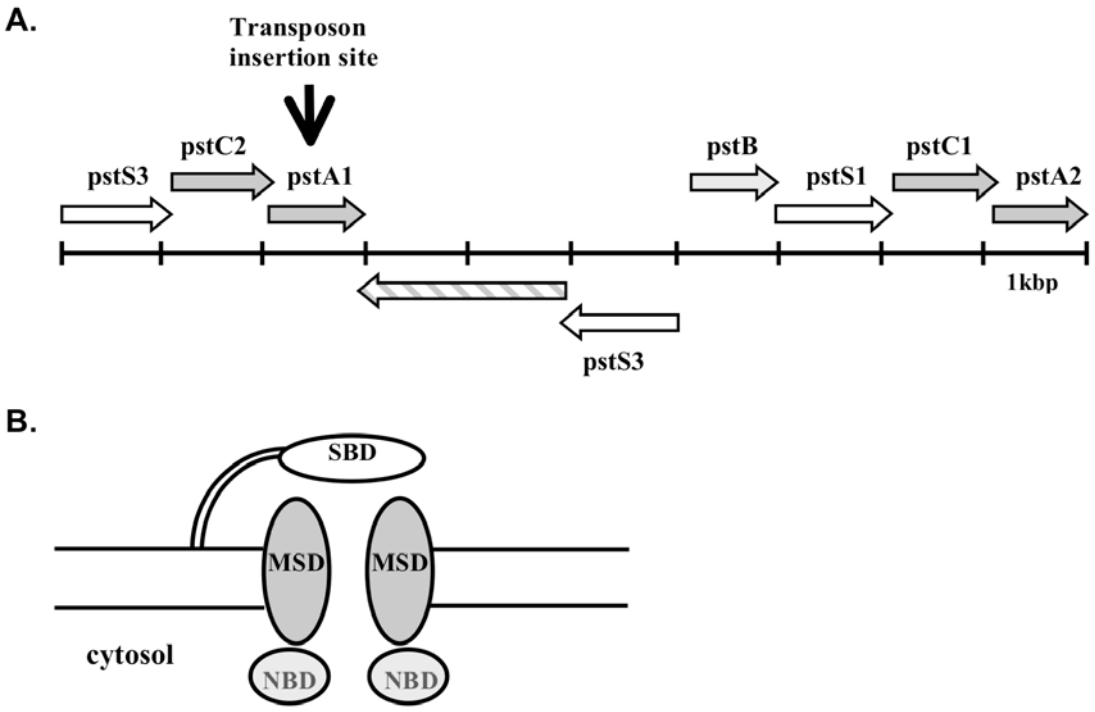

Figure 4.2. Identification of *pstA1* Mutant: a Component of the Pst Inorganic Phosphate Uptake System. A *pstA1* mutant was identified by inverse PCR in the counterimmune (*cim*) mutant dSTM screen. (A) Organization of the *pst* locus containing the *pstA1* gene. (B) Schematic of the organization of a prokaryotic ABC importer. SBD, substrate binding domain; MSD, membrane spanning domain; NBD, nucleotide binding domain.

last open reading frame in what appears to be an operon encoding another MSD subunit (Rv0929/*pstC2*) and an SBD subunit (Rv0928/*pstS3*) of a putative inorganic phosphate transporter. A homologous locus located ~4.2 kb downstream of the *pstA1* locus encodes another operon homologous to the Pst high-affinity phosphate transporter; the order of the genes in the two putative operons is conserved (Figure 4.2A) although the homology between the corresponding genes is limited (25-64%). The significant, complementable, *in vitro* phenotypes of the *pstA1* mutant suggest that the two *pstA* genes and the two operons are not functionally redundant.

Confirmation of the *pstA1* Mutant's *In Vivo* Phenotype

As with the other PDIM deficient mutants isolated from the dSTM screen, the *in vivo* phenotype of the *pstA1* mutant was confirmed by tail-vein infection of wild-type (C57BL/6), IFN-$\gamma^{-/-}$, and NOS2$^{-/-}$ mice with the individual strain. The *pstA1* mutant displayed a significant growth advantage in IFN-$\gamma^{-/-}$ mice as compared to C57BL/6 mice and was rapidly lethal, as were the other PDIM deficient strains. However, time-to-death for NOS2$^{-/-}$ animals was markedly delayed when animals were infected with the *pstA1* mutant as compared to the other PDIM deficient strains (Figure 4.3H). These results suggest that *pstA1* is required for progressive bacterial growth in the presence of an IFN-γ-dependent immune mechanism other than NOS2. It must be noted, however, that the attenuation caused by *pstA1* deficiency might be more or less pronounced or even completely absent in a PDIM proficient background.

IFN-γ-Dependent and Independent Attenuation in Aerosol-Infected Mice

Differential replication of PDIM proficient H37Rv in NOS2$^{-/-}$ and IFN-$\gamma^{-/-}$ mice is absent by 4 weeks post aerosol infection, eliminating much of the cfu difference seen after tail-vein infection (Figures 4.3A, 4.4A). The host-pathogen dynamic is influenced by the route of infection; in aerosol-infected mice, NOS2 appears to account almost entirely for the early IFN-γ dependent control of PDIM+ H37Rv (Figure 4.4A). In contrast, PDIM- H37Rv demonstrates differential growth in WT (C57BL/6), NOS2-/-, and IFN-$\gamma^{-/-}$ mice between one and four weeks post infection, indicating early action of an IFN-γ dependent pathway other than NOS2 on PDIM deficient bacteria (Figure 4.4B). Thus, by utilizing a counter-immune (*cim*) mutant, we have uncovered an otherwise

minimal differential phenotype of two immunodeficient mouse strains. In the absence of NOS2, an early IFN-γ dependent pathway is able to contain PDIM- bacterial infection but not PDIM+ H37Rv.

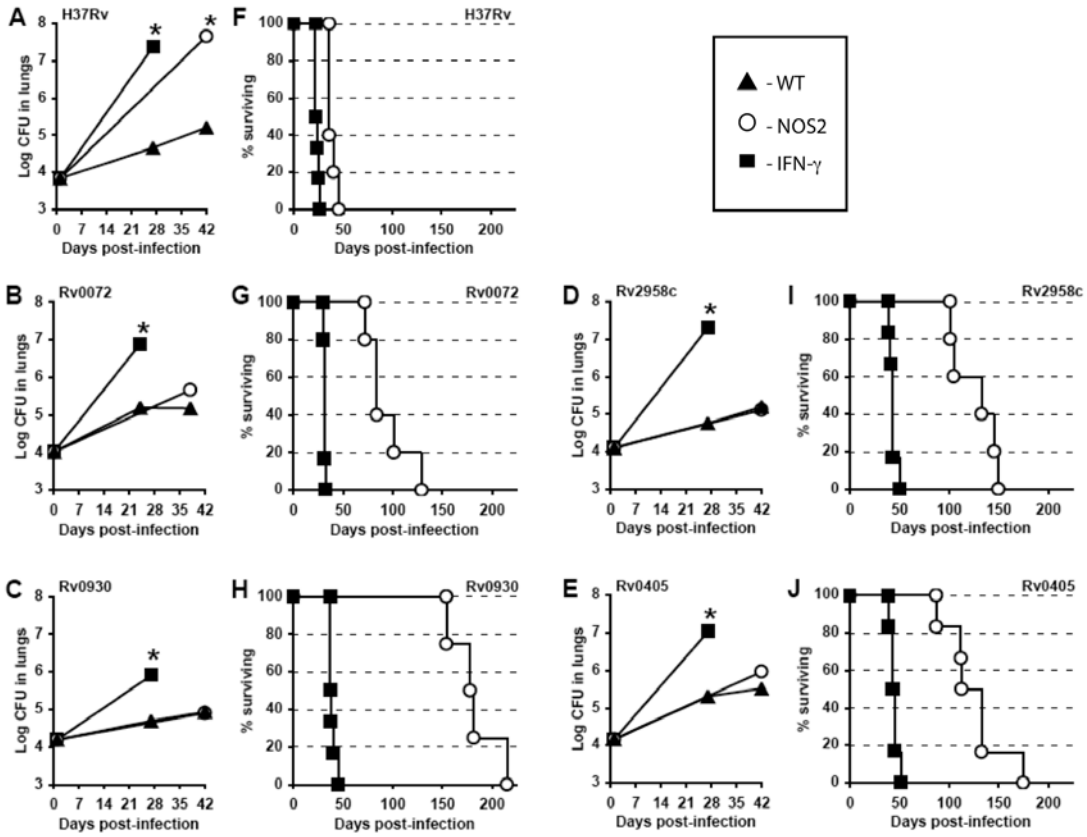

Figure 4.3: *pstA1* Mutant Phenotype by Monotypic Intravenous Infection. WT (C57BL/6), NOS2$^{-/-}$, and IFN-γ$^{-/-}$ mice were infected by tail vein injection with H37Rv-mixed DIM+/DIM- (A, F), DIM- Rv0072 mutant (B, G), DIM- Rv0930/*pstA1* mutant (C, H), DIM- Rv2958c mutant (D, I), and DIM- Rv0405/*pks6* mutant (E, J). (A-E) Colony forming units (cfu) in the lungs of WT (black triangles), NOS2$^{-/-}$ (white circles) and IFN-γ$^{-/-}$ (black squares) mice over time. (F-J) Percent survival of infected NOS2$^{-/-}$ (white circles) and IFN-γ$^{-/-}$ (black squares) mice over time.

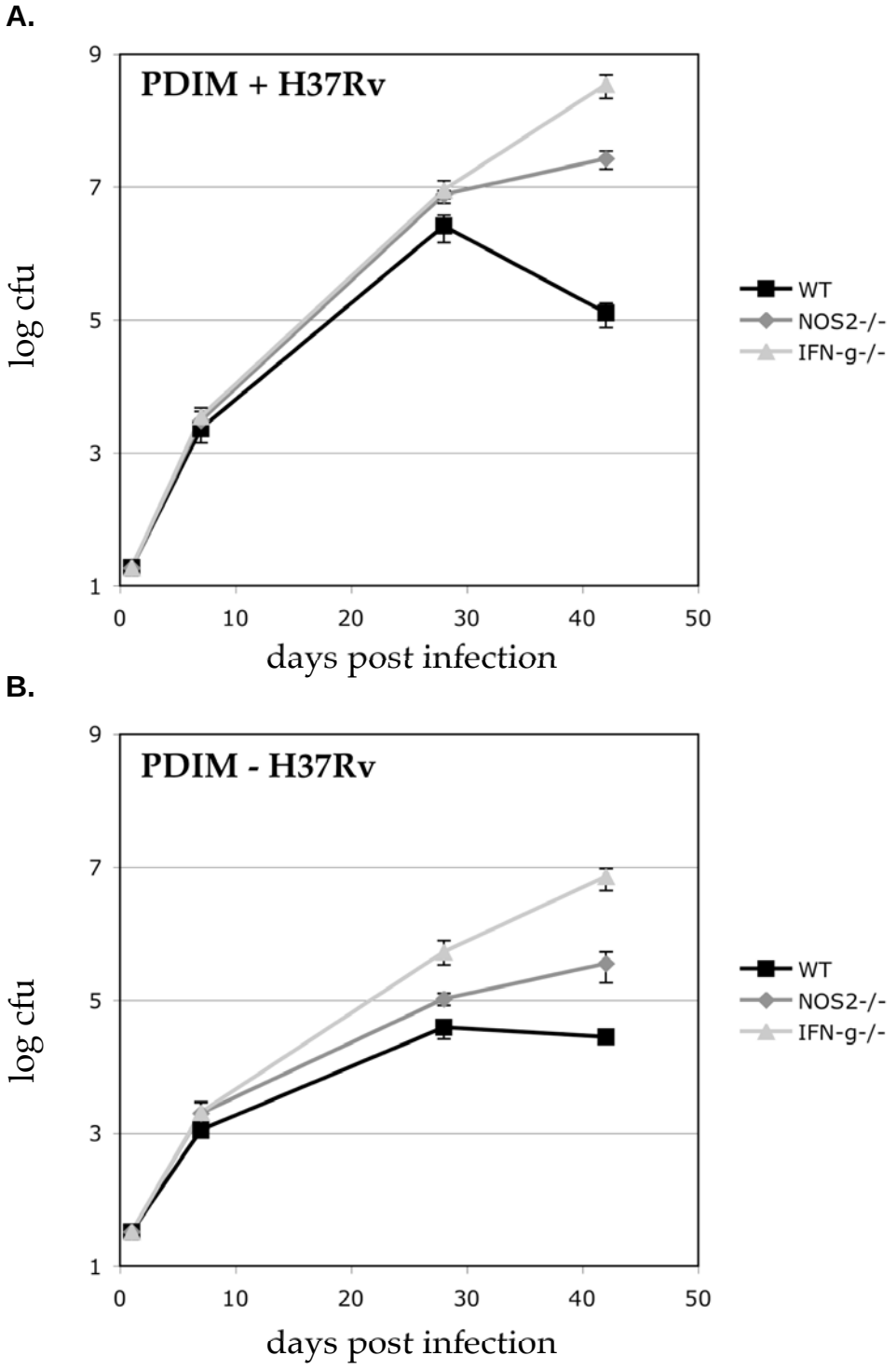

Figure 4.4: Aerosol Infection of Mice with PDIM+ versus PDIM- H37Rv. WT C57BL/6 (black squares), NOS2$^{-/-}$ (grey diamonds), and IFN-$\gamma^{-/-}$ (light grey triangles) mice were aerosol-infected with (A) PDIM+ H37Rv and (B) PDIM- H37Rv.

We examined in detail the *in vivo* growth of the *pstA1* mutant after aerosol infection of WT (C57BL/6), NOS2$^{-/-}$, and IFN-γ$^{-/-}$ mice. Consistent with our IV infection results, the *pstA1* mutant demonstrated a substantial growth advantage in and rapidly killed IFN-γ$^{-/-}$ mice as compared to WT mice (Figure 4.5). Also consistent with the IV infection data, the *pstA1* mutant displayed no significant growth advantage in aerosol-infected NOS2$^{-/-}$ mice compared to WT mice during the first 6 weeks of infection and NOS2$^{-/-}$ mice exhibited prolonged ability to control replication of *pstA1* bacteria (Figure 4.5). When adjusted for starting cfu, it appears that the *pstA1* mutant gains less of a growth advantage in IFN-γ$^{-/-}$ and NOS2$^{-/-}$ mice than its parent PDIM deficient H37Rv (Figure 4.6). However, due to differences in starting inoculum, statistical significance is difficult to establish without further experimentation. Moreover, it remains to be determined how a *pstA1* mutant would behave in a PDIM proficient background.

Infection of Murine Bone Marrow Derived Macrophages (BMMΦ)

To determine whether the phenotype of the *pstA1* mutant could be replicated *ex vivo*, we infected murine BMMΦ with *pstA1* deficient bacteria. Resting WT (C57BL/6) BMMΦ permit replication of H37Rv and the *pstA1* mutant with similar kinetics, while the *pstA1* mutant fared less well in IFN-γ activated WT BMMΦ (Figure 4.7). In contrast, the *pstA1* mutant is attenuated in both resting and activated NOS2$^{-/-}$ macrophages (Figure 4.8). This suggests the possibility that the IFN-γ independent pathway(s) that is responsible for restricting growth of *pstA1* deficient bacteria at the level of the macrophage is upregulated in the absence of NOS2 [74].

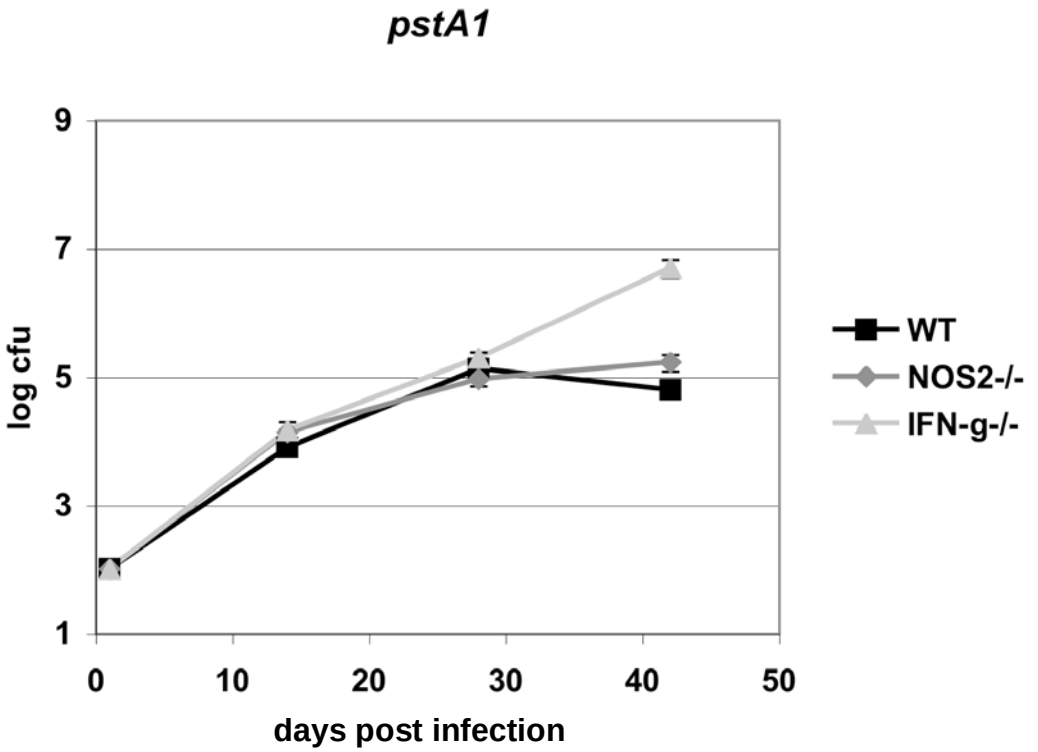

Figure 4.5: Aerosol Infection of Mice with the *pstA1* Mutant. WT C57BL/6 (black squares), NOS2$^{-/-}$ (grey diamonds), and IFN-γ$^{-/-}$ (light grey triangles) mice were aerosol-infected with the *pstA1* mutant.

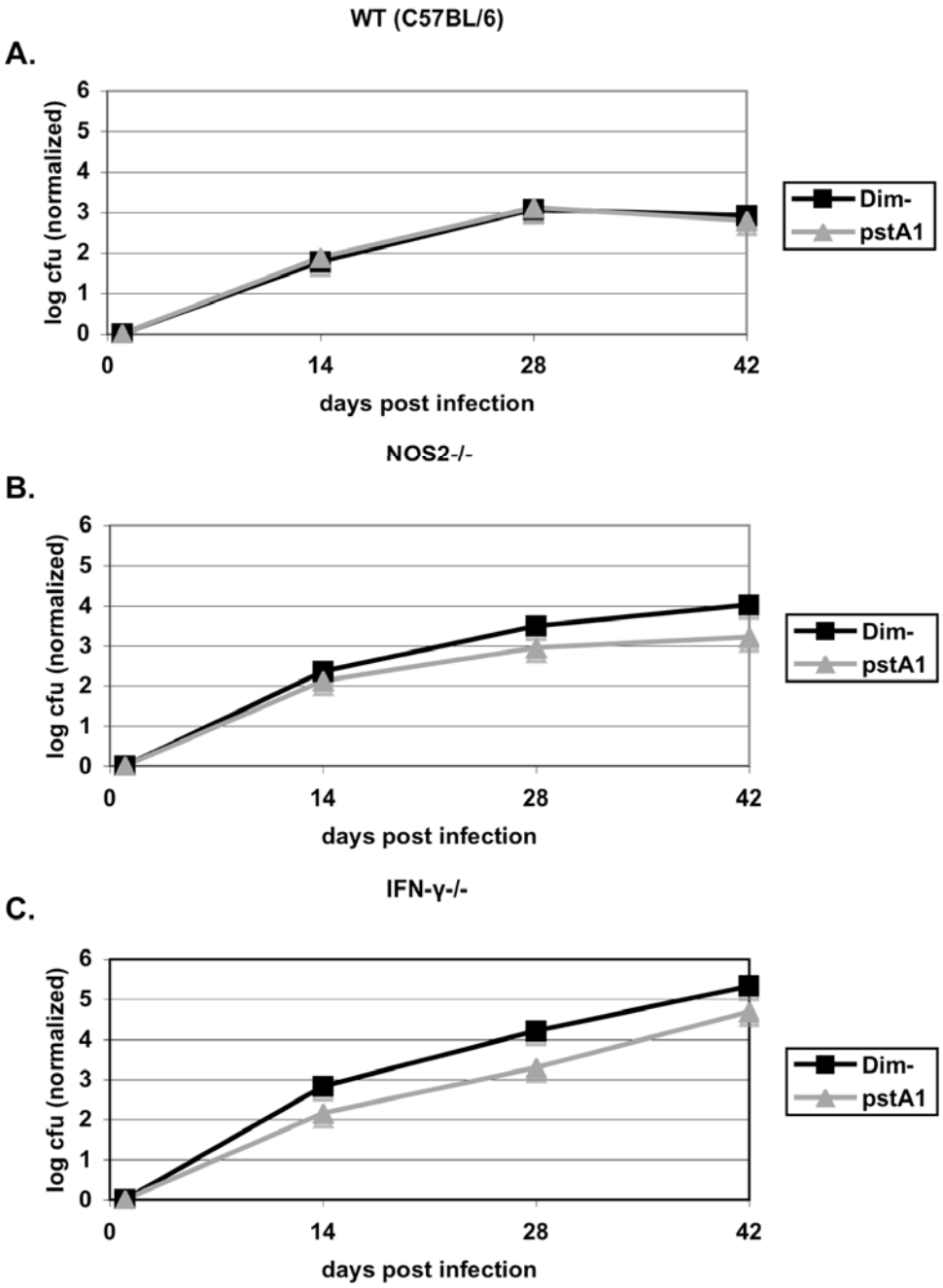

Figure 4.6: Aerosol Infection of Mice with PDIM- H37Rv versus the PDIM- *pstA1* Mutant. (A) WT (C57BL/6), (B) NOS2$^{-/-}$, and (C) IFN-γ$^{-/-}$ mice were aerosol-infected with PDIM- H37Rv (black squares) or the PDIM- *pstA1* mutant (grey triangles).

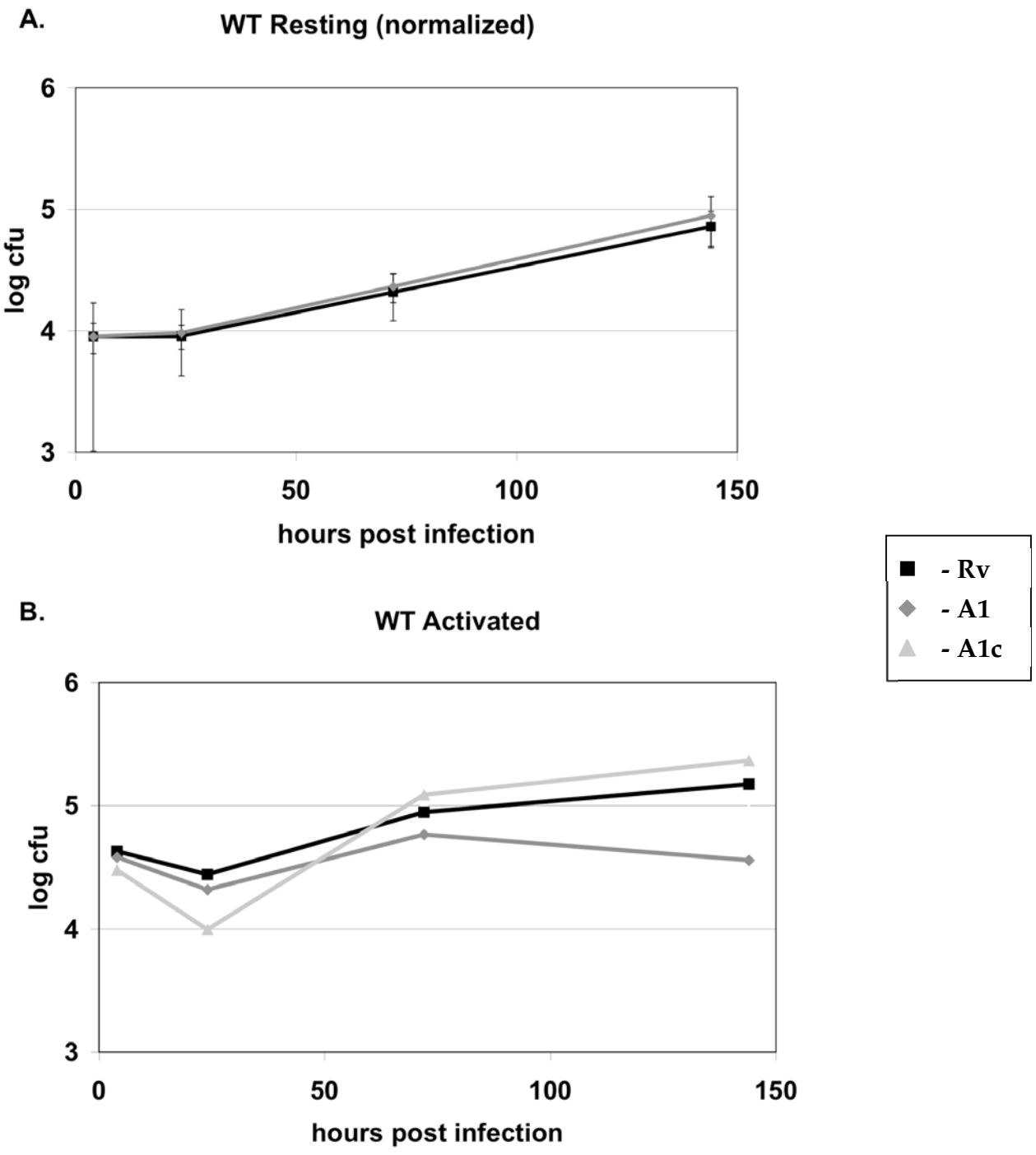

Figure 4.7: Replication and Survival of the *pstA1* Mutant in Murine BMMΦ from WT (C57BL/6) Mice. Intracellular cfu of H37Rv (black squares), *pstA1* mutant (grey diamonds), and complemented *pstA1* mutant (light grey triangles) per well of (A) resting, or (B) IFN-γ activated WT BMMΦ.

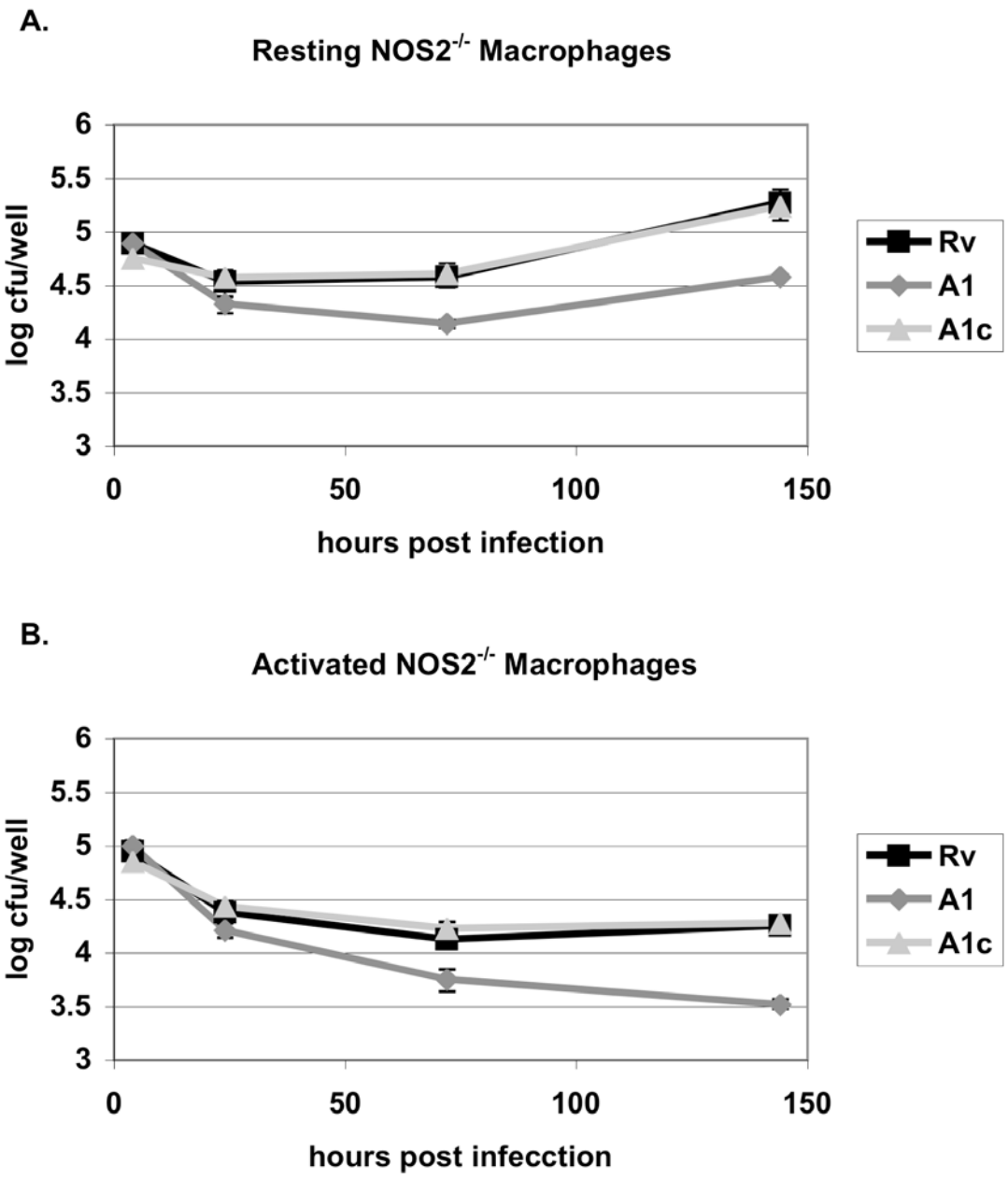

Figure 4.8: Replication and Survival of the *pstA1* Mutant in Murine BMMΦ from NOS2$^{-/-}$ Mice. Intracellular cfu of H37Rv (black squares), *pstA1* mutant (grey diamonds), and complemented *pstA1* mutant (light grey triangles) per well of (A) resting, or (B) IFN-γ activated NOS2$^{-/-}$ BMMΦ.

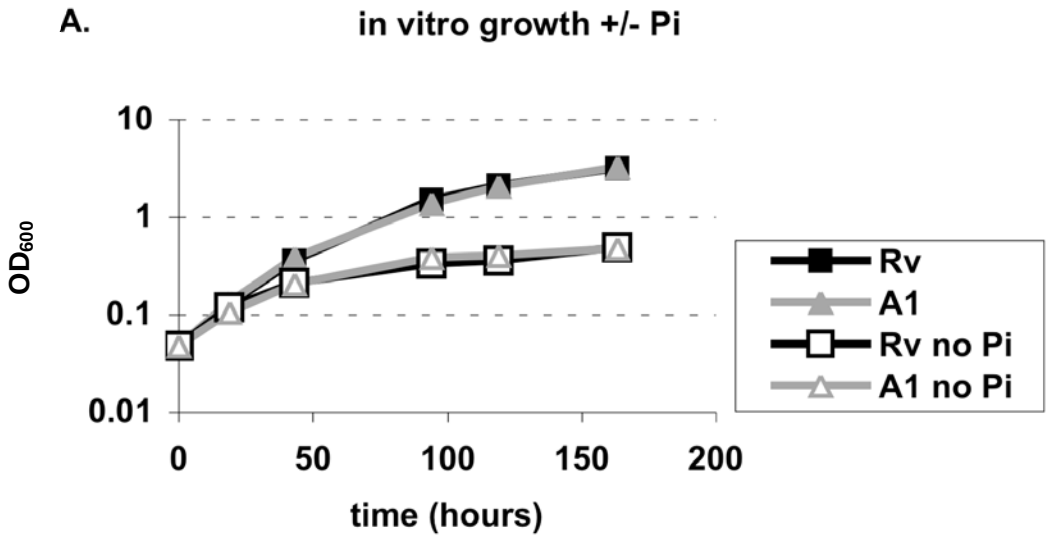
A.
in vitro growth +/- Pi
10
1
0.1
0.01
OD600
0
50
100
150
200
time (hours)
Rv
A1
Rv no Pi
A1 no Pi

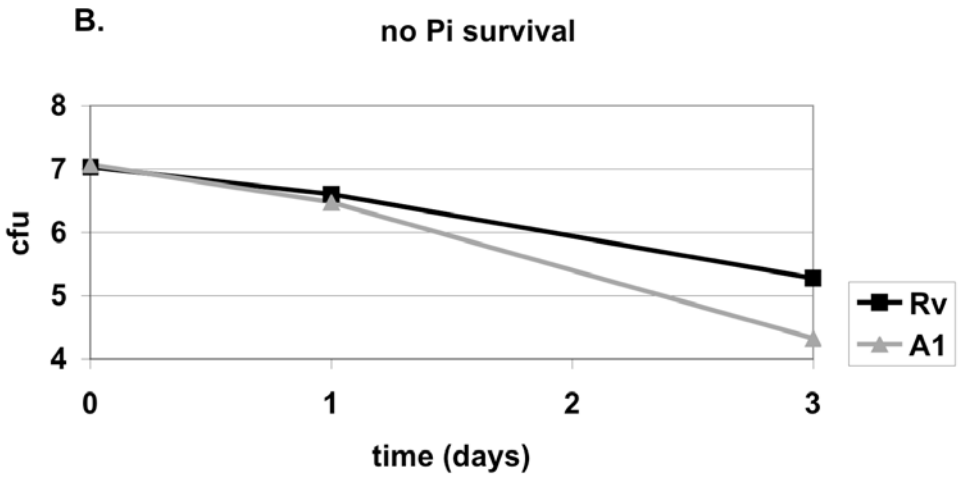
B.
no Pi survival
8
7
6
5
4
cfu
0
1
2
3
time (days)
Rv
A1

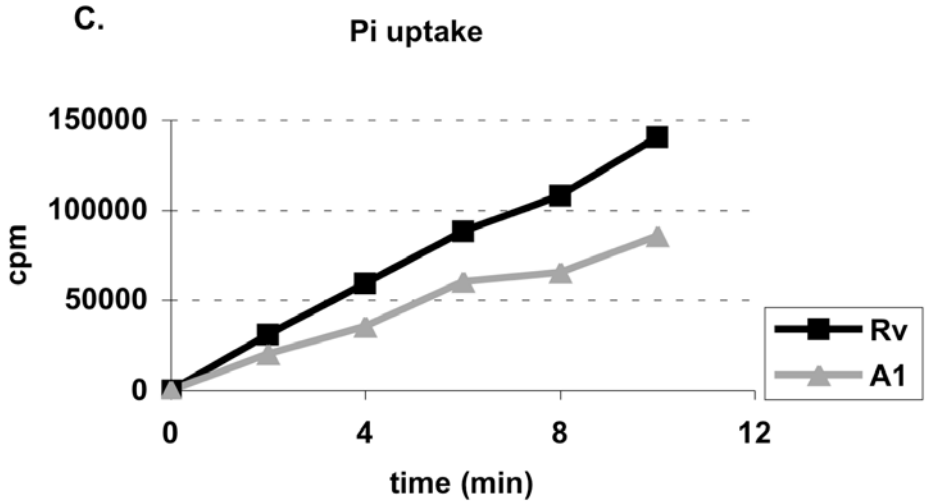
C.
Pi uptake
150000
100000
50000
0
cpm
0
4
8
12
time (min)
Rv
A1

Figure 4.9: *In vitro* Growth, Survival, and P_i Uptake of the *pstA1* Mutant. (A) Growth of H37Rv (squares) and *pstA1* mutant (triangles) in P_i replete 7H9 medium (filled symbols) and in 7H9 medium prepared without P_i (open symbols) assayed by optical density (OD_{600}). (B) Survival of H37Rv (black squares) and *pstA1* mutant (grey triangles) over time in 7H9 medium prepared without P_i as assayed by plating for colony forming units (cfu). (C) Uptake of ^{32}P-orthophosphate by H37Rv (black squares) and *pstA1* mutant (grey triangles) after 24 hours of incubation in 7H9 medium prepared without P_i.

The Role of PstA1 in High Affinity Phosphate Uptake

The *pstA1* mutant replicates as well as wildtype H37Rv *in vitro* in both phosphate replete 7H9 medium and in 7H9 prepared without phosphate (Figure 4.9A). However, the *pstA1* mutant survives less well in 7H9 without phosphate than H37Rv (Figure 4.9B). In addition, after 24 hours of phosphate starvation, *pstA1* is deficient in its ability to take up radiolabeled orthophosphate (Figure 4.9C). This evidence suggests that PstA1 is an important component of the Mtb high affinity P_i uptake system *in vitro*.

***In vitro* Stress Sensitivity of the *pstA1* Mutant**

Because both phox and NOS2 are known downstream effectors of IFN-γ, the *in vitro* sensitivity of *pstA1* to acidified nitrite and H_2O_2 were tested. The slight, but significant enhanced sensitivity of *pstA1* to acidified nitrite (Figure 4.10A) was consistent with the slight growth advantage observed in $NOS2^{-/-}$ mice 82 days post aerosol infection and the shortened time to death of $NOS2^{-/-}$ mice compared to wildtype C57BL/6 mice (data not shown).

The *pstA1* mutant is markedly more sensitive to H_2O_2 stress than wildtype H37Rv (Figure 4.10B). Catalase is a primary mediator of Mtb defense against

reactive oxygen species (ROS). Exposure to H_2O_2 leads to comparable activation of catalase activity in both H37Rv and the *pstA1* mutant. It does not appear that the sensitivity of *pstA1* deficient bacteria to H_2O_2 is due to a defect in catalase production or induction (Figure 4.12A). In fact, preliminary results indicate that the *pstA1* mutant exhibits accelerated H_2O_2 consumption *in vitro* compared to H37Rv (Figure 4.12B). It is possible that this is due to increased permeability, consistent with the hypersensitivity of the *pstA1* mutant to SDS exposure (Figure 4.10C). However, *pstA1* is not required for global stress resistance, as *pstA1* deficient bacteria do not appear to be hypersensitive to heat or osmotic stress and are hyper-resistant to low pH (data not shown, Figure 4.14). Surprisingly, in spite of its sensitivity to H_2O_2 *in vitro*, the *pstA1* mutant fares no better in phox$^{-/-}$ mice than in wildtype mice (Figure 4.13).

H37Rv is sensitized to both H_2O_2 and SDS by 24 hours of phosphate starvation (Figure 4.11). Taken together, these observations suggest that PstA1 plays a role in phosphate uptake or signaling that is required for an effective stress response *in vitro* and that the *in vitro* phenotype can be mimicked by subjecting H37Rv to phosphate starvation.

Expression of *pst* Genes *In Vitro*

Evidence from various organisms indicates that Pst systems are generally upregulated during phosphate starvation as part of the Pho regulon. The Pst system is, in turn, often required for repression of the Pho regulon under conditions of high phosphate. We used Sybr Green real time quantitative RT-PCR to examine the regulation of the *pstS* and *pstA* genes of Mtb grown under phosphate replete and phosphate starved conditions.

The first and second operons, encoding PstS3/PstA1 and PstS2, are upregulated under phosphate starvation conditions, while expression of the genes in the third operon (*pstS1* and *pstA2*) remain unchanged (Figure 4.15). Constitutively high expression of *pstS3* in the *pstA1* mutant suggests that PstA1 is required for repression of the first operon under high phosphate conditions. Notably phosphate dependent upregulation of *pstS2* and *pstS3* is partially maintained in the *pstA1* mutant and is therefore not fully dependent on PstA1. In addition *pstS2* is highly expressed in both H37Rv and the *pstA1* mutant in phosphate replete conditions (Figure 4.15). These data suggest the existence of both PstA1 dependent and PstA1 independent modes of *pst* gene regulation.

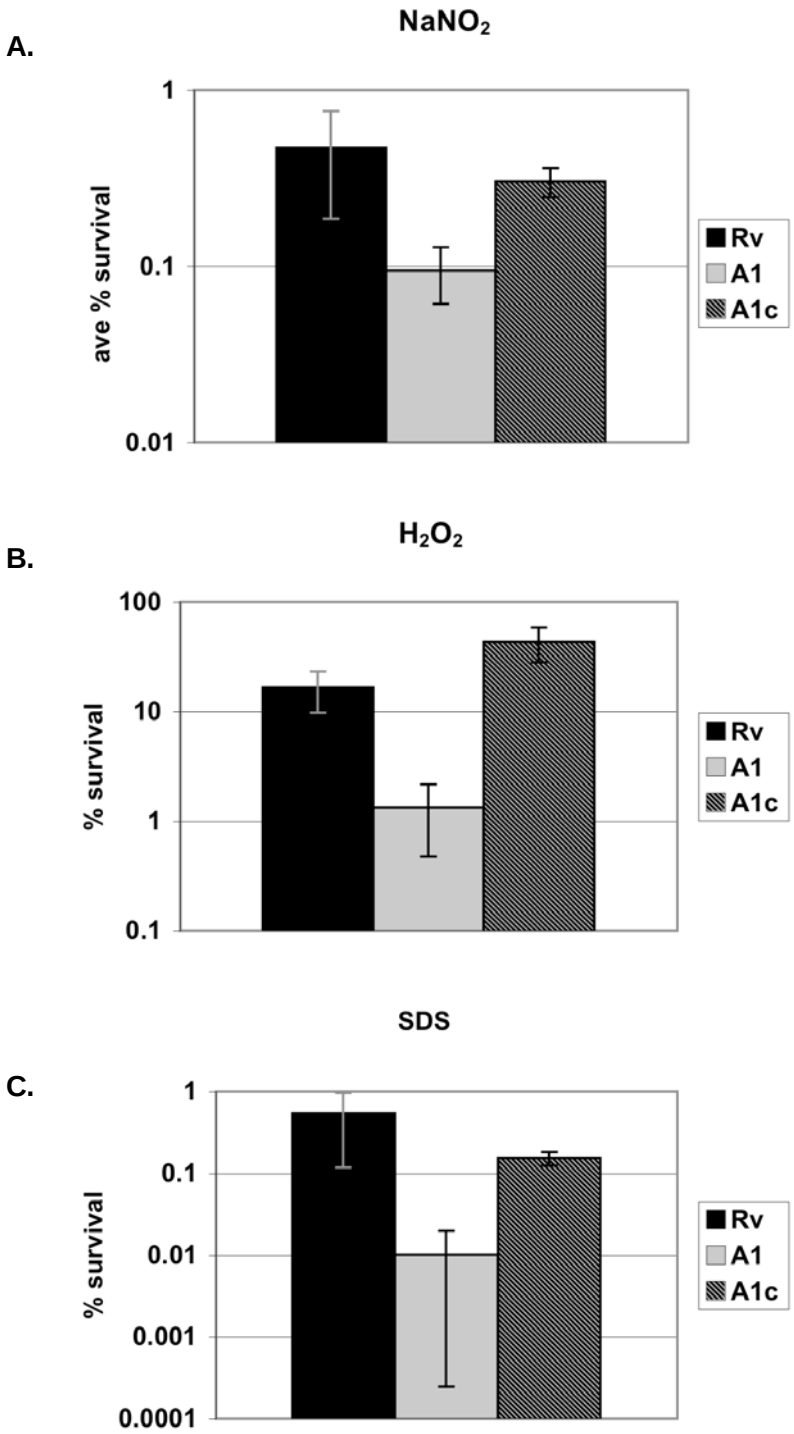

Figure 4.10: Sensitivity of H37Rv and the *pstA1* Mutant to $NaNO_2$, H_2O_2, and SDS. Percent survival of H37Rv (black bars), the *pstA1* mutant (grey bars) and the complemented *pstA1* mutant (hatched bars) after incubation in 7H9 in the presence of (A) acidified 3 mM $NaNO_2$, (B) 1 mM H_2O_2, (C) 5 % SDS.

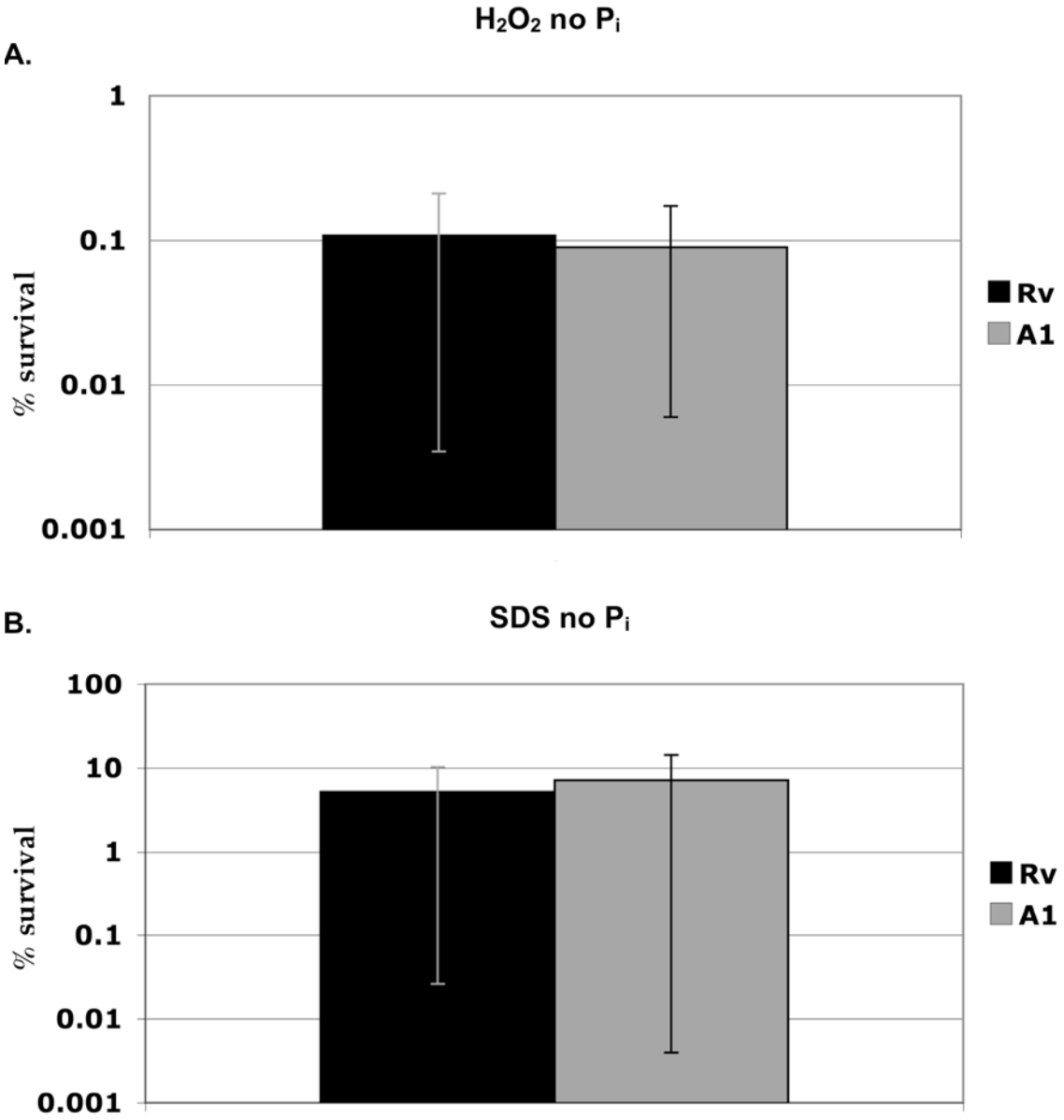

Figure 4.11: Sensitivity of Phosphate-Starved H37Rv and *pstA1* Mutant to H_2O_2 and SDS. Percent survival of H37Rv (black bars) and *pstA1* mutant (grey bars) after incubation for 24 hours in phosphate limited 7H9 followed by 24 incubation in the presence of (A) 1 mM H_2O_2 and (B) 0.5 % SDS.

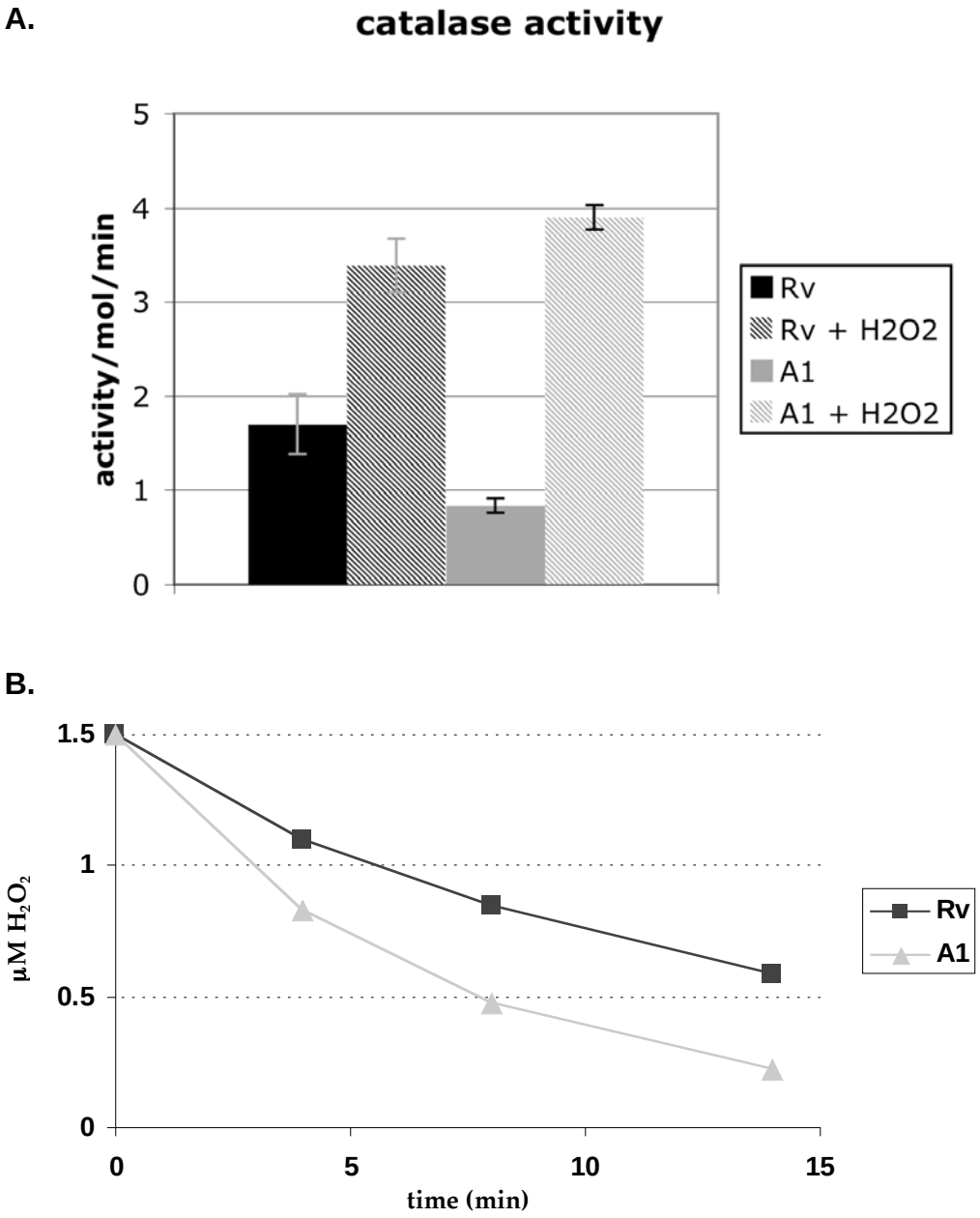

Figure 4.12: Catalase Activity and H_2O_2 Consumption. (A) Catalase activity of cell-free extracts of H37Rv (black bars) and *pstA1* mutant (grey bars) incubated for 3 hours in 7H9 alone (solid bars) or 7H9 + 0.01 mM H_2O_2 (hatched bars). (B) H_2O_2 consumption over time of H37Rv (black line) and *pstA1* mutant (grey line).

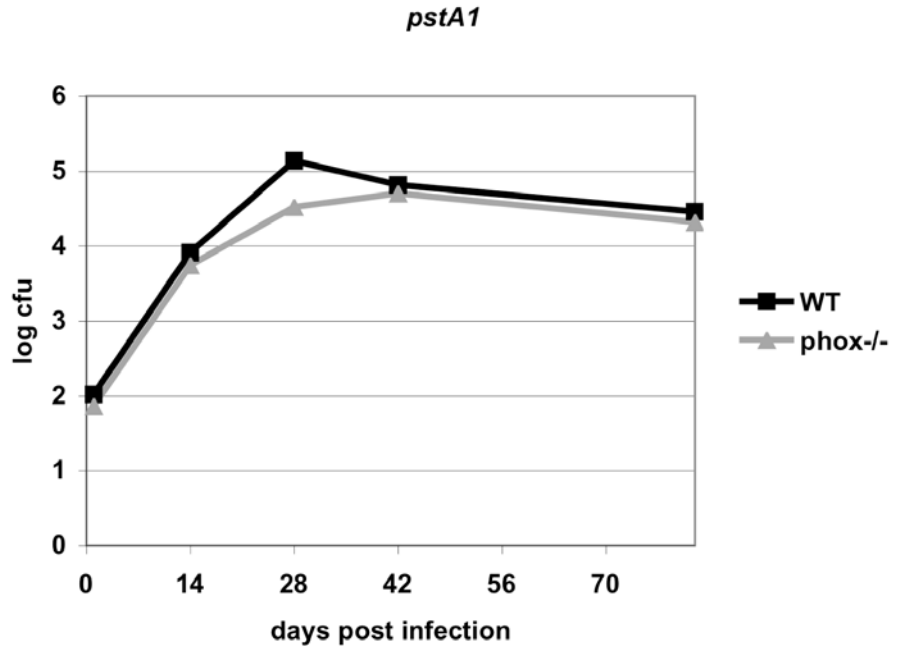

Figure 4.13: Aerosol Infection of Wildtype (C57BL/6) and phox$^{-/-}$ Mice with the *pstA1* Mutant. WT (black squares) and phox$^{-/-}$ (grey triangles) mice were aerosol-infected with *pstA1* mutant bacteria.

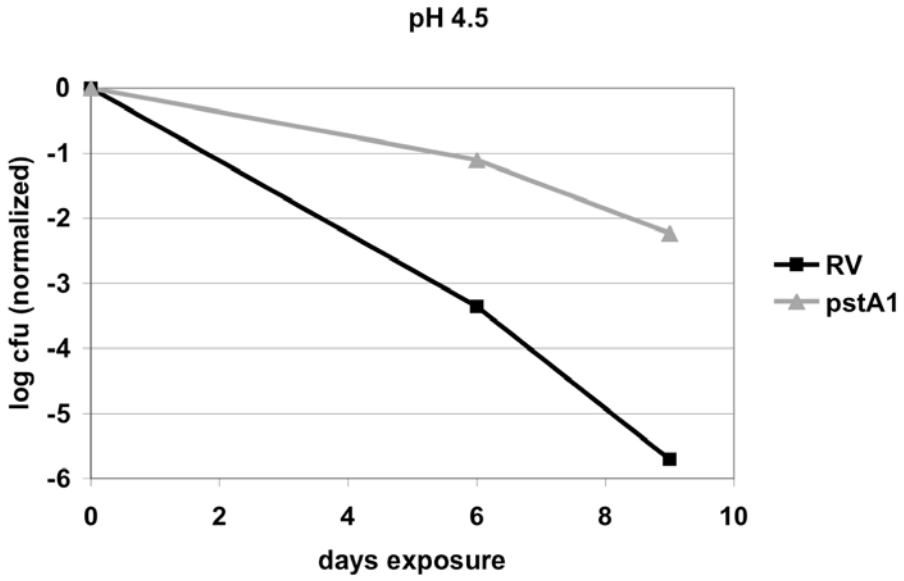

Figure 4.14: Sensitivity of H37Rv and *pstA1* Mutant to pH 4.5. Survival (cfu) of H37Rv (black bars) and *pstA1* mutant (grey bars) during incubation in 7H9 at pH 4.5.

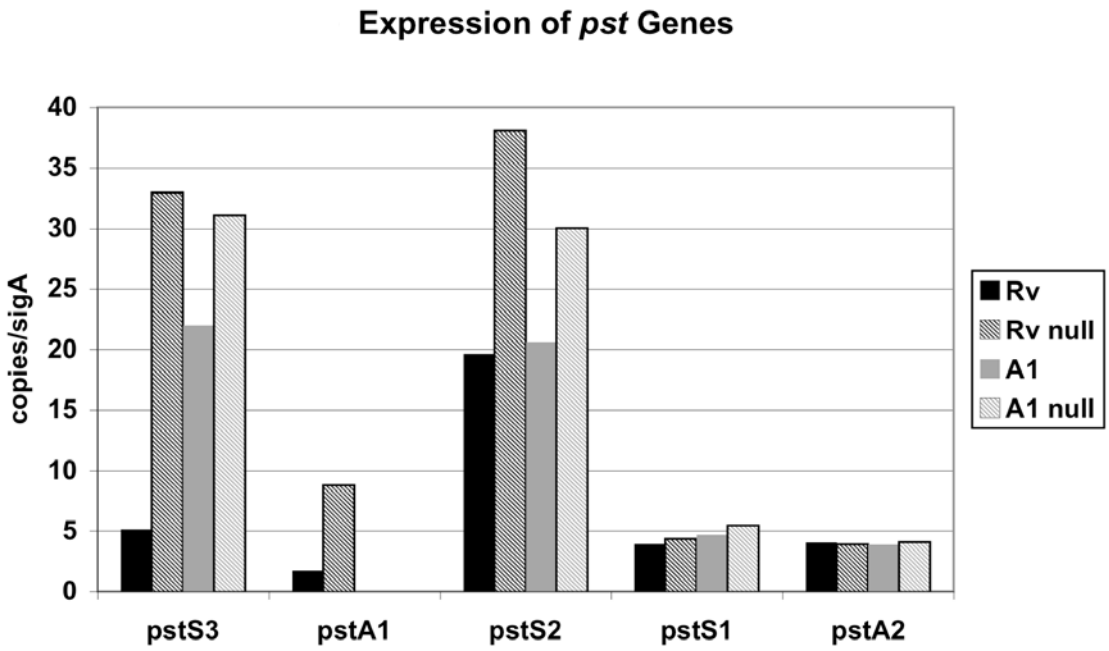

Figure 4.15: Expression of *pst* Genes in H37Rv and the *pstA1* Mutant. Quantitative real-time RT-PCR of *pstS* and *pstA* mRNAs relative to the *sigA* mRNA (encoding the housekeeping RNA polymerase sigma factor) using Sybr Green. RNA was isolated from H37Rv (black bars) or *pstA1* mutant (grey bars) after incubation in phosphate replete 7H9 (solid bars) or 7H9 prepared without phosphate (hatched bars).

Chapter 5:

A Role for PstS3

pstS Results and Discussion

An in-frame unmarked deletion of *pstS3*, the SBD gene that is upstream of *pstA1*, was generated in an effort to further characterize the locus (Figure 4.2). Notably, this mutant shares all of the *in vitro* phenotypes of *pstA1* deficient bacteria described thus far (except $NaNO_2$ sensitivity), albeit with lesser severity (Figures 5.1, 5.2).

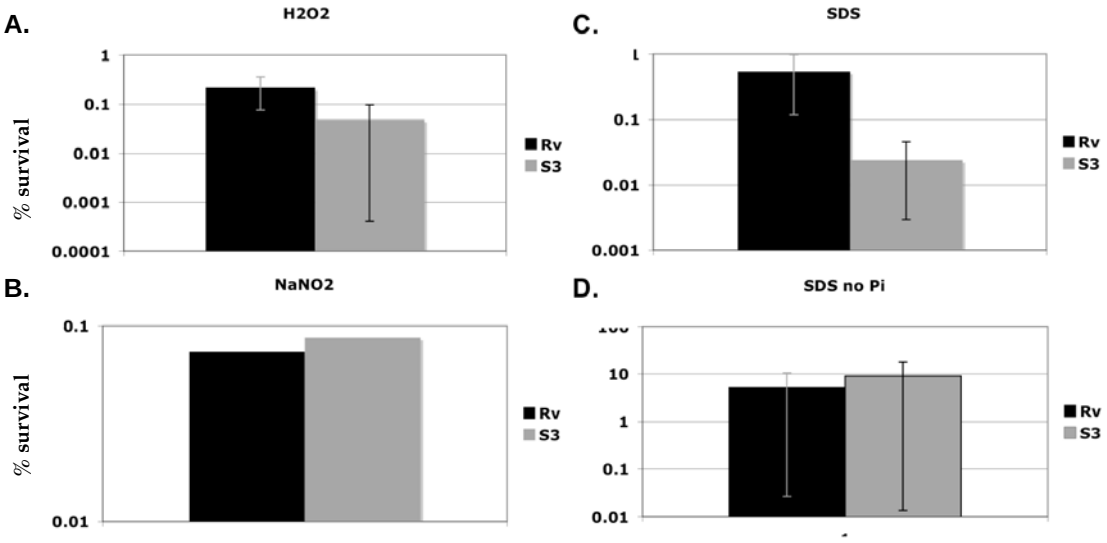

Figure 5.1: Sensitivity of the *pstS3* Mutant to *in vitro* Stresses. Percent survival of H37Rv (black bars) and *pstS3* mutant (grey bars) after incubation in 7H9 in the presence of (A) 1 mM H_2O_2, (B) acidified 3 mM $NaNO_2$, (C) 0.5 % SDS, and (D) 0.5 % SDS after 24 hours of phosphate starvation.

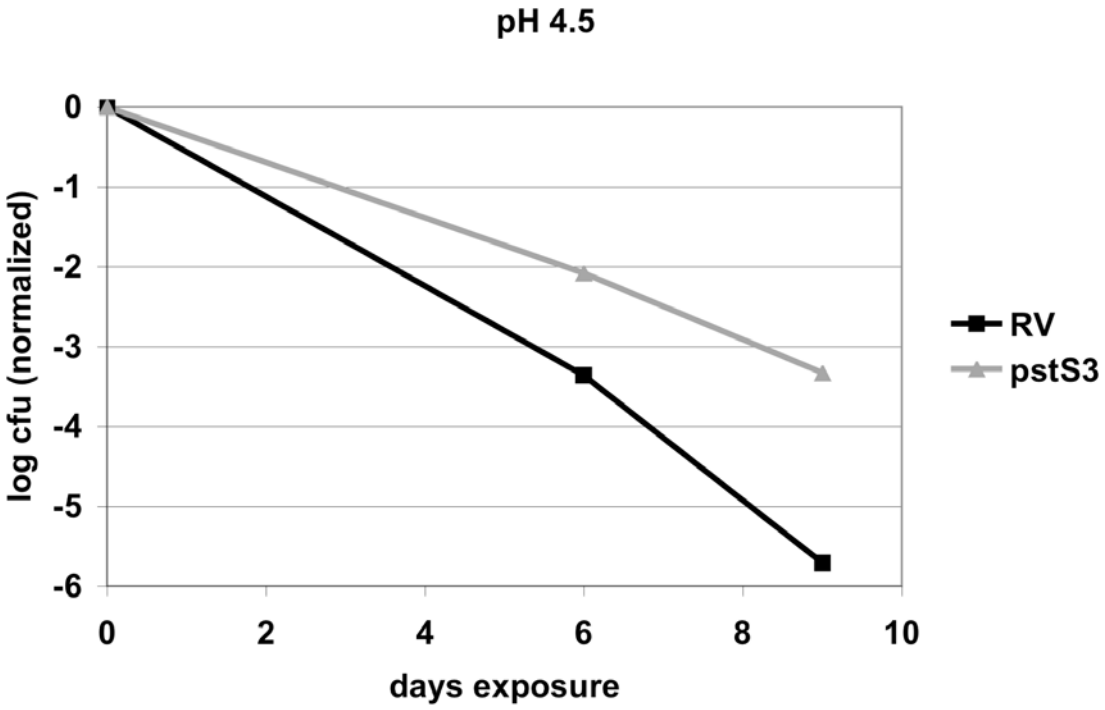

Figure 5.2: Resistance of the *pstS3* Mutant to pH 4.5. Bacterial cfu (normalized to match starting cfu) of H37Rv (black squares) and *pstS3* mutant (grey triangles) after incubation in 7H9 at pH 4.5.

Due to the sensitivity of the *pstS3* mutant and phosphate starved H37Rv to H_2O_2, expression of oxidative stress genes was examined in each strain *in vitro* in the presence and absence of phosphate. Both strains exhibited five-fold upregulation of *ahpC* and *ahpD* in response to growth in the absence of phosphate. However, under both growth conditions, expression of the *ahp* genes was significantly lower in the *pstS3* mutant than in H37Rv. Consistent with the catalase activity seen in *pstA1* and *pstS3* deficient bacteria, there was no difference in expression of *katG* between the mutants and H37Rv (Figure 5.3). Taken together, these data suggest that phosphate restriction induces oxidative stress, triggering upregulation of *ahpC* and *ahpD*, but not *katG*. Significantly,

preliminary experiments indicate that Mtb accumulates H_2O_2 during growth on limiting phosphate (Figure 5.4).

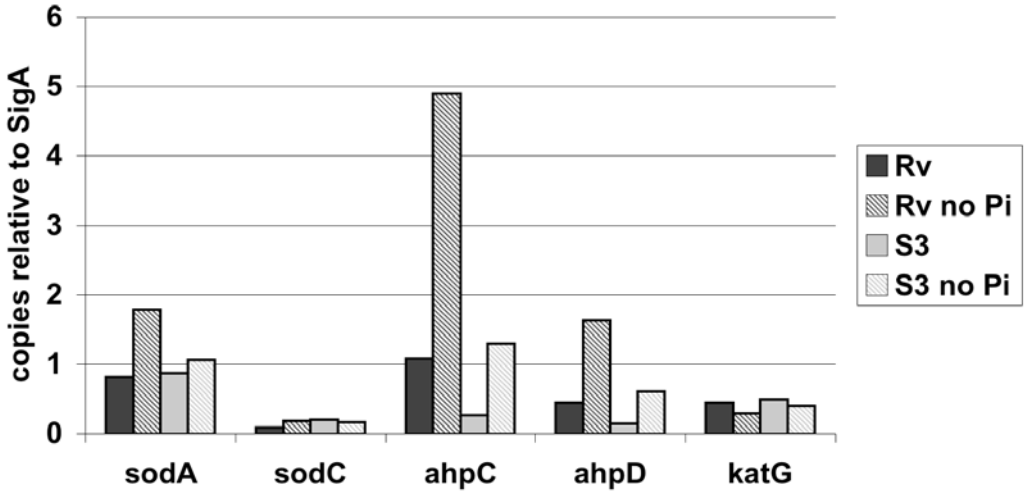

Figure 5.3: Expression of Oxidative Stress Response Genes in H37Rv and the *psts3* Mutant Cultured with and without Phosphate. Quantitative real-time RT-PCR of the indicated target mRNAs relative to the *sigA* mRNA using Sybr Green. RNA was isolated from H37Rv (black bars) or the *pstS3* mutant (grey bars) after incubation in phosphate replete 7H9 (solid bars) or 7H9 prepared without phosphate (hatched bars).

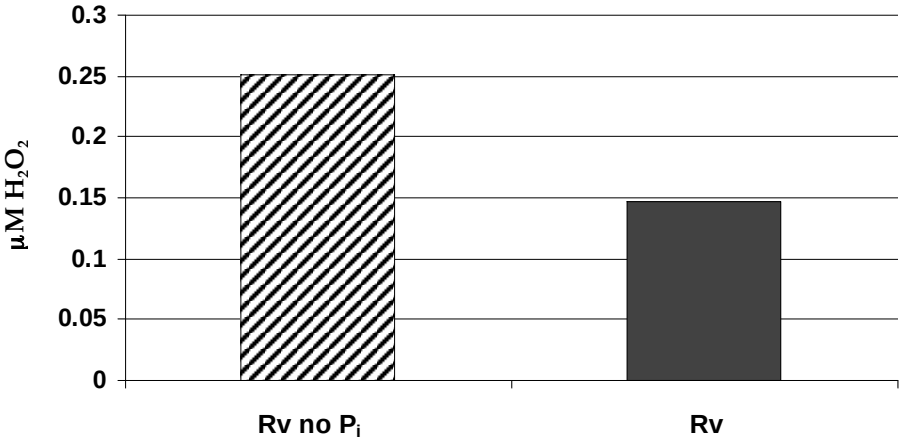

Figure 5.4: H_2O_2 Generation by H37Rv. Spectrophotometric assay of H_2O_2 production using Amplex Red. H37Rv incubated for 24 hours in phosphate replete 7H9 (solid bars) or 7H9 prepared without phosphate (hatched bars).

Multi-gene in-frame unmarked deletion mutants were constructed to examine the role of the *pstS* genes in virulence of Mtb. Surprisingly, none of the mutants were attenuated in aerosol-infected mice (Figure 5.5). in contrast to a previous report claiming that loss of *pstS1* or *pstS2* causes attenuation *in vivo* [167]. However, it should be noted that all of our *pstS* mutants were generated in a PDIM deficient background and it is possible that PDIM deficiency masks the effects of loss of *pstS* genes.

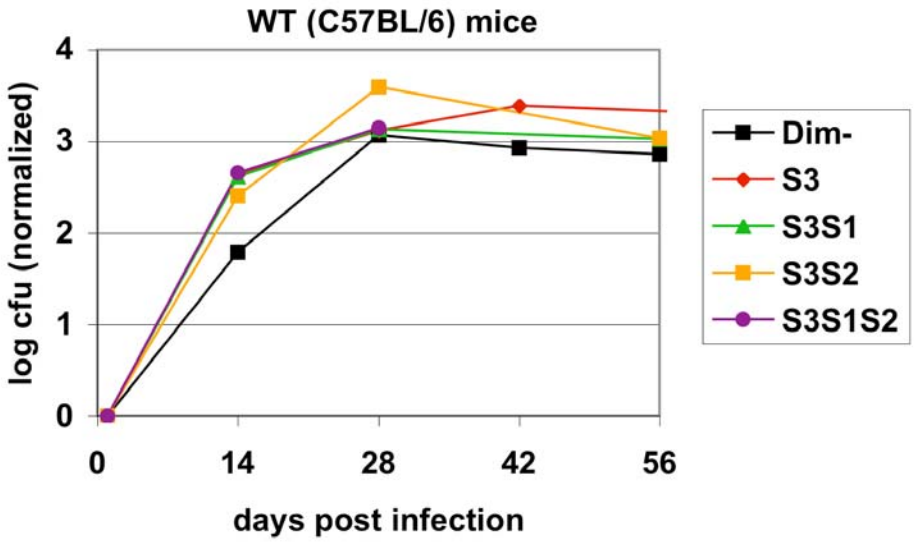

Figure 5.5: Aerosol Infection of WT (C57BL/6) Mice with PDIM- H37Rv versus *pstS* Mutants. Lung cfu (normalized to match starting inoculum) from WT mice infected by aerosol with PDIM- H37Rv (black squares), the *pstS3* mutant (red diamonds), the *pstS3S1* mutant (green triangles), the *pstS3S2* mutant (orange squares), and the *pstS3S1S2* mutant (purple circles).

Chapter 6:

Summary, Conclusions, and Future Directions

dSTM and PDIM

Mtb encounters a multitude of stresses during infection of a mammalian host. The purpose of this work was to identify pathways utilized by Mtb to counter immune-specific stresses and allow for bacterial replication and persistence in the mouse model of infection. A differential signature-tagged transposon mutagenesis (dSTM) screen was designed to reveal Mtb mutants that were underrepresented after passage through $NOS2^{-/-}$ mice but which were well represented after passage through IFN-$\gamma^{-/-}$ mice. It was hypothesized that such mutants would be deficient in counter-immune (*cim*) defenses required for survival in the face of IFN-γ dependent pathways other than NOS2. Considering the disputed role of NOS2 in control of Mtb infections in humans, such genes might be of particular interest as potential drug targets.

Our preliminary dSTM experiment identified four mutants of interest from 96 that were screened, all of which were confirmed by monotypic intravenous retest. Two mutants were not immediately chosen for follow-up. One mutation was in the gene for polyketide synthase 6 (*pks6*), a gene of unknown function that is being studied by a number of other laboratories. A second mutant had a transposon insertion in one membrane spanning domain (MSD) protein of a putative glutamine ABC transporter. Considering the fact that Mtb has a well characterized and highly active glutamine synthase, it was unclear to us why a glutamine transporter would be required for virulence [181].

Two mutants were examined in detail for their growth kinetics in and lethality to mice after aerosol infection: a glycosyltransferase mutant (Rv2958c) and an inorganic phosphate ABC transporter MSD protein mutant (*pstA1*). Both

mutants were similarly attenuated early in infection of C57BL/6 (wildtype), NOS2$^{-/-}$, and IFN-$\gamma^{-/-}$ mice. Consistent with the phenotype for which they were screened, both mutants were capable of rapid growth kinetics in IFN-$\gamma^{-/-}$ mice and these mice quickly succumbed to infection with the mutant bacteria. In contrast, NOS2$^{-/-}$ mice were able to suppress replication of these mutants for a minimum of several months before succumbing.

Concurrent with publication of our dSTM screen, C. Guilhot and colleagues published biochemical characterization of several glycosyltransferase mutants that were deficient in glycosylation of the *p*HBAD precursor of the phenolic glycolipid of Mtb (PGLtb) [161]. One of the mutants contained an insertion in Rv2958c, a gene that was shown to be defective for addition of the second sugar to the phenol group of the triglycosylated *p*HBADII and/or the intact PGLtb. As H37Rv is lacking the intact *pks15-1* gene, it is unable to form the intact PGLtb and this molecule was therefore ruled out as the source of attenuation in our Rv2958c mutant. Our interest focused, therefore, on characterization of the pathogenic importance of the three *p*HBAD gycosyltransferases (Rv2958c, Rv2959, and Rv2962c) using the strains generated by Guilhot and colleagues, which they generously provided for our experiments. Surprisingly, none of these mutants, including their Rv2958c mutant, exhibited a significant virulence defect compared to their H37Rv parent strain. Our H37Rv strain produces triglycosylated *p*HBADII and our Rv2958c mutant has the same glycosylation defect as the Guilhot Rv2958c mutant by TLC analysis [182].

Preliminary MALDI-TOF analysis done by Guilhot and colleagues suggested that our Rv2958c mutant might be deficient in PDIM synthesis [182].

We were able to confirm by TLC of ^{14}C-propionate-labeled lipid extracts that our Rv2958c mutant was PDIM deficient. Surprisingly, we found that all four of the mutants isolated from the dSTM screen lacked PDIM production, as did an attenuated H37Rv strain that was subcultured from the same parent stock. Upon further examination, it was found that approximately 50% of our parent H37Rv stock consisted of PDIM deficient bacteria.

Aerosol infection experiments in mice with clonal PDIM+ and PDIM- H37Rv confirmed that PDIM deficiency accounted for the bulk of attenuation we observed in the dSTM mutants. Apparently, PDIM deficiency arises as an occult secondary defect in a number of Mtb strains, presumably due to spontaneous mutations. It has been hypothesized that genetic manipulation, especially phage mediated transposon mutagenesis, might select for PDIM mutations [27]. However, the pre-existence of PDIM mutants in high numbers in our parent H37Rv stock argues against this hypothesis. Moreover, we were able to establish that PDIM- bacterial cultures have a significant *in vitro* growth advantage that could enable spontaneous mutants to take over a culture with serial passaging. It is likely that spontaneously arising PDIM deficient mutants were preferentially selected in the dSTM screen due to their severe attenuation in NOS2$^{-/-}$ mice and retention of virulence in IFN-$\gamma^{-/-}$ mice, the phenotype for which we screened.

In light of our experience, which is unlikely to be unique, it is important to note that a large number of attenuated mutants described in the literature have not been complemented and may suffer from the same PDIM synthesis defect as ours. Moreover, there are a number of genes that have been ascribed a role in PDIM synthesis based on their lack of PDIM synthesis. Several of these mutants have not been complemented and have no obvious biochemical link to the PDIM

biosynthetic pathway. It is possible that these mutants also have an undetected secondary mutation(s) leading to PDIM deficiency. These observations underscore the importance of bringing genetic analysis to completion via complementation. The possibility that other virulence-attenuating mutations could be selected during *in vitro* passage of bacteria must also be ruled out by complementation analysis.

pstA1 and the *pstS* Genes

The *pstS* mutants generated in this study do not appear to have virulence defects in mice when compared to their PDIM deficient parent. However, in spite of the confounding influence of PDIM, the *pstA1* mutant appears to be attenuated in a PDIM-independent manner. NOS2 mice survived 50-100% longer when infected intravenously with the PDIM-deficient *pstA1* mutant compared to the other PDIM-deficient strains isolated from the screen. Results of direct competition of the *pstA1* mutant and the PDIM- parental strain of H37Rv in aerosol-infected mice are pending.

Notably, the *pstA1* mutant exhibits significant *ex vivo* phenotypes in murine bone marrow derived macrophages. While previous reports suggest that PDIM deficiency does not influence virulence in macrophages [26], the *pstA1* mutant is attenuated in IFN-γ activated WT macrophages and in both resting and activated NOS2$^{-/-}$ macrophages. Both of these phenotypes are complemented with an episomal copy of the *pstA1* gene, confirming the role of *pstA1* in generating the phenotype. The enhanced attenuation of *pstA1* in NOS2$^{-/-}$ macrophages compared to WT (C57BL/6) macrophages suggests two possibilities: (1) the *pstA1* mutant might be sensitive to a non-NOS2 immune

pathway that is constitutively upregulated in the absence of NOS2, or (2) the *pstA1* mutant might depend on NOS2 for induction of bacterial responses required for intraphagosomal survival. Each of these hypotheses is consistent with published evidence that (1) absence of NOS2 influences macrophage gene expression [74, 92], and (2) macrophage immune status influences Mtb gene expression [74, 92].

Even more striking are the complementable *in vitro* phenotypes of the *pstA1* mutant, which is markedly sensitive to H_2O_2, SDS, and acidified $NaNO_2$ in a manner that is mimicked by phosphate starved H37Rv. The *pstS3* deletion mutant also exhibits H_2O_2 and SDS hypersensitivity. Evidence from other bacteria indicates that the Pst system has evolved as a phosphate responsive environmental sensor that is involved in regulation of the Pho regulon as well as other stress response and virulence genes. Consistent with a role for the Pst systems in gene regulation in Mtb, the *pstA1* mutant exhibits constitutive overexpression of *pstS3* while phosphate starvation leads to induction of this gene in H37Rv. Gene expression in the *pstA1* mutant appears to mimic gene expression in response to phosphate starvation, potentially explaining the similar stress sensitivity of the *pstA1* mutant and phosphate starved H37Rv.

It is unclear why phosphate starvation and *pst* gene disruption lead to sensitivity to H_2O_2, SDS, and acidified $NaNO_2$. The *pstA1* mutant is hyper-resistant to low pH and normo-sensitive to osmotic stress, arguing against a generalized stress response defect. An in-frame, unmarked, deletion mutant of *pstS3* exhibits the same stress sensitivity profile as the *pstA1* transposon mutant, indicating that the complete transporter is required for an appropriate stress response in phosphate replete conditions.

Notably, H37Rv exhibits five-fold induction of the alkylhydroperoxide reductase genes *ahpC* and *ahpD* (but not catalase) during growth on limiting phosphate as compared to phosphate replete media. However, the *pstS3* mutant under-expresses these genes under both phosphate replete and phosphate starved growth conditions. Intriguingly, it has been shown that in *E. coli* the Ahp system is necessary and sufficient for detoxification of endogenously generated reactive oxygen species (ROS) during growth on limiting phosphate. Failure to detoxify endogenous ROS generated during aerobic growth due to underexpression of *ahpC* and *ahpD* may be the cause of the enhanced sensitivity of the Mtb *pst* mutants to exogenous ROS and reactive nitrogen species (RNS). Preliminary results indicate that H37Rv accumulates H_2O_2 during growth on limiting phosphate. Therefore, toxic endogenous ROS production may be the reason for upregulation of *ahpC* and *ahpD* by H37Rv and decreased survival of the *pstA1* mutant during phosphate starvation.

It is interesting to note that an *M. smegmatis pstB* mutant and an *M. bovis phoT* mutant are hypersensitive to fluoroquinolones [176, 177]. As described previously, a role for these Pst NBD proteins in active drug efflux is possible. However, fluoroquinolones are known to induce oxidative stress, providing another intriguing candidate for the cause of enhanced fluoroquinolone toxicity to *pst* mutants [183, 184]. It remains to be seen whether mutations in the other *pst* subunits of Mtb exhibit this drug sensitivity.

Suprisingly, preliminary results indicate that the *pstA1* mutant exhibits accelerated degradation of exogenous H_2O_2 compared to H37Rv. This observation is confounding, considering that the *pstA1* mutant does not overexpress *katG* or catalase activity and the mutant is hypersensitive to the toxic

effects of H_2O_2. It is possible that the *pstA1* mutant has a membrane defect that makes it more permeable to H_2O_2 allowing both enhanced sensitivity and accelerated uptake from the medium. The exquisite sensitivity of the mutant to SDS is consistent with this hypothesis.

The phenotypes of *pst* mutants generate more questions than answers. It is possible that the complexities of the defects generated by disruption of the Pst system are more dynamic and intricate than we currently realize. It cannot be ruled out that the *in vitro* phenotypes of the *pst* mutants are linked to their *in vivo* phenotypes in ways that are not obvious. For example, *katA* and *katB* mutants of *Legionella pneumophila* fail to prevent LAMP-1 association with their phagosomes, suggesting a role for antioxidant genes in vesicular trafficking [7]. It is also possible that the *in vitro* and *in vivo* phenotypes of the Mtb *pst* mutants are unrelated. For example, in spite of its sensitivity to H_2O_2 *in vitro*, *pstA1* deficient bacteria fare no better in phox$^{-/-}$ mice than in WT mice.

Much work remains to be done in order to elucidate the role of the Mtb Pst system in virulence and stress response. It is clear that PstA1 and PstS3 play a role in gene regulation. It remains to be seen if and how the other Pst subunits may contribute to regulatory control. Microarray comparison of these mutants with their wildtype parents will enhance our understanding of their regulatory functions. It is likely that regulatory defects in these mutants are linked to virulence defects. Therefore, expression of genes of interest should be examined in macrophages and lung tissues of mice during infection with the mutants and with wildtype bacteria.

Finally, PDIM deficiency causes profound virulence defects during mouse infection. Therefore, it will be essential to generate an in-frame unmarked

deletion of *pstA1* in a PDIM+ background in order to clarify the role of this gene in Mtb virulence. PDIM proficient mutants of the *pstS* genes will also provide valuable information on the role of the Pst system in phosphate acquisition, stress response, and virulence.

Chapter 7:

Materials and Methods

Bacterial Growth Conditions

Wildtype Mtb H37Rv and derivative strains were cultured at 37°C in Middlebrook 7H9 broth containing 10% OADC (Difco), 0.5% glycerol, and 0.05% Tween-80, or on Middlebook 7H10 agar containing 10% ADS (DifCo) and 0.5% glycerol unless otherwise noted. Cycloheximide was used at 10 μg/mL to prevent culture contamination as needed. Kanamycin (25 μg/mL), hygromycin (50 μg/mL), sucrose (2.5 %), and X-gal (40 μg/mL) were used for selection on agar plates as needed. Frozen stocks were prepared by growing liquid cultures to mid-log phase (~ OD_{600} 0.5) and freezing in aliquots at -80°C.

Mouse Strains

C57BL/6 wildtype, IFN-$\gamma^{-/-}$, $NOS2^{-/-}$, and $phox^{gp91-/-}$ mice were bought from Jackson Laboratories. LRG-$47^{-/-}$ mice were kindly provided by Gregory A. Taylor's laboratory at Duke University and bred at the Rockefeller University's Specific Pathogen Free (SPF) animal facility. $phox^{gp91-/-}$ $NOS2^{-/-}$ double knockout mice were generously provided by Carl Nathan's laboratory at Weill Medical College and Graduate School of Medical Sciences. All mice were maintained on sterile food and water *ad libitum* on cob/alpha-dri bedding with the exception of the $phox^{gp91-/-}$ $NOS2^{-/-}$ mice which required maintenance on alpha-dri bedding and prophylactic Baytril (4mL/L of 100mg/mL stock) and Sporonox (3 mL/L of 10 mg/mL stock) in their water supply.

Construction of Bacterial Mutants

The STM mutant library was generated as described [76, 77]. In-frame

unmarked gene deletions were generated by allelic recombination. Briefly, 500-1000 bp PCR fragments were generated of the upstream and downstream regions of the gene to be deleted. PCR products were cloned by Topo TA (Invitrogen) and confirmed by sequencing. Upstream fragments were designed with 3′ PacI and 5′ AvrII restriction sites and downstream fragments with 3′ AvrII and 5′ AscI sites such that they could be stitched together in vector pJG1111b (provided by James Gomez, The Rockefeller University). The resulting vector contained a small number of 3′ and 5′ nucleotides from the gene of interest that were fused in frame to encode a short peptide. The backbone of the pJG1111b vector contained hygromycin and kanamycin resistance genes as well as *lacZ* and *sacB*. Bacteria were transformed with the vector plus insert and single cross-over mutants were picked from blue colonies formed on Hyg/Kn agar plates prepared with X-gal. Individual colonies were inoculated into 7H9 broth, incubated for several days for outgrowth, and plated on X-gal plates with sucrose for counter-selection. White colonies were picked for double cross-overs and deletion mutants were confirmed by PCR and/or Southern Blot.

Differential Signature Tagged Mutagenesis Screen (dSTM)

dSTM was performed by Katherine Hisert as described [76, 77]. Briefly, C57BL/6 wildtype, IFN-$\gamma^{-/-}$, and NOS2$^{-/-}$ mice were infected by tail-vein infection with STM pools. Mice were sacrificed at specified timepoints and lung homogenates were plated for cfu enumeration, tag amplification, and tag hybridization.

STM Mutant Identification and IV Retest

Transposon insertion sites of mutants were determined by inverse PCR as described [26]. Individual clones were grown up and phenotypically confirmed by monotypic IV infection in mice. Mice were infected by injection of 0.1 mL ($1x10^5$ to $1x10^6$ cfu) of diluted bacterial stocks and were sacrificed at specified timepoints for cfu enumeration. Bacterial cfu were determined by plating serial dilutions of drill or hand homogenized organs on 7H10 agar plates and counting colonies after 2-4 weeks incubation at 37°C.

***p*HBAD Glycosylation and PDIM Production**

*p*HBAD production in our H37Rv and Rv2958c mutant was analyzed by Christophe Guilhot and colleagues at the Institut de Pharmacologie et Biologie Structurale, Toulouse using thin layer chromatography (TLC) of extracted and purified glycolipids [161].

PDIMs were labeled by 24 hour incubation of mid-log 10 mL inkwell bottle cultures of Mtb with 10 μCi ^{14}C-propionate, a PDIM precursor. Bacteria were pelleted at 3800 rpm in a Sorvall tabletop centrifuge for 10-15 minutes and resuspended in 5 mL 10:1 methanol : 0.3 % NaCl plus 5 mL petroleum ether. Suspensions were vortexed vigourously for 3-5 minutes and spun at 1800 rpm in a Sorvall tabletop centrifuge for 10 min. The upper layer, containing the apolar lipids, was stored during a re-extraction of lipids from the remaining methanol with 5 mL of fresh petroleum ether. Remaining bacteria in the pooled apolar lipid extracts were killed by one hour incubation in an equal volume of added chloroform. Extracts were removed from BSL3 and evaporated down in the BSL2 chemical hood overnight. 20-30 μl of extract were spotted on TLC plates

and run in 9:1 petroleum ether:diethyl ether solvent. Labeled PDIM was imaged from phosphoimager plates exposed to dried TLC plates overnight.

Aerosol Infections

Bacterial cultures were grown to mid-log phase before being spun down for 15 min at 3800 rpm in a Sorvall tabletop centrifuge. Bacterial pellets were resuspended in PBS with 0.05 % Tween-80 and spun for 5 min at 800 rpm to eliminate clumps of bacteria. The declumped culture suspension was diluted to an OD_{600} of 0.01-0.015 to allow for pulmonary seeding of approximately 50-150 cfu/mouse. Mice were infected by exposure to 15 min aerosolization of the diluted cultures in a custom-made aerosol exposure chamber from the University of Wisconsin, Dept. of Mechanical Engineering.

Mice were sacrificed at indicated timepoints and organs were isolated for enumeration of cfu. For survival experiments, mice were observed post infection and time to death was recorded. As needed, lungs were isolated from post-mortem mice for cfu enumeration.

Macrophage Infections

Mice were sacrificed and bone marrow was flushed from femurs and tibia using cold RPMI. Marrow was passaged through a 5 mL pipette to generate a single cell suspension before being filtered through a 2361 cellstrainer (BD Falcon) into a 50 mL Falcon tube to remove debris. The cell suspension was brought up to 40 mL in RPMI and spun at 1300 rpm for 8 min in a Sorvall tabletop centrifuge. Cell pellets were resuspended in 2 mL RPMI + 2 mL 3 mM NaOAc for 2 min to lyse red blood cells, and brought up to 40 mL in RPMI before

spinning again. Cells were then resuspended in 10 mL of BMMΦ medium containing RPMI with 20 % L-cell supernatant, 10 % FBS, and Pen/Strep, counted, and seeded into Fisher Petri dishes (catalogue #0875712) at $4x10^5$ cells/mL in 10 mL/plate. At day 4 post seeding, 5 mL of medium per plate were replaced with fresh pre-warmed BMMΦ medium.

At day 6 post seeding, plates were placed at 4°C for 15 minutes before macrophages were flushed from the bottom of the plate with a 5 mL serological pipette. Suspended macrophages were collected in 50 mL falcon tubes, spun at 1300 rpm for 8 min in a Sorvall tabletop centrifuge, resuspended in 10 mL BMMΦ medium with 5 % L-cell supernatant, 5 % FBS, and 5 % Horse Serum, and counted. Macrophages were then seeded into 12 well tissue culture plates at a density of $1x10^5$ cells/mL in a volume of 2 mL/well. As needed, wells were pre-activated with 100 units of recombinant IFN-γ (Beohringer Manheim) 12-16 hours prior to bacterial infection.

On day 7, media was removed from macrophage wells and replaced with 600 μL of media containing $4x10^5$ cfu/mL bacteria. After 4 hours incubation, wells were washed thrice with PBS to remove free bacteria and fresh media was placed on wells. At timepoints for bacterial harvest, wells were washed once with PBS before incubation for several minutes in 0.5 mL of 0.5 % Triton-X for macrophage lysis. Serial dilutions of the lysates were plated on 7H10 agar plates and incubated at 37°C for 3-4 weeks for CFU enumeration.

In vitro Stresses

Survival of bacteria was determined after incubation of bacterial cultures at OD_{600} 0.05 for 24 hours in the presence of the following stresses: 1 mM H_2O_2, 0.5 % SDS, 3 mM $NaNO_2$ (at pH 5.5), 0.625 mM NaCl. Acidic 7H9 was titrated to a pH of 4.5 or 5.5 as indicated and bacterial survival was measured after 4 and 7 days incubation. 500 mL of a 100X liquid stock of phosphate free reconstituted 7H9 base was made with the following ingredients: dH_2O, 25 g ammonium sulfate, 25 g L-glutamic acid, 5 g sodium citrate, 50 mg pyridoxine, 25 mg biotin, 2 g ferric ammonium sulfate, 2.5 g magnesium sulfate, 25 mg calcium chloride, 50 mg zinc sulfate, 50 mg copper sulfate, 61.5 g sodium chloride, 27.5 g potassium chloride. 1X phosphate free 7H9 was made with 0.5 % glycerol, 10 % ADS, 0.05 % Tween-80, and 50 mM MOPS buffer. Phosphate was added back to phosphate replete control cultures from a 100X Pi stock (0.25 % disodium phosphate, 0.1 % monopotassium phosphate in dH_2O). Survival in phosphate free media was determined in the presence of various stresses and at various timepoints as indicated.

RNA Isolation and Gene Expression

In vitro grown bacteria were spun down for 10 min at 3800 rpm in a Sorvall tabletop centrifuge. Bacterial pellets were resuspended in 2 mL TriReagent (Invitrogen) and transferred to 2 mL O-ring screw cap tubes containing ~250 μL silicone beads. Infected mouse lungs were homogenized directly in TriReagent. TriReagent immersed samples were homogenized with silicone beads in a bead-beater for two 45 sec pulses separated by a 1 min period of cooling. RNA isolation from TriReagent was conducted in the BSL2 lab

according to the manufacturer's instructions. Residual DNA was removed by treatment with DNA-free or TurboDNA-free (Invitrogen) as specified by the manufacturer.

In vitro gene expression was quantified by reverse transcription and Sybr Green quantitative RT-PCR (qRT-PCR). *In vivo* gene expression was determined by reverse transcription and Taqman qRT-PCR. qRT-PCR reactions were done in an ABI Prism 7900.

Catalase Activity, H_2O_2 Consumption, and H_2O_2 Accumulation

To measure catalase activity, cultures were grown to mid-log phase and spun down for 10 min at 3800 rpm in a Sorvall tabletop centrifuge. Bacterial pellets were resuspended in potassium phosphate buffer and bead-beaten (as described above for RNA isolation). Protein concentrations in clarified cell-free bacterial lysates were quantified using Bradford reagent and diluted to equal concentrations. H_2O_2 was added to lysates and H_2O_2 quantities were measured over time by spectrophotometrical measurement at OD_{570} and comparison to an H_2O_2 standard curve.

To measure H_2O_2 consumption, mid-log phase cultures were exposed to 1.5 μM H_2O_2 and H_2O_2 levels were measured spectrophotometrically at OD_{570} using Amplex Red (Invitrogen) as specified by the manufacturer. H_2O_2 accumulation was measured directly in aliquots of growing cultures using Amplex Red. Quantification was accomplished by comparison to an H_2O_2 standard curve.

Appendix:

Tables of Plasmids and Primers:

Table A.1: Plasmids

Name	Use	Features	Source
pMV261	Complementation constructs	episomal	This study
pMV361	Complementation constructs	integrating	This study
pMV306	Complementation constructs	integrating	This study
TopoTA	cloning PCR products		Invitrogen
pJG1100	knockout constructs	lacZ, Kn^R Hyg^R, sacB	James Gomez (Rockefeller University)

Table A.2: Primers for Knockout Constructs

Name	Forward sequence 1	Reverse sequence 1	Forward sequence 2	Reverse sequence 2
pstA1 k/o	TTAATTAACAAGC TCGAGCCGATCGC GA	CCTAGGGGGACTC ACCCGTTGACCTT CC	CCTAGGGGCGGCG ACTCCCGTTATGA	GGCGCGCCCAGAC CGTGCTACCGTTC
pstS1 k/o	TTAATTAAGCTGTT CCAGCGCCCGAAT CCG	CCTAGGAATTTTC ACGCCATACCTTT CT	CCTAGGTCCAGCT AGCCTCGTTGACC AC	GGCGCGCCAGCGA TGTGATGAGCGATG AAC
pstS1 *not used	TTAATTAATGGTG GTCAGCAGCAGTT GTTGT	CGACGACGCGGG GGTAGTCCTAGG	CCTAGGCGCCCGC GGTGGTGAAGTTG TCT	CGGAGCGATGTGA TGAGCGATGAACC GCGCGG
pstS2 k/o	TTAATTAATCGGA GGCGGCACGGGC AA	CCTAGGATTTCTTG ACCTAGTGAAGGG A	CCTAGGGAACTTC ACGCAACTCCTCT CG	GGCGCGCCTCGCG GTAGTTGAAGATG CT
pstS3 k/o	TTAATTAAAAGCT CCGACGGCCTGAC CAG	CCTAGGGAGTTTC AATTCAGTTCCTA AC	CCTAGGATCGCCT GATCTGAGGTTGA CG	GGCGCGCCCCCAA GTTGCGATTGAGA AA
ManT2 k/o	TTAATTAATTGCTG GAAATCCGTCAGC GA	CCTAGGGCTTGTTT CCTCCATACTCGC C	CCTAGGCGGCTCG TCTGCTAAAGGGT GC	GGCGCGCCACGAT CGTCGACAAGGAG TTTT

Table A.3: Primers for Knockout Confirmations

(-) no product in deletion; (+) different size products in wildtype and deletion

Name	Use	Forward Sequence	Reverse Sequence
PstS3 k/o probe	southern probe	CGACGAAATGGGAGGTAGTGC	AACGCCGCCACGATAGAGG
pstA1-SP	southern probe	TGCGAGAAGCCAGCTACG	GCGACCACGATGATCAGG
Rv2958cdel	deletion (-)	ACCCTTTAGCAGACGAGC	ATTTCTGATCCGCAACTAGC
pstS1 del	deletion (-)	CCTTTCACGAGAGGTATCC	AACAAGAAATTGCCAGAGC
pstS2 del	deletion (-)	CAGTTTCTCAACAACGAAACC	TTGCATAAACGCCCTTACC
pstS3 del	deletion (-)	GCCAAACCCTGAACTACACG	ACTTTCCAGCGCCCTTACC
pstA1 del	deletion (-)	AACGTTTTTCTTCACCTCG	TTGATGGAGTGGCTGTACC
PstA1-PP	transposon (-)	TCCGCTTACGCTGCGACG	ATAACGCCGCCACGATAGAGG
Tn o84L-F2 & R2	transposon primer for k/o	ATCCGGCTCATCACCAGGTAGG	ATCTCTCCGGCTTCACCGATCC
pstS3del2	deletion (+)	GCCGAAACGGTAACAAGC	ATCATCACCGACAGCACG
pstS2del2	deletion (+)	CATAAACCTCGCCCATCC	ACAACAACTGCTGCTGACC
pstS1del2	deletion (+)	GACGCAGCATCTTCAACTACC	CTATCCCACCCAACCACC
pstA1	deletion (+)	CTGCCTATCGTCACATCG	GGAACCGTCTACGTCACC

Table A.4: Primers for Gene Expression Analysis by qRT-PCR

Name	Use	Forward Sequence	Reverse Sequence	RT Sequence
PhoY2	beacon	ATGCGGACCGCCTACCATGA	TGCCTGCAACGCCAGAAGAA	TGGCGCTCACAATGGCTCTG
PhoY1	beacon	TGGCCGGGATAGCGATGAAA	GGATGTTGCAACGCCAGCAG	TCGGTGTCGGCGATGATCTG
PhoT	beacon	ATGCGGTCGCTGATGTGTCG	GGTCGATACCGGGGGCGTAG	TTCGGCCGCTGAAACAACCAT
PstS1	beacon	GGGGCCTCCGACGCCTATCT	GCGGGTCGTCCCAGGTTTTG	GGGTTGAGCGCAGCGATCTG
PstS2	beacon	ATACCTCGACGGCGCATCCA	ATCGACCCGTCGGTCGGTCTG	CCCACCGCAAACGACCACTC
PstS3	beacon	CAACGGTGCGTGGGGTAAGG	TTGGCCATGGTCAGGTGCTG	GTCCCCACCAGCCGAAGTGA
PstA1	beacon	GCACCGGTTCTGGTGCTGGT	GCGTGCTCGGGATTGGTGAG	TGGCGACCACGATGATCAGG
UgpA	beacon	CGGGGTGCCCGACTTTTACC	ATTTCGGCCGCCTCCAACAG	CAGCTGCGGCAACAGCACTC
pstC2	Sybr	GCCAATTTCTTCACCAGTACC	AACACCAGAGCCGTTATCG	
pknD	Sybr	TATGAGGCCGAGGACACC	ATCCGTGCTCGAAACACC	
phoT	Sybr	TCTACTACGGGTCATTTCATGC	ATCGAGCAGTACGGCACC	
phoR	Sybr	CCCCTACCCTGGTCATAACCC	GGCAGTGTTGTCGTTGAGTGC	AATGGCGACGGTGGTCAAG
katG	Sybr	CGTCGGCGGTCACACTTTC	CAGCAGGGCTCTTCGTCAGC	GGCTGGCAATCTCGGCTTC
sodA	Sybr	AAGCACCACGCCACCT	GAGTGTGTCCCAGCCC	CTTGTTGCCGAGTGTGT

		ACG	AGTG	CCC
sodC	Sybr	TTCGGGTCACGACGAG GAG	GCGGAATGTTGGCAAA GTTGTC	GCGTTCTGGCGGAATG TTG
oxyS	Sybr	GGTGAGCGGTTGGTGG TATG	CACTGTCTTGGGTCTC GGGG	GGTGTGCGGAACGATG GAC
ahpC	Sybr	CAAGTGGCGGGTGGTG TTC	CGTTTTGAGGTCGTTGT GCTGTG	GAGCATCGGGAAGGG TAACG
ahpD	Sybr	CGACCAGGAACAACTA TGGGG	GACACTGCGAAGGAC CAGAGC	ACGAGGCAATGCGAG CACC
phoP	Sybr	CAAGTTCCAGGGCTTT GAAGTCTAC	CTTTGTCACATAGTCGT CACCACC	ATTCGGTGGGCGACAG CGACAC
pstA1	Sybr	GGGGTGTATCACGCCC TGTA	GAAGGTAGTCACCCGC GACA	AATAACGCCGCCACG ATAGA
pstA2	Sybr	GTGGCACGGTGAGTGT GTTG	GGCCAAATAGCCGAC GTAGC	CGAAAACCCCCAATCG AAGT
pstS1	Sybr	CTCAACCCCGGCGTGA AC	CGGGAAGTCGACGGTG GT	CCGATATAGGCCACGC AGC
pstS2	Sybr	GCGTGAGCACGCTGAA TCTT	TGAGGGGCTTGGATCT GTGGA	TGTCGCTGCGGAAGAT AACG
pstS3	Sybr	ATTTGGTGCCGCCGTA GGT	CGACCCACTGGCTTTG AGTG	GTTGACAAAGCGGGTC ATCG
pstS3-Taq	Taqman	CGCTTTGTCAACGTGTT CGA	CTGAACTACACGGCCA ATGGT	
pstA1-Taq	Taqman	GGGTGTATCACGCCCT GTAC	CTTGATGACCGCGGTT TACCT	
pstS1-Taq	Taqman	TCAGGGCACCGGTTCT G	TCAACATTGGGGCCTC CG	
pstS2-Taq	Taqman	GCAGTTCGTCTATGCCT ACGT	GACTACAACGCCAAC GGGT	
sigA-Taq	Taqman	GGCCCGGTCCGTCAAG	ACCATCCCGAAAAGG AAGACC	

References

1. Cave, A., *The evidence for the incidenced of tuberculosis in ancient Egypt.* Brit. J. Tuberculosis, 1939. **33**: p. 142.

2. Gutierrez, M.C., et al., *Ancient origin and gene mosaicism of the progenitor of Mycobacterium tuberculosis.* PLoS Pathog, 2005. **1**(1): p. e5.

3. Dye, C., et al., *Consensus statement. Global burden of tuberculosis: estimated incidence, prevalence, and mortality by country. WHO Global Surveillance and Monitoring Project.* Jama, 1999. **282**(7): p. 677-86.

4. Tiruviluamala, P. and L.B. Reichman, *Tuberculosis.* Annu Rev Public Health, 2002. **23**: p. 403-26.

5. Murray, J.F., *Tuberculosis and HIV infection: a global perspective.* Respiration, 1998. **65**(5): p. 335-42.

6. Nunn, P., et al., *Tuberculosis control in the era of HIV.* Nat Rev Immunol, 2005. **5**(10): p. 819-26.

7. Bandyopadhyay, P., et al., *Legionella pneumophila catalase-peroxidases are required for proper trafficking and growth in primary macrophages.* Infect Immun, 2003. **71**(8): p. 4526-35.

8. Gomez-Reino, J.J., et al., *Treatment of rheumatoid arthritis with tumor necrosis factor inhibitors may predispose to significant increase in tuberculosis risk: a multicenter active-surveillance report.* Arthritis Rheum, 2003. **48**(8): p. 2122-7.

9. Doffinger, R., et al., *Autoantibodies to interferon-gamma in a patient with selective susceptibility to mycobacterial infection and organ-specific autoimmunity.* Clin Infect Dis, 2004. **38**(1): p. e10-4.

10. Hoflich, C., et al., *Naturally occurring anti-IFN-gamma autoantibody and severe infections with Mycobacterium cheloneae and Burkholderia cocovenenans.* Blood, 2004. **103**(2): p. 673-5.

11. Bloom, B.R., Fine, P.E.M, *Tuberculosis: Pathogenesis, Protection, and Control*. 1994, Washington, D.C: ASM Press. 531-557.

12. Wang, C.Y., *Latent tuberculosis.* Lancet, 1916. **2**: p. 417-419.

13. Feldman, W.H. and A.H. Baggentoss, *The Residual Infectivity of the primary complex of tuberculosis.* Am. J. Pathol., 1938. **14**: p. 473-490.

14. Feldman, W.H. and A.H. Baggentoss, *The occurrence of virulent tubercle bacilli in presumably non-tuberculous lung tissue.* Am. J. Pathol., 1939. **15**: p. 501.

15. Hernandez-Pando, R., et al., *Persistence of DNA from Mycobacterium*

tuberculosis in superficially normal lung tissue during latent infection. Lancet, 2000. **356**(9248): p. 2133-8.

16. Snider, G.L., *Tuberculosis then and now: a personal perspective on the last 50 years.* Ann Intern Med, 1997. **126**(3): p. 237-43.

17. Corbett, E.L., et al., *The growing burden of tuberculosis: global trends and interactions with the HIV epidemic.* Arch Intern Med, 2003. **163**(9): p. 1009-21.

18. Blumberg, H.M., et al., *American Thoracic Society/Centers for Disease Control and Prevention/Infectious Diseases Society of America: treatment of tuberculosis.* Am J Respir Crit Care Med, 2003. **167**(4): p. 603-62.

19. McKinney, J.D., *In vivo veritas: the search for TB drug targets goes live.* Nat Med, 2000. **6**(12): p. 1330-3.

20. Iseman, M.D., *A Clinician's Guide to Tuberculosis*. 2000, Philadelphia, PA: Lippincott Williams & Wilkins. 327-329.

21. World Health Organization, W.P. (2004) *Anti-Tuberculosis Drug Resistance in the World. .* **Volume**,

22. Forget, E.J. and D. Menzies, *Adverse reactions to first-line antituberculosis drugs.* Expert Opin Drug Saf, 2006. **5**(2): p. 231-49.

23. Sreevatsan, S., et al., *Restricted structural gene polymorphism in the Mycobacterium tuberculosis complex indicates evolutionarily recent global dissemination.* Proc Natl Acad Sci U S A, 1997. **94**(18): p. 9869-74.

24. Rastogi, N., R. Hellio, and H.L. David, *A new insight into the mycobacterial cell envelope architecture by the localization of antigens in ultrathin sections.* Zentralbl Bakteriol, 1991. **275**(3): p. 287-302.

25. Chan, J., et al., *Lipoarabinomannan, a possible virulence factor involved in persistence of Mycobacterium tuberculosis within macrophages.* Infect Immun, 1991. **59**(5): p. 1755-61.

26. Cox, J.S., et al., *Complex lipid determines tissue-specific replication of Mycobacterium tuberculosis in mice [In Process Citation].* Nature, 1999. **402**(6757): p. 79-83.

27. Reed, M.B., et al., *A glycolipid of hypervirulent tuberculosis strains that inhibits the innate immune response.* Nature, 2004. **431**(7004): p. 84-7.

28. Karakousis, P.C., W.R. Bishai, and S.E. Dorman, *Mycobacterium tuberculosis cell envelope lipids and the host immune response.* Cell Microbiol, 2004. **6**(2): p. 105-16.

29. Wiker, H.G. and M. Harboe, *The antigen 85 complex: a major secretion product of Mycobacterium tuberculosis.* Microbiol Rev, 1992. **56**(4): p. 648-61.

30. Harboe, M. and H.G. Wiker, *The 38-kDa protein of Mycobacterium tuberculosis: a review.* J Infect Dis, 1992. **166**(4): p. 874-84.

31. Langermans, J.A., et al., *Protection of macaques against Mycobacterium tuberculosis infection by a subunit vaccine based on a fusion protein of antigen 85B and ESAT-6.* Vaccine, 2005. **23**(21): p. 2740-50.

32. Wilkinson, R.J., et al., *Evaluation of the recombinant 38-kilodalton antigen of Mycobacterium tuberculosis as a potential immunodiagnostic reagent.* J Clin Microbiol, 1997. **35**(3): p. 553-7.

33. Mahairas, G.G., et al., *Molecular analysis of genetic differences between Mycobacterium bovis BCG and virulent M. bovis.* J Bacteriol, 1996. **178**(5): p. 1274-82.

34. Arend, S.M., et al., *Antigenic equivalence of human T-cell responses to Mycobacterium tuberculosis-specific RD1-encoded protein antigens ESAT-6 and culture filtrate protein 10 and to mixtures of synthetic peptides.* Infect Immun, 2000. **68**(6): p. 3314-21.

35. Cole, S.T., et al., *Deciphering the biology of Mycobacterium tuberculosis from the complete genome sequence.* Nature, 1998. **393**(6685): p. 537-44.

36. Cole, S.T. and B.G. Barrell, *Analysis of the genome of Mycobacterium tuberculosis H37Rv.* Novartis Found Symp, 1998. **217**: p. 160-72; discussion 172-7.

37. Fleischmann, R.D., et al., *Whole-genome comparison of Mycobacterium tuberculosis clinical and laboratory strains.* J Bacteriol, 2002. **184**(19): p. 5479-90.

38. Musser, J.M., A. Amin, and S. Ramaswamy, *Negligible genetic diversity of mycobacterium tuberculosis host immune system protein targets: evidence of limited selective pressure.* Genetics, 2000. **155**(1): p. 7-16.

39. Sassetti, C.M., D.H. Boyd, and E.J. Rubin, *Genes required for mycobacterial growth defined by high density mutagenesis.* Mol Microbiol, 2003. **48**(1): p. 77-84.

40. McKinney, J., Jacobs, WR, Bloom, BR, *Persisting Problems in Tuberculosis*. Biomedical Research Reports, ed. J. Gallin, Fauci, AS. 1998, New York: Academic Press. 64.

41. *Histology Laboratory, Pulmonary System I, Station 13: Caseating Granuloma*. Pathology Education Resources Laboratory- PERLjam 2.01 1998 [cited 2006; Available from: http://erl.pathology.iupui.edu/C604/GENE662.HTM.

42. Scanga, C.A., et al., *Reactivation of Latent Tuberculosis: Variations on the Cornell Murine Model.* Infect. Immun., 1999. **67**(9): p. 4531-4538.

43. Orme, I.M., *Immune responses in animal models.* Curr Top Microbiol Immunol, 1996. **215**: p. 181-96.

44. Converse, P.J., et al., *Cavitary tuberculosis produced in rabbits by aerosolized virulent tubercle bacilli.* Infect Immun, 1996. **64**(11): p. 4776-87.

45. Lin, P.L., et al., *Early events in Mycobacterium tuberculosis infection in cynomolgus macaques.* Infect Immun, 2006. **74**(7): p. 3790-803.

46. Ernst, J.D., *Macrophage receptors for Mycobacterium tuberculosis.* Infect Immun, 1998. **66**(4): p. 1277-81.

47. Ehlers, M.R. and M. Daffe, *Interactions between Mycobacterium tuberculosis and host cells: are mycobacterial sugars the key?* Trends Microbiol, 1998. **6**(8): p. 328-35.

48. Means, T.K., et al., *Human toll-like receptors mediate cellular activation by Mycobacterium tuberculosis.* J Immunol, 1999. **163**(7): p. 3920-7.

49. Kaufmann, S.H. and U.E. Schaible, *A dangerous liaison between two major killers: Mycobacterium tuberculosis and HIV target dendritic cells through DC-SIGN.* J Exp Med, 2003. **197**(1): p. 1-5.

50. Armstrong, J.A. and P.D. Hart, *Phagosome-Lysosome Interactions in Cultured Macrophages Infected with Virulent Tubercle Bacilli.* Journal of Experimental Medicine, 1975. **142**: p. 1-16.

51. Le Cabec, V., et al., *Complement receptor 3 (CD11b/CD18) mediates type I and type II phagocytosis during nonopsonic and opsonic phagocytosis, respectively.* J Immunol, 2002. **169**(4): p. 2003-9.

52. Li, Y.J., M. Petrofsky, and L.E. Bermudez, *Mycobacterium tuberculosis uptake by recipient host macrophages is influenced by environmental conditions in the granuloma of the infectious individual and is associated with impaired production of interleukin-12 and tumor necrosis factor alpha.* Infect Immun, 2002. **70**(11): p. 6223-30.

53. Scanga, C.A., et al., *Depletion of CD4(+) T cells causes reactivation of murine persistent tuberculosis despite continued expression of interferon gamma and nitric oxide synthase 2.* J Exp Med, 2000. **192**(3): p. 347-58.

54. Serbina, N.V., V. Lazarevic, and J.L. Flynn, *CD4(+) T cells are required for the development of cytotoxic CD8(+) T cells during Mycobacterium tuberculosis infection.* J Immunol, 2001. **167**(12): p. 6991-7000.

55. Caruso, A.M., et al., *Mice deficient in CD4 T cells have only transiently diminished levels of IFN-gamma, yet succumb to tuberculosis.* J Immunol, 1999. **162**(9): p. 5407-16.

56. Rolph, M.S., et al., *MHC class Ia-restricted T cells partially account for beta2-*

microglobulin-dependent resistance to Mycobacterium tuberculosis. Eur J Immunol, 2001. **31**(6): p. 1944-9.

57. Behar, S.M., et al., *Susceptibility of mice deficient in CD1D or TAP1 to infection with Mycobacterium tuberculosis.* J Exp Med, 1999. **189**(12): p. 1973-80.

58. Sousa, A.O., et al., *Relative contributions of distinct MHC class I-dependent cell populations in protection to tuberculosis infection in mice.* Proc Natl Acad Sci, 2000. **97**(8): p. 4204-8.

59. Sieling, P.A., et al., *CD1-restricted T cell recognition of microbial lipoglycan antigens.* Science, 1995. **269**(5221): p. 227-30.

60. Sieling, P.A., *CD1-Restricted T cells: T cells with a unique immunological niche.* Clin Immunol, 2000. **96**(1): p. 3-10.

61. Rosat, J.P., et al., *CD1-restricted microbial lipid antigen-specific recognition found in the CD8+ alpha beta T cell pool.* J Immunol, 1999. **162**(1): p. 366-71.

62. Stenger, S., et al., *Differential effects of cytolytic T cell subsets on intracellular infection.* Science, 1997. **276**(5319): p. 1684-7.

63. Sieling, P.A., et al., *Evidence for human CD4+ T cells in the CD1-restricted repertoire: derivation of mycobacteria-reactive T cells from leprosy lesions.* J Immunol, 2000. **164**(9): p. 4790-6.

64. Steinman, R.M., *Dendritic cells: from the fabric of immunology.* Clin Invest Med, 2004. **27**(5): p. 231-6.

65. Moody, D.B., et al., *CD1b-mediated T cell recognition of a glycolipid antigen generated from mycobacterial lipid and host carbohydrate during infection.* J Exp Med, 2000. **192**(7): p. 965-76.

66. Giacomini, E., et al., *Infection of human macrophages and dendritic cells with Mycobacterium tuberculosis induces a differential cytokine gene expression that modulates T cell response.* J Immunol, 2001. **166**(12): p. 7033-41.

67. Ragno, S., et al., *Changes in gene expression in macrophages infected with Mycobacterium tuberculosis: a combined transcriptomic and proteomic approach.* Immunology, 2001. **104**(1): p. 99-108.

68. Rook, G.A., et al., *Activation of macrophages to inhibit proliferation of Mycobacterium tuberculosis: comparison of the effects of recombinant gamma-interferon on human monocytes and murine peritoneal macrophages.* Immunology, 1986. **59**(3): p. 333-8.

69. Cooper, A.M., et al., *Disseminated tuberculosis in interferon gamma gene-disrupted mice.* J Exp Med, 1993. **178**(6): p. 2243-7.

70. Flynn, J.L., et al., *An essential role for interferon gamma in resistance to Mycobacterium tuberculosis infection.* J Exp Med, 1993. **178**(6): p. 2249-54.

71. Flynn, J.L., et al., *Tumor necrosis factor-alpha is required in the protective immune response against Mycobacterium tuberculosis in mice.* Immunity, 1995. **2**(6): p. 561-72.

72. Jouanguy, E., et al., *Interferon-gamma-receptor deficiency in an infant with fatal bacille Calmette-Guerin infection.* N Engl J Med, 1996. **335**(26): p. 1956-61.

73. Keane, J., et al., *Tuberculosis associated with infliximab, a tumor necrosis factor alpha-neutralizing agent.* N Engl J Med, 2001. **345**(15): p. 1098-104.

74. Ehrt, S., et al., *Reprogramming of the Macrophage Transcriptome in Response to Interferon-{gamma} and Mycobacterium tuberculosis: Signaling Roles of Nitric Oxide Synthase-2 and Phagocyte Oxidase.* J. Exp. Med., 2001. **194**(8): p. 1123-1140.

75. MacMicking, J.D., et al., *Identification of nitric oxide synthase as a protective locus against tuberculosis.* Proc Natl Acad Sci U S A, 1997. **94**(10): p. 5243-8.

76. Hisert, K.B., et al., *Identification of Mycobacterium tuberculosis counterimmune (cim) mutants in immunodeficient mice by differential screening.* Infect Immun, 2004. **72**(9): p. 5315-21.

77. Jung, Y.J., et al., *Virulent but not avirulent Mycobacterium tuberculosis can evade the growth inhibitory action of a T helper 1-dependent, nitric oxide Synthase 2-independent defense in mice.* J Exp Med, 2002. **196**(7): p. 991-8.

78. MacMicking, J.D., G.A. Taylor, and J.D. McKinney, *Immune control of tuberculosis by IFN-gamma-inducible LRG-47.* Science, 2003. **302**(5645): p. 654-9.

79. Ulrichs, T. and S.H. Kaufmann, *New insights into the function of granulomas in human tuberculosis.* J Pathol, 2006. **208**(2): p. 261-9.

80. Segal, W. and H. Bloch, *Biochemical Differentiation of Mycobacterium tuberculosis Grown in vivo and in vitro.* Journal of Bacteriology, 1956. **72**: p. 132-141.

81. McKinney, J.D., et al., *Persistence of Mycobacterium tuberculosis in macrophages and mice requires the glyoxylate shunt enzyme isocitrate lyase.* Nature, 2000. **406**(6797): p. 735-8.

82. Munoz-Elias, E.J. and J.D. McKinney, *Mycobacterium tuberculosis isocitrate lyases 1 and 2 are jointly required for in vivo growth and virulence.* Nat Med, 2005. **11**(6): p. 638-44.

83. Berthet, F.X., et al., *Attenuation of virulence by disruption of the*

Mycobacterium tuberculosis erp gene. Science, 1998. **282**(5389): p. 759-62.

84. Buchmeier, N., et al., *A parallel intraphagosomal survival strategy shared by mycobacterium tuberculosis and Salmonella enterica.* Mol Microbiol, 2000. **35**(6): p. 1375-82.

85. Glickman, M.S., J.S. Cox, and W.R. Jacobs, Jr., *A novel mycolic acid cyclopropane synthetase is required for cording, persistence, and virulence of Mycobacterium tuberculosis.* Mol Cell, 2000. **5**(4): p. 717-27.

86. Stewart, G.R., et al., *Overexpression of heat-shock proteins reduces survival of Mycobacterium tuberculosis in the chronic phase of infection.* Nat Med, 2001. **7**(6): p. 732-7.

87. McAdam, R.A., et al., *Characterization of a Mycobacterium tuberculosis H37Rv transposon library reveals insertions in 351 ORFs and mutants with altered virulence.* Microbiology, 2002. **148**(Pt 10): p. 2975-86.

88. Plum, G. and J.E. Clark-Curtiss, *Induction of Mycobacterium avium gene expression following phagocytosis by human macrophages.* Infect Immun, 1994. **62**(2): p. 476-83.

89. Graham, J.E. and J.E. Clark-Curtiss, *Identification of Mycobacterium tuberculosis RNAs synthesized in response to phagocytosis by human macrophages by selective capture of transcribed sequences (SCOTS).* Proc Natl Acad Sci U S A, 1999. **96**(20): p. 11554-9.

90. Triccas, J.A., et al., *Use of fluorescence induction and sucrose counterselection to identify Mycobacterium tuberculosis genes expressed within host cells [In Process Citation].* Microbiology, 1999. **145**(Pt 10): p. 2923-30.

91. Triccas, J.A., W.J. Britton, and B. Gicquel, *Isolation of strong expression signals of Mycobacterium tuberculosis.* Microbiology, 2001. **147**(Pt 5): p. 1253-8.

92. Schnappinger, D., et al., *Transcriptional Adaptation of Mycobacterium tuberculosis within Macrophages: Insights into the Phagosomal Environment.* J. Exp. Med., 2003. **198**(5): p. 693-704.

93. Talaat, A.M., et al., *The temporal expression profile of Mycobacterium tuberculosis infection in mice.* Proc Natl Acad Sci U S A, 2004. **101**(13): p. 4602-7.

94. Ramakrishnan, L., N.A. Federspiel, and S. Falkow, *Granuloma-specific expression of Mycobacterium virulence proteins from the glycine-rich PE-PGRS family.* Science, 2000. **288**(5470): p. 1436-9.

95. Hensel, M., et al., *Simultaneous identification of bacterial virulence genes by negative selection.* Science, 1995. **269**(5222): p. 400-3.

96. Camacho, L.R., et al., *Identification of a virulence gene cluster of Mycobacterium tuberculosis by signature-tagged transposon mutagenesis.* Mol Microbiol, 1999. **34**(2): p. 257-67.

97. Ng, V.H., et al., *Role of KatG catalase-peroxidase in mycobacterial pathogenesis: countering the phagocyte oxidative burst.* Mol Microbiol, 2004. **52**(5): p. 1291-1302.

98. Darwin, K.H., et al., *The proteasome of Mycobacterium tuberculosis is required for resistance to nitric oxide.* Science, 2003. **302**(5652): p. 1963-6.

99. Rosenberg, H., R.G. Gerdes, and K. Chegwidden, *Two systems for the uptake of phosphate in Escherichia coli.* J Bacteriol, 1977. **131**(2): p. 505-11.

100. Surin, B.P., H. Rosenberg, and G.B. Cox, *Phosphate-specific transport system of Escherichia coli: nucleotide sequence and gene-polypeptide relationships.* J Bacteriol, 1985. **161**(1): p. 189-98.

101. Webb, D.C., H. Rosenberg, and G.B. Cox, *Mutational analysis of the Escherichia coli phosphate-specific transport system, a member of the traffic ATPase (or ABC) family of membrane transporters. A role for proline residues in transmembrane helices.* J Biol Chem, 1992. **267**(34): p. 24661-8.

102. Steed, P.M. and B.L. Wanner, *Use of the rep technique for allele replacement to construct mutants with deletions of the pstSCAB-phoU operon: evidence of a new role for the PhoU protein in the phosphate regulon.* J Bacteriol, 1993. **175**(21): p. 6797-809.

103. Wanner, B.L., *Gene regulation by phosphate in enteric bacteria.* J Cell Biochem, 1993. **51**(1): p. 47-54.

104. Aguena, M., E. Yagil, and B. Spira, *Transcriptional analysis of the pst operon of Escherichia coli.* Mol Genet Genomics, 2002. **268**(4): p. 518-24.

105. Wanner, B.L., *Signal transduction in the control of phosphate-regulated genes of Escherichia coli.* Kidney Int, 1996. **49**(4): p. 964-7.

106. Cox, G.B., D. Webb, and H. Rosenberg, *Specific amino acid residues in both the PstB and PstC proteins are required for phosphate transport by the Escherichia coli Pst system.* J Bacteriol, 1989. **171**(3): p. 1531-4.

107. Cox, G.B., et al., *Arg-220 of the PstA protein is required for phosphate transport through the phosphate-specific transport system in Escherichia coli but not for alkaline phosphatase repression.* J Bacteriol, 1988. **170**(5): p. 2283-6.

108. Hoffer, S.M. and J. Tommassen, *The phosphate-binding protein of Escherichia coli is not essential for P(i)-regulated expression of the pho regulon.* J Bacteriol, 2001. **183**(19): p. 5768-71.

109. Atalla, A. and W. Schumann, *The pst operon of Bacillus subtilis is specifically*

induced by alkali stress. J Bacteriol, 2003. **185**(16): p. 5019-22.

110. Makino, K., et al., *Role of the sigma 70 subunit of RNA polymerase in transcriptional activation by activator protein PhoB in Escherichia coli.* Genes Dev, 1993. **7**(1): p. 149-60.

111. Cox, G.B., et al., *Genetic analysis of mutants affected in the Pst inorganic phosphate transport system.* J Bacteriol, 1981. **148**(1): p. 1-9.

112. Muda, M., N.N. Rao, and A. Torriani, *Role of PhoU in phosphate transport and alkaline phosphatase regulation.* J Bacteriol, 1992. **174**(24): p. 8057-64.

113. Morohoshi, T., et al., *Accumulation of inorganic polyphosphate in phoU mutants of Escherichia coli and Synechocystis sp. strain PCC6803.* Appl Environ Microbiol, 2002. **68**(8): p. 4107-10.

114. Diaz, M., et al., *The high-affinity phosphate-binding protein PstS is accumulated under high fructose concentrations and mutation of the corresponding gene affects differentiation in Streptomyces lividans.* Microbiology, 2005. **151**(Pt 8): p. 2583-92.

115. Rao, N.N. and A. Kornberg, *Inorganic polyphosphate supports resistance and survival of stationary-phase Escherichia coli.* J Bacteriol, 1996. **178**(5): p. 1394-400.

116. Kuroda, A., et al., *Role of inorganic polyphosphate in promoting ribosomal protein degradation by the Lon protease in E. coli.* Science, 2001. **293**(5530): p. 705-8.

117. Ault-Riche, D., et al., *Novel assay reveals multiple pathways regulating stress-induced accumulations of inorganic polyphosphate in Escherichia coli.* J Bacteriol, 1998. **180**(7): p. 1841-7.

118. Ruiz, N. and T.J. Silhavy, *Constitutive activation of the Escherichia coli Pho regulon upregulates rpoS translation in an Hfq-dependent fashion.* J Bacteriol, 2003. **185**(20): p. 5984-92.

119. Sledjeski, D.D., C. Whitman, and A. Zhang, *Hfq is necessary for regulation by the untranslated RNA DsrA.* J Bacteriol, 2001. **183**(6): p. 1997-2005.

120. Zhang, A., et al., *The OxyS regulatory RNA represses rpoS translation and binds the Hfq (HF-I) protein.* Embo J, 1998. **17**(20): p. 6061-8.

121. Taschner, N.P., E. Yagil, and B. Spira, *A differential effect of sigmaS on the expression of the PHO regulon genes of Escherichia coli.* Microbiology, 2004. **150**(Pt 9): p. 2985-92.

122. Hengge-Aronis, R., *Back to log phase: sigma S as a global regulator in the osmotic control of gene expression in Escherichia coli.* Mol Microbiol, 1996. **21**(5): p. 887-93.

123. Hengge-Aronis, R., *Stationary phase gene regulation: what makes an Escherichia coli promoter sigmaS-selective?* Curr Opin Microbiol, 2002. **5**(6): p. 591-5.

124. Dukan, S. and T. Nystrom, *Bacterial senescence: stasis results in increased and differential oxidation of cytoplasmic proteins leading to developmental induction of the heat shock regulon.* Genes Dev, 1998. **12**(21): p. 3431-41.

125. Moreau, P.L., et al., *Non-growing Escherichia coli cells starved for glucose or phosphate use different mechanisms to survive oxidative stress.* Mol Microbiol, 2001. **39**(4): p. 1048-60.

126. Dukan, S. and T. Nystrom, *Oxidative stress defense and deterioration of growth-arrested Escherichia coli cells.* J Biol Chem, 1999. **274**(37): p. 26027-32.

127. VanBogelen, R.A., et al., *Global analysis of proteins synthesized during phosphorus restriction in Escherichia coli.* J Bacteriol, 1996. **178**(15): p. 4344-66.

128. Yuan, Z.C., R. Zaheer, and T.M. Finan, *Phosphate limitation induces catalase expression in Sinorhizobium meliloti, Pseudomonas aeruginosa and Agrobacterium tumefaciens.* Mol Microbiol, 2005. **58**(3): p. 877-94.

129. Orihuela, C.J., et al., *Streptococcus pneumoniae PstS production is phosphate responsive and enhanced during growth in the murine peritoneal cavity.* Infect Immun, 2001. **69**(12): p. 7565-71.

130. Runyen-Janecky, L.J. and S.M. Payne, *Identification of chromosomal Shigella flexneri genes induced by the eukaryotic intracellular environment.* Infect Immun, 2002. **70**(8): p. 4379-88.

131. Martin, J.F., *Phosphate control of the biosynthesis of antibiotics and other secondary metabolites is mediated by the PhoR-PhoP system: an unfinished story.* J Bacteriol, 2004. **186**(16): p. 5197-201.

132. Monds, R.D., M.W. Silby, and H.K. Mahanty, *Expression of the Pho regulon negatively regulates biofilm formation by Pseudomonas aureofaciens PA147-2.* Mol Microbiol, 2001. **42**(2): p. 415-26.

133. Slater, H., et al., *Phosphate availability regulates biosynthesis of two antibiotics, prodigiosin and carbapenem, in Serratia via both quorum-sensing-dependent and -independent pathways.* Mol Microbiol, 2003. **47**(2): p. 303-20.

134. Sola-Landa, A., R.S. Moura, and J.F. Martin, *The two-component PhoR-PhoP system controls both primary metabolism and secondary metabolite biosynthesis in Streptomyces lividans.* Proc Natl Acad Sci U S A, 2003. **100**(10): p. 6133-8.

135. Gonin, M., et al., *Regulation of stalk elongation by phosphate in Caulobacter crescentus.* J Bacteriol, 2000. **182**(2): p. 337-47.

136. Duwat, P., S.D. Ehrlich, and A. Gruss, *The recA gene of Lactococcus lactis:*

characterization and involvement in oxidative and thermal stress. Mol Microbiol, 1995. **17**(6): p. 1121-31.

137. Duwat, P., S.D. Ehrlich, and A. Gruss, *Effects of metabolic flux on stress response pathways in Lactococcus lactis.* Mol Microbiol, 1999. **31**(3): p. 845-58.

138. Rallu, F., et al., *Acid- and multistress-resistant mutants of Lactococcus lactis : identification of intracellular stress signals.* Mol Microbiol, 2000. **35**(3): p. 517-28.

139. Lamarche, M.G., et al., *Inactivation of the pst system reduces the virulence of an avian pathogenic Escherichia coli O78 strain.* Infect Immun, 2005. **73**(7): p. 4138-45.

140. Daigle, F., J.M. Fairbrother, and J. Harel, *Identification of a mutation in the pst-phoU operon that reduces pathogenicity of an Escherichia coli strain causing septicemia in pigs.* Infect Immun, 1995. **63**(12): p. 4924-7.

141. Srinivasa Rao, P.S., T.M. Lim, and K.Y. Leung, *Opsonized virulent Edwardsiella tarda strains are able to adhere to and survive and replicate within fish phagocytes but fail to stimulate reactive oxygen intermediates.* Infect Immun, 2001. **69**(9): p. 5689-97.

142. Srinivasa Rao, P.S., T.M. Lim, and K.Y. Leung, *Functional genomics approach to the identification of virulence genes involved in Edwardsiella tarda pathogenesis.* Infect Immun, 2003. **71**(3): p. 1343-51.

143. Wagner, D., et al., *Elemental analysis of Mycobacterium avium-, Mycobacterium tuberculosis-, and Mycobacterium smegmatis-containing phagosomes indicates pathogen-induced microenvironments within the host cell's endosomal system.* J Immunol, 2005. **174**(3): p. 1491-500.

144. Neild, A., *Expression of M. tuberculosis pst genes during bone-marrow-derived murine macroophage infection*, M. Kirksey, Editor. 2005: New York.

145. Kocan, M., et al., *Two-component systems of Corynebacterium glutamicum: deletion analysis and involvement of the PhoS-PhoR system in the phosphate starvation response.* J Bacteriol, 2006. **188**(2): p. 724-32.

146. Ren, J. and J.F. Prescott, *The effect of mutation on Rhodococcus equi virulence plasmid gene expression and mouse virulence.* Vet Microbiol, 2004. **103**(3-4): p. 219-30.

147. Perez, E., et al., *An essential role for phoP in Mycobacterium tuberculosis virulence.* Mol Microbiol, 2001. **41**(1): p. 179-87.

148. Walters, S.B., et al., *The Mycobacterium tuberculosis PhoPR two-component system regulates genes essential for virulence and complex lipid biosynthesis.* Mol Microbiol, 2006. **60**(2): p. 312-30.

149. Daffe, M. and M.A. Laneelle, *Distribution of phthiocerol diester, phenolic mycosides and related compounds in mycobacteria.* J Gen Microbiol, 1988. **134**(7): p. 2049-55.

150. Daffe, M., *Glycomicrobiology*, ed. R.J. Doyle. 2000: Plenum Pub Corp.

151. Onwueme, K.C., et al., *The dimycocerosate ester polyketide virulence factors of mycobacteria.* Prog Lipid Res, 2005. **44**(5): p. 259-302.

152. Goren, M.B., O. Brokl, and W.B. Schaefer, *Lipids of putative relevance to virulence in Mycobacterium tuberculosis: phthiocerol dimycocerosate and the attenuation indicator lipid.* Infect Immun, 1974. **9**(1): p. 150-8.

153. Kondo, E. and K. Kanai, *A suggested role of a host-parasite lipid complex in mycobacterial infection.* Jpn J Med Sci Biol, 1976. **29**(4): p. 199-201.

154. Camacho, L.R., et al., *Analysis of the phthiocerol dimycocerosate locus of Mycobacterium tuberculosis. Evidence that this lipid is involved in the cell wall permeability barrier.* J Biol Chem, 2001. **276**(23): p. 19845-54.

155. Jain, M. and J.S. Cox, *Interaction between polyketide synthase and transporter suggests coupled synthesis and export of virulence lipid in M. tuberculosis.* PLoS Pathog, 2005. **1**(1): p. e2.

156. Sulzenbacher, G., et al., *LppX is a lipoprotein required for the translocation of phthiocerol dimycocerosates to the surface of Mycobacterium tuberculosis.* Embo J, 2006. **25**(7): p. 1436-44.

157. Jackson, M., et al., *Inactivation of the antigen 85C gene profoundly affects the mycolate content and alters the permeability of the Mycobacterium tuberculosis cell envelope [In Process Citation].* Mol Microbiol, 1999. **31**(5): p. 1573-87.

158. Rousseau, C., et al., *Production of phthiocerol dimycocerosates protects Mycobacterium tuberculosis from the cidal activity of reactive nitrogen intermediates produced by macrophages and modulates the early immune response to infection.* Cell Microbiol, 2004. **6**(3): p. 277-87.

159. Ng, V., et al., *Role of the cell wall phenolic glycolipid-1 in the peripheral nerve predilection of Mycobacterium leprae.* Cell, 2000. **103**(3): p. 511-24.

160. Schlesinger, L.S. and M.A. Horwitz, *Phenolic glycolipid-1 of Mycobacterium leprae binds complement component C3 in serum and mediates phagocytosis by human monocytes.* J Exp Med, 1991. **174**(5): p. 1031-8.

161. Perez, E., et al., *Characterization of three glycosyltransferases involved in the biosynthesis of the phenolic glycolipid antigens from the Mycobacterium tuberculosis complex.* J Biol Chem, 2004. **279**(41): p. 42574-83.

162. Constant, P., et al., *Role of the pks15/1 gene in the biosynthesis of phenolglycolipids in the Mycobacterium tuberculosis complex. Evidence that all*

strains synthesize glycosylated p-hydroxybenzoic methly esters and that strains devoid of phenolglycolipids harbor a frameshift mutation in the pks15/1 gene. J Biol Chem, 2002. **277**(41): p. 38148-58.

163. Onwueme, K.C., *Biosynthesis of the Polyketide Synthase-Derived Phthiocerol Dimycocerosate Virulence Factors of Mycobacterium tuberculosis*, in *Microbiology and Immunology*. 2005, Graduate School of Cornell University: New York. p. 194.
164. Lefevre, P., et al., *Three different putative phosphate transport receptors are encoded by the Mycobacterium tuberculosis genome and are present at the surface of Mycobacterium bovis BCG.* J Bacteriol, 1997. **179**(9): p. 2900-6.

165. Andersen, A.B., L. Ljungqvist, and M. Olsen, *Evidence that protein antigen b of Mycobacterium tuberculosis is involved in phosphate metabolism.* J Gen Microbiol, 1990. **136**(3): p. 477-80.

166. Torres, A., et al., *Molecular analysis of Mycobacterium tuberculosis phosphate specific transport system in Mycobacterium smegmatis. Characterization of recombinant 38 kDa (PstS-1).* Microb Pathog, 2001. **30**(5): p. 289-97.

167. Braibant, M., et al., *A Mycobacterium tuberculosis gene cluster encoding proteins of a phosphate transporter homologous to the Escherichia coli Pst system.* Gene, 1996. **176**(1-2): p. 171-6.

168. Braibant, M., et al., *Identification of a second Mycobacterium tuberculosis gene cluster encoding proteins of an ABC phosphate transporter.* FEBS Lett, 1996. **394**(2): p. 206-12.

169. Kriakov, J., S. Lee, and W.R. Jacobs, Jr., *Identification of a regulated alkaline phosphatase, a cell surface-associated lipoprotein, in Mycobacterium smegmatis.* J Bacteriol, 2003. **185**(16): p. 4983-91.

170. Betts, J.C., et al., *Evaluation of a nutrient starvation model of Mycobacterium tuberculosis persistence by gene and protein expression profiling.* Mol Microbiol, 2002. **43**(3): p. 717-31.

171. Dahl, J.L., et al., *The role of RelMtb-mediated adaptation to stationary phase in long-term persistence of Mycobacterium tuberculosis in mice.* Proc Natl Acad Sci U S A, 2003. **100**(17): p. 10026-31.

172. Mariani, F., et al., *Mycobacterium tuberculosis H37Rv comparative gene-expression analysis in synthetic medium and human macrophage.* Gene, 2000. **253**(2): p. 281-91.

173. Wagner, D., et al., *Changes of the phagosomal elemental concentrations by Mycobacterium tuberculosis Mramp.* Microbiology, 2005. **151**(Pt 1): p. 323-32.

174. Banerjee, S.K., et al., *Identification of an ABC transporter gene that exhibits mRNA level overexpression in fluoroquinolone-resistant Mycobacterium smegmatis.* FEBS Lett, 1998. **425**(1): p. 151-6.

175. Bhatt, K., S.K. Banerjee, and P.K. Chakraborti, *Evidence that phosphate specific transporter is amplified in a fluoroquinolone resistant Mycobacterium smegmatis.* Eur J Biochem, 2000. **267**(13): p. 4028-32.

176. Banerjee, S.K., et al., *Involvement of a natural transport system in the process of efflux-mediated drug resistance in Mycobacterium smegmatis.* Mol Gen Genet, 2000. **262**(6): p. 949-56.

177. Collins, D.M., et al., *Different susceptibility of two animal species infected with isogenic mutants of Mycobacterium bovis identifies phoT as having roles in tuberculosis virulence and phosphate transport.* Microbiology, 2003. **149**(11): p. 3203-3212.

178. Rengarajan, J., B.R. Bloom, and E.J. Rubin, *From The Cover: Genome-wide requirements for Mycobacterium tuberculosis adaptation and survival in macrophages.* PNAS, 2005. **102**(23): p. 8327-8332.

179. Peirs, P., et al., *Mycobacterium tuberculosis with disruption in genes encoding the phosphate binding proteins PstS1 and PstS2 is deficient in phosphate uptake and demonstrates reduced in vivo virulence.* Infect Immun, 2005. **73**(3): p. 1898-902.

180. Braibant, M., P. Gilot, and J. Content, *The ATP binding cassette (ABC) transport systems of Mycobacterium tuberculosis.* FEMS Microbiol Rev, 2000. **24**(4): p. 449-67.

181. Tullius, M.V., G. Harth, and M.A. Horwitz, *The extracellular levels of Mycobacterium tuberculosis glutamine synthase and superoxide dismutase in actively growing cultures are due to high expression and extracellular stability rather than to a protein-specific export mechanism.* Infect Immun, 2001. **69**: p. 6348-63.

182. Guilhot, C., *Personal Communication regarding pHBAD glycosylation and PDIM synthesis of various H37Rv strains.* 2005.

183. Becerra, M. and I. Albesa, *Oxidative stress induced by ciprofloxacin in Staphylococcus aureus.* Biochem Biophys Res Commun, 2002. **297**(4): p. 1003-7.

184. Albesa, I., et al., *Oxidative stress involved in the antibacterial action of different antibiotics.* Biochem Biophys Res Commun, 2004. **317**(2): p. 605-9.